POLITECHNIKA GDAŃSKA

OPIS ROZPRAWY DOKTORSKIEJ

Autor rozprawy doktorskiej: mgr inż. Michał Struk

Tytuł rozprawy doktorskiej w języku polskim: Badania eksperymentalne zjawiska surf-ridingu w warunkach nadążającej fali bi-chromatycznej.

Tytuł rozprawy w języku angielskim: Experimental exploration of the ship surf-riding in bi-chromatic following seas.

Język rozprawy doktorskiej: angielski

Promotor rozprawy doktorskiej: dr hab. inż. Przemysław Krata

Data obrony: ……

Słowa kluczowe rozprawy doktorskiej w języku polskim: fala bi-chromatyczna; fala nadążająca; surf-riding; basen modelowy; badania modelowe; nieliniowa mechanika ruchu okrętu

Słowa kluczowe rozprawy doktorskiej w języku angielskim: bi-chromatic wave; following seas; surf-riding; towing tank; model test; nonlinear ship dynamics

Streszczenie rozprawy w języku polskim: Niniejsza rozprawa potwierdza obowiązującą teorię surf-ridingu w warunkach nadążającej fali bi-chromatycznej poprzez eksperymenty przeprowadzone w basenach modelowych. Przeanalizowano cztery główne zagadnienia: wykonalność badań dotyczących surf-ridingu na fali nadążającej, zgodność z przewidywaniami numerycznymi, użyteczność eksperymentów przeprowadzonych w basenie modelowym o długości 40m, skalowalność zjawiska. Eksperymenty zostały przeprowadzone na basenie modelowym Politechniki Gdańskiej (40m długości) oraz na basenie modelowym Centrum Techniki Okrętowej (270m długości) umożliwiając badania przy użyciu dwóch modeli statków wykonanych w dwóch różnych skalach (1/64 i 1/14). Wyniki badań poszerzają wiedzę w temacie analizowanych zagadnień: eksperymenty w danych warunkach zapewniają adekwatne wyniki; obserwowane zjawiska pokrywają się z przewidywaniami numerycznymi zarówno jakościowo i ilościowo; basen modelowy o długości 40m jest wystarczający pomimo ograniczonej liczby napotkań fali; zjawisko jest skalowalne, choć parametry krytyczne wymagają dalszej identyfikacji. Niniejsza praca jest pierwszym na świecie podejściem do eksperymentalnych badań surf-ridingu na fali bi-chromatycznej - badania te podkreślają aplikowalność istniejącej teorii w warunkach rzeczywistych, oferując narzędzia dla eksperymentatorów i obliczeniowców.

Streszczenie rozprawy w języku angielskim: This research validates the standing theory of ship surf-riding in bi-chromatic following wave conditions through towing tank experiments. The scope of the study mainly covers four issues: feasibility of surf-riding experiments in following waves, alignment with numerical predictions, viability of experiments in a 40m tank, and scalability of the phenomenon. Experiments were conducted at Gdansk Tech towing tank (40m long), as well as at CTO towing tank (270m long), using two ship models at two different scales (1/64 and 1/14). The findings address all of the research questions: experiments are feasible in bi-chromatic following wave conditions, observed phenomena match numerical predictions both qualitatively and quantitatively, 40m towing tank is adequate despite limited number of wave encounters, and the experiment is scalable, however critical parameters require further identification. This work represents the first attempt at experiments of ship surf-riding in bi-chromatic waves, providing scientific novelty. The research highlights real-world applicability of the surf-riding theory, offering utility for towing tank researchers and numerical specialists.

GDAŃSK UNIVERSITY OF TECHNOLOGY

DESCRIPTION OF DOCTORAL DISSERTATION

The Author of the doctoral dissertation: mgr inż. Michał Struk

Title of doctoral dissertation: Experimental exploration of the ship surf-riding in bi-chromatic following seas.

Title of doctoral dissertation in Polish: Badania eksperymentalne zjawiska surf-ridingu w warunkach nadążającej fali bi-chromatycznej.

Language of doctoral dissertation: English

Supervisor: dr hab. inż. Przemysław Krata

Date of doctoral defense: ……

Keywords of doctoral dissertation in Polish: fala bi-chromatyczna; fala nadążająca; surf-riding; basen modelowy; badania modelowe; nieliniowa mechanika ruchu okrętu

Keywords of doctoral dissertation in English: bi-chromatic wave; following seas; surf-riding; towing tank; model test, nonlinear ship dynamics

Summary of doctoral dissertation in Polish: Niniejsza rozprawa potwierdza obowiązującą teorię surf-ridingu w warunkach nadążającej fali bi-chromatycznej poprzez eksperymenty przeprowadzone w basenach modelowych. Przeanalizowano cztery główne zagadnienia: wykonalność badań dotyczących surf-ridingu na fali nadążającej, zgodność z przewidywaniami numerycznymi, użyteczność eksperymentów przeprowadzonych w basenie modelowym o długości 40m, skalowalność zjawiska. Eksperymenty zostały przeprowadzone na basenie modelowym Politechniki Gdańskiej (40m długości) oraz na basenie modelowym Centrum Techniki Okrętowej (270m długości) umożliwiając badania przy użyciu dwóch modeli statków wykonanych w dwóch różnych skalach (1/64 i 1/14). Wyniki badań poszerzają wiedzę w temacie analizowanych zagadnień: eksperymenty w danych warunkach zapewniają adekwatne wyniki; obserwowane zjawiska pokrywają się z przewidywaniami numerycznymi zarówno jakościowo i ilościowo; basen modelowy o długości 40m jest wystarczający pomimo ograniczonej liczby napotkań fali; zjawisko jest skalowalne, choć parametry krytyczne wymagają dalszej identyfikacji. Niniejsza praca jest pierwszym na świecie podejściem do eksperymentalnych badań surf-ridingu na fali bi-chromatycznej - badania te podkreślają aplikowalność istniejącej teorii w warunkach rzeczywistych, oferując narzędzia dla eksperymentatorów i obliczeniowców.

Summary of doctoral dissertation in English: This research validates the standing theory of ship surf-riding in bi-chromatic following wave conditions through towing tank experiments. The scope of the study mainly covers four issues: feasibility of surf-riding experiments in following waves, alignment with numerical predictions, viability of experiments in a 40m tank, and scalability of the phenomenon. Experiments were conducted at Gdansk Tech towing tank (40m long), as well as at CTO towing tank (270m long), using two ship models at two different scales (1/64 and 1/14). The findings address all of the research questions: experiments are feasible in bi-chromatic following wave conditions, observed phenomena match numerical predictions both qualitatively and quantitatively, 40m towing tank is adequate despite limited number of wave encounters, and the experiment is scalable, however critical parameters require further identification. This work represents the first attempt at experiments of ship surf-riding in bi-chromatic waves, providing scientific novelty. The research highlights real-world applicability of the surf-riding theory, offering utility for towing tank researchers and numerical specialists.

ACKNOWLEDGEMENTS

I would like to express my sincere gratitude to Professor Przemysław Krata for his patience, expertise and invaluable guidance as my supervisor. Without his support, this research would not have been possible. I would also like to thank my friend Emil Roch for his unwavering support throughout our academic journey, from our first day at university to the present day. My thanks also go to Miguel Quintero from the Naval Surface Warfare Center for his insightful discussions on the experimental methodology. Thanks also go to my towing tank colleagues, Mirosław Grygorowicz and Piotr Pruszko, who introduced me to experimental hydrodynamics and provided constructive feedback on my methods. Special thanks go to Katarzyna Warnke-Olewniczak and Zbigniew Macikowski for their partnership on surf-riding related research and for their practical insights into my work. I would also like to acknowledge my KSTO KORAB science club colleagues for volunteering during experimental campaigns. Finally, I would like to express my profound gratitude to my wife, Adrianna, for her patience and support throughout this journey.

The study was performed as a part of the “Experimental exploration of the ship surf-riding in bi-chromatic following seas with the view to expand the understanding of this phenomenon in irregular wave conditions” research project (number N62909-23-1-2083), funded by the US Office of Naval Research and US Office of Naval Research Global under supervision of Dr. Martina Siwek, Dr.Woei-Min Lin, Dr. Robert Brizzolara and Dr. Richard Meyer.

TABLE OF CONTENTS

LIST OF IMPORTANT SYMBOLS AND ABBREVIATIONS

v_c - commanded speed of the ship model [m/s];

λ_i - length of the *i* wave component [m/s];

c_i - celerity of the *i* wave component [m/s];

f_i - frequency of the *i* wave component [Hz];

A_i - amplitude of the *i* wave component [m];

T_{Ei} - encounter period of the *i* wave component [s];

t - time [s];

L_{BP} - length between perpendiculars of the ship model [m];

L_{OA} - length overall of the ship mode [m];

B - beam of the ship model [m];

d - draft of the ship model [m];

m - mass of the ship model [kg];

VCG - vertical center of gravity [m];

ITTC - International Towing Tank Conference;

IMO - International Maritime Organization;

CTO - Maritime Advanced Research Centre (Poland);

NRIFE - National Research Institute of Fisheries Engineering (Japan);

LHEEA - The Research Laboratory in Hydrodynamics (France);

HSVA - The Hamburg Ship Model Basin (Germany);

CSSRC - China Ship Scientific Research Center (China).

1. INTRODUCTION

1.1. Background and motivation

Although the simplest way a ship can move is in a straight line at a constant speed, this happens only when there is a balance between the ship's resistance and the thrust. Such situation only occurs when the ship is on a steady course with absolutely no waves nor wind, which is very rare. In reality, under the influence of wind and wave forces, the ship moves in a complex motion in all six degrees of freedom. Most often, in the context of navigation safety, rolling is the main concern, but this does not cover all issues. For centuries sailors have experienced the danger of sudden acceleration in following waves, which can cause a sudden change in the ship's course (Spyrou, 2010). The first of these phenomena is referred to as surf-riding, which may result in course instability known as broaching-to (IMO, 2023).

Surf-riding is a dynamic phenomenon occurring when a ship is captured by a wave approaching from its stern, accelerating it to the wave celerity. This is a state where the ship’s propulsion force combines with the wave surging force to exceed its commanded calm water speed. This phenomenon is particularly hazardous because it serves as a precursor to broaching-to, the violent directional instability that can trigger collisions, large-angle heeling, or even capsizing (Szozda and Krata, 2022). Broaching-to, a behavior historically documented since the sail era, itself is a critical safety concern. When a ship broaches, recovery is frequently, though not always, possible(Spyrou, 2010). Given the inherent vulnerability of fast, small to mid-size vessels to surf-riding, the potential loss of directional stability in waves represents a significant navigational risk.

The fundamental mechanism in regular waves involves a dynamic equilibrium established at the front slope of the wave. If the approaching wave is sufficiently steep, its surging force can accelerate the ship to the wave celerity, where the combined propulsion and wave forces balance the ship’s resistance, as shown in Figure 1.1. This equilibrium effectively "captures" the vessel, drawing it toward the wave’s front slope (Belenky et al., 2016; Spyrou, 1995; Umeda, 1990). However, many ships exhibit directional instability under these conditions, tending to veer away from their commanded course. As yaw instability intensifies, the rudder response may become insufficient to maintain directional stability, leading to broaching and subsequent stability failure (Hashimoto et al., 2004; Spyrou, 1996a; Umeda, 1999).

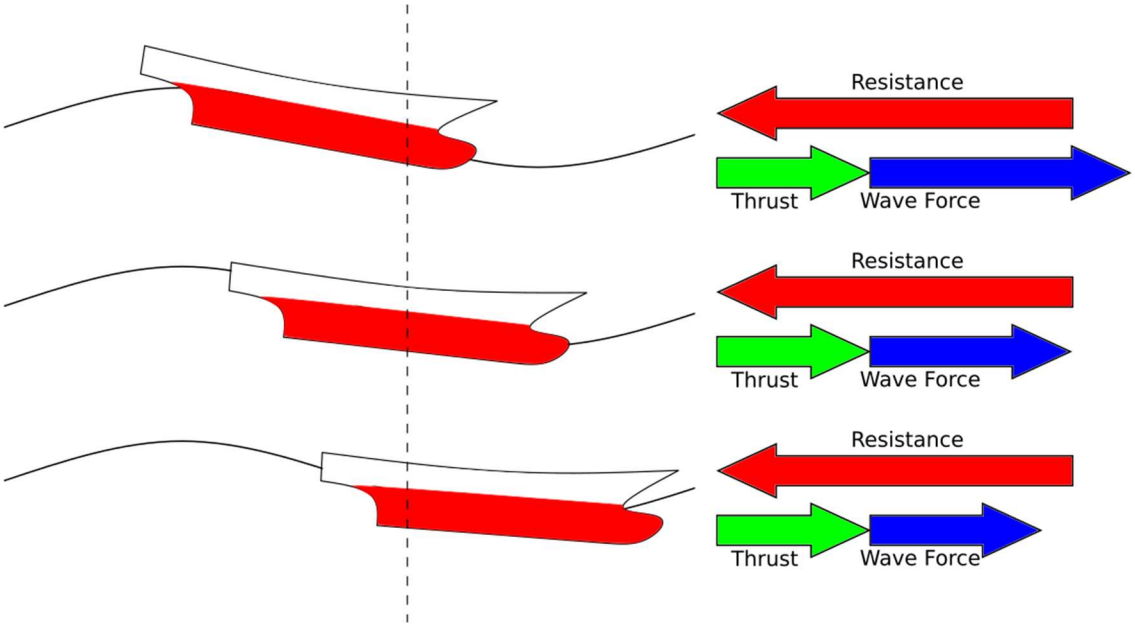

Figure 1.1 Diagram showing how surge forces change when position on the wave changes

Critical to mitigating such a risk is the identification of conditions that facilitate development of surf-riding, as this phenomenon itself can lead to occurrence of broaching-to. For instance, the dynamic equilibrium in regular waves is a state where propulsion and wave forces match resistance at wave celerity due to high enough wave steepness or fast enough ship commanded speed. The ability to predict and avoid these critical thresholds is paramount for safe navigation of vulnerable vessels. Consequently, rigorous research into surf-riding dynamics, particularly for high-speed small to mid-size ships, remains essential to prevent catastrophic outcomes like capsizing or structural damage in marine environments. Ensuring operational safety hinges on understanding and addressing the intricate interplay between wave forces, ship hydrodynamics, and directional stability during surf-riding events. The ships most likely to be affected by surf-riding are those moving at high speeds, such as fishing vessels, small passenger ships, recreational boats, and naval vessels, especially unmanned surface vehicles (USV). In an era where small autonomous drones capable of operating in all conditions are being developed rapidly, this research is crucial.

In regular following seas, there are limited response types:

- surging - oscillatory movement where the ship's velocity consistently increases and decreases with roughly equal acceleration and deceleration times;
- high-run - prolonged periods of increased speed followed by short, rapid drops in velocity (Themelis et al., 2016);
- surf-riding - when the ship accelerates due to wave forces until it reaches wave celerity, then maintains that speed in quasi-stationary motion;
- wave blocking - when the bow of the ship pushes into the waves in front of it, the ship roots and decelerates (Harold E. Saunders, 1965).

While asymmetrical deceleration to a speed close to wave celerity (low-run) is theoretically possible when the ship's commanded speed exceeds the wave celerity, this phenomenon is rarely significant in practice, though light boats with high-powered propulsion can achieve it (Warnke-Olewniczak and Krata, 2024).

The physics of surf-riding phenomena in irregular waves differs from the physics of surf-riding in regular seas. The consequence of irregularity of sea waves is the impossibility of achieving a balance of forces (an equilibrium) in any given time interval. For a balance of forces to be possible, the time interval would have to be zero seconds. Over a longer period, the low frequency wave components of irregular seas will always be ahead of the ship, while high frequency components will be overtaken by the ship. Hence, there is always a fluctuation in the force exerted by these waves in the longitudinal direction. This phenomenon means that ship navigation in irregular seas generates complex phenomena that remain largely unexplored in scientific literature.

For the sake of simplification of studying a ship response during sailing in irregular following seas, an imaginary case of sailing in bi-chromatic waves has been invented (Bulian and Francescutto, 2013; Spyrou et al., 2016, 2014). According to that idea, the first step towards understanding surf-riding in irregular seas is implementing a second wave component to the regular wave surf-riding case. Following this concept, this work focuses specifically on experimental research into the motion of a ship in bi-chromatic following seas.

1.2. State of the art

Since the dawn of sailing, this phenomenon of surf-riding has been observed, and in practice, sailors have tried to avoid it, often successfully. However, in those days, practical knowledge was not supported by scientific theories explaining the causes of surf-riding or broaching (Spyrou, 2010). Systematic studies of both broaching and surf-riding phenomena started from the mid-20th century (Davidson, 1948; Du Cane and Goodrich, 1962; Grim, 1951; Makov, 1969; Wahab and Swaan, 1964). The state of knowledge at that time is well summarized in a subsection from the textbook Hydrodynamics in ship design: "*A craft which can manage to maintain position on the advancing side of a long-crested wave travelling at about the same speed without encountering the steering difficulties to be described presently, is helped along appreciably* [in the context of an ocean regatta] *by the slope thrust exerted on it. To do this, however, requires excellent course-keeping characteristics and almost superlative skill on the part of the stern steersman* [...]. *Actually, the principal danger to a boat or ship running in following or overtaking seas is loss of directional control, considering again, the rudder at the stern, which are supposed to provide steering control, are now in a region of high wake due to the forward orbital velocity of the water particles in the adjacent crest. Wake components, due to potential flow to friction resistance, would, if considered, increase the forward particle velocity still more. Under these conditions, a rudder large enough for normal steering can become completely ineffective, because it can exert no lateral force at zero relative speed through the water. Unless*

the situation is saved by the presence of a propulsion device outflow jet steering past the rudder, steering control may be almost completely lost." (Harold E. Saunders, 1965).

Model tests by (Kan, 1990a, 1990b) were pivotal in the research of the surf-riding phenomena. Kan's work identified three critical regions of the considered ship speed: below the first critical speed, surf-riding never occurs (only periodic surging); between critical speed values, surf-riding depends on initial conditions; above the second critical speed, surf-riding is inevitable. Crucially, Kan proposed a practical, empirically grounded guideline to avoid surf-riding through precise identification of ship speed and wave height thresholds, a framework later validated by real-world applications. This empirical foundation directly facilitated the development of the currently standing theory of surf-riding and broaching in regular waves (Spyrou, 2017, 1997, 1996b, 1996a; Umeda, 1999).

The threat of surf-riding and its aftermath, broaching, was formally recognized by the International Maritime Organization through its 1995 Guidance to the Master for Avoiding Dangerous Situations in Following and Quartering Seas (IMO, 1995). This document, rooted in Umeda's (1990) theoretical analysis of surf-riding probability in irregular seas, has established the first operational thresholds for mitigating broaching risks. The application of the Melnikov method for establishing surf-riding threshold was established by Spyrou (2006), who developed a mathematical model incorporating propulsion, resistance, and hull characteristics to derive a closed-form analytical solution. The method's key advantage is providing a simplified formula for assessing broaching-to tendency under the assumption of small damping terms. The relevant recommendations were subsequently updated in the IMO's 2007 revised guidance (IMO, 2007), and later formalized into Level 1 vulnerability criteria within the Second Generation Intact Stability Criteria (IMO, 2020, 2023). These criteria explicitly integrate insights from Spyrou (2006), A. Maki et al. (2010), and Sakai et al. (2017), who demonstrated that surf-riding transitions to broaching via heteroclinic bifurcations in nonlinear ship dynamics. The small damping assumption for these transitions was rigorously justified by Wu et al. (2010) through extended Melnikov analysis, which overcame the traditional limitations of linear damping models. A comprehensive review of IMO-related works on surf-riding and broaching further contextualizes these developments (IMO, 2021). All of the aforementioned work was based on the results of surf-riding and broaching-to in regular waves research.

However, in irregular waves, the physics of surf-riding and broaching-to phenomena diverges significantly from that applicable within the regular wave theory. While regular wave models result in a stable equilibrium point where wave, propulsion, and resistance forces balance, irregular seas introduce stochastic variations in a wave shape and forces. This randomness causes the "balanced position" to move around over time, as an accelerating frame of reference. Spyrou et al. (2014) demonstrated that in such conditions, the absence of a fixed equilibrium renders traditional stability assessments obsolete. The resulting transient nature of surf-riding conditions implies that even in the brief window where theoretical thresholds might be met, the

phenomenon may not manifest due to the time-dependent acceleration of the quasi-equilibrium frame. This indeterministic behavior justifies the extensive global research effort highlighted by Belenky et al. (2016; 2019), which emphasizes the need for probabilistic rather than deterministic prediction tools.

Critical advances in irregular wave modeling emerged from free-running experiments conducted in following seas (Matsubara et al., 2023; Umeda et al., 2016). These studies employed Umeda's (1990) theoretical approach, using a deterministic surf-riding threshold and joint probability distributions of local wave heights and periods, to quantify surf-riding risk in real world conditions. The methodology revealed that surf-riding probability in irregular seas is not negligible, contrary to assumptions in regular wave theory, and depends on ship specific parameters like hull form and propulsion efficiency. Umeda's work further showed that minor reductions in propeller revolution rates can significantly lower surf-riding susceptibility, offering a practical control strategy for operators. Although these experiments were a milestone in surf-riding research, they did not fully explain the phenomenon. They approached it in probabilistic terms, focusing on the effects, i.e., the occurrence or non-occurrence of surf-riding. However, they did not analyze in depth the details of the phenomena accompanying surf-riding.

Spyrou's (1996a, 1996b, 1997) research provides a foundational nonlinear dynamical explanation for these phenomena on the theoretical ground. By applying state-space analysis to quartering waves, Spyrou identified surf-riding as a homoclinic event that triggers broaching. This work classified four distinct broaching mechanisms, mapped initial conditions for surf-riding and periodic motions, and demonstrated how roll instability cascades into capsize through heteroclinic transitions. Similarly, Umeda (1999) developed a 4 DOF model to prove that heteroclinic bifurcations in ship motion represent the critical transition to capsizing, a finding that directly informed the IMO's vulnerability criteria. These insights underscore that broaching is not merely a hydrodynamic failure but a nonlinear dynamical cascade rooted in phase-space topology.

The Melnikov-based analytical approaches further refine predictive capabilities. A. Maki et al. (2010) extended Melnikov's method using continuous piecewise linear approximations to derive explicit formulas for surf-riding thresholds, validated against experiments on the ONR Tumblehome vessel. Sakai et al. (2017) demonstrated that modeling propeller thrust as a quadratic polynomial allows analytical solutions for surf-riding thresholds via quadratic equations, eliminating the need for numerical iterations. Wu et al. (2010) advanced this framework by relaxing the small-damping constraint inherent in traditional Melnikov analysis, though their method required numerically optimized "best fit" approximations for practical use. Collectively, these methodologies bridge theoretical rigor and operational implementation, enabling precise threshold identification without excessive computational burden.

The IMO's MSC/Circ. 707 (IMO, 1995) (and its 2007 revision (IMO, 2007)) integrates these insights into actionable guidelines. It emphasizes that surf-riding risks escalate when ship speed approaches $1.8\sqrt{L}$ knots (L = ship length), with marginal zones ($1.4–1.8\sqrt{L}$ knots) posing

surging hazards. Crucially, the guidance acknowledges that wave group velocity effects, where a ship encounters successive high waves that double observed wave height, can accelerate broaching. Recent developments, such as Spyrou's (2017) review of homoclinic phenomena, further clarify that surging to broaching transitions are inherently non stationary and statistically rare, necessitating operational adjustments rather than design only solutions. This aligns with the need for dynamic, adaptive strategies in irregular seas (Margari and Spyrou, 2025a, 2025b).

Ultimately, the transition from regular to irregular wave regimes exposes a fundamental challenge: the absence of a universal equilibrium point. In irregular seas, surf-riding conditions become time dependent, probabilistic, and sensitive to minute perturbations. While Umeda's (1990) joint probability framework and Spyrou's (Spyrou et al., 2014) frame of reference analysis provides analytical tools to address this, practical implementation requires integrating real time sea state data with nonlinear dynamics models. The current research frontier, highlighted by Belenky et al. (2019), further stresses that surf-riding risk must be assessed not as a binary threshold but as a spectrum influenced by ship speed, wave spectra, and control systems. As naval architecture increasingly adopts nonlinear stability criteria (e.g., Level 2 vulnerability), the field must continue to leverage advances from Kan's empirical guidelines to Spyrou's homoclinic bifurcation theory, ensuring that future IMO recommendations and regulations evolve with scientific rigor and operational realism. The recalled here brief review of these multidisciplinary efforts underscores their collective role in transforming surf-riding from a historical concern into a quantifiable, preventable risk in modern maritime engineering. As can be seen in the world literature, significant progress has been made in research, but there is still a lack of full understanding of the phenomenon on an irregular wave, as it is only described statistically in the context of the end result, which is the ship entering surf-riding or not.

The next step in expanding our knowledge of surf-riding and understanding how it occurs in irregular waves was to introduce a second wave component to a regular wave. The result of this superposition is a bi-chromatic wave that can be defined using the parameters of two regular wave components and the phase shift between these components. Numerical experiments applying this concept with the implementation of a simple 1DOF motion model yielded intriguing results. Equations 2.1 to 2.4 present the mathematical model used by Spyrou, to predict phenomena occurring in surf-riding in bi-chromatic following waves (Spyrou et al., 2016). It is this model that I wish to validate or disprove in this study.

$$(m + A_{11})\ddot{\xi} + R(\dot{\xi}) - T(\dot{\xi}, n) = F_W(\xi, t) \quad (2.1)$$

$$R(\dot{\xi}) = r_1\dot{\xi} + r_2\dot{\xi}^2 + r_3\dot{\xi}^3 \quad (2.2)$$

$$T(\dot{\xi}, n) = \tau_0 n^2 + \tau_1 n\dot{\xi} + \tau_2\dot{\xi}^2 \quad (2.3)$$

$$F_W(\xi, t) = \sum_{i=1}^{N} F_{A_i} cos(k_i\xi - \omega_i t + \varphi_i + \gamma_i) \quad (2.4)$$

where:

m - mass of the ship [kg],
A_{11} - added mass in surge [kg]
ξ - longitudinal position of the center of gravity in the Earth-fixed coordinate system [m],
R - resistance [N],
T - thrust [N],
n - the propeller rate [$^1/_s$],
F_W - wave surging force [N],
t - time [s],
r_i - resistance coefficient [-],
τ_i - thrust coefficient [-],
F_{Ai} - wave force amplitude of wave component *i* [N],
k_i - wave number of wave component *i* [$^1/_m$],
ω_i - frequency of wave component *i* [$^1/_s$],
φ_i - phase of the surge wave force for wave component *i* [-],
γ_i - wave component *i* random phase [-].

In recent years, a classification of phenomena related to surf-riding in bi-chromatic following waves has been proposed by Warnke-Olewniczak & Krata (2024). This division is based on the fact that both components of the wave can act as attractors, and phenomena known from surf-riding in regular waves also occur in a modified form in the case of multi-chromatic waves. In this work, the primary wave is consistently defined as the slower component of the considered bi-chromatic wave, and the secondary wave as the faster component of that wave. Below eight categories of responses of a ship moving in a bi-chromatic following seas are listed (Warnke-Olewniczak and Krata, 2024):

- Beating oscillations in surge;
- High-runs on primary wave;
- Surf-riding on primary wave;
- Low-runs on primary wave;
- Surging due to attraction to secondary wave;
- High-runs on secondary wave;
- Surf-riding on secondary wave;
- Low-runs on secondary wave.

However, the categorization presented above may not yet fully cover the phenomena occurring in a bi-chromatic following seas, since the research work on that topic is still in progress. Furthermore, according to the discussed literature, it is expected on the theoretical front that the aforementioned phenomena may occur temporarily as oscillatory (Spyrou et al., 2018) or combined as hybrid (Tigkas and Spyrou, 2023).

In summary, the literature review on this subject reveal that theoretical works cover a wide range of studies, from ship behavior in regular waves and bi-chromatic waves thru statistical descriptions of ship response to description of forces resulting from sailing in fully irregular waves. However, in terms of experiments, a significantly narrower range of research has been carried out worldwide. A summary of relevant experiments published in the global literature is presented in Table 1.1. It is understandable given the high costs and enormous labor intensity of experiments involving a ship sailing on following waves. However, the limited number of experiments on irregular waves and the complete absence of experiments on bi-chromatic waves mean there is an opportunity to make a significant contribution to the global trend.

Table 1.1 Experimental works focused on the ship surf-riding phenomenon published to date

Type of experiment	Year	Testing facility	Country	Publication
free-running	1962	HSVA	Germany	(Du Cane and Goodrich, 1962)
free-running	1990	Ship Research Institute	Japan	(Kan, 1990a)
captive	1995	NRIFE	Japan	(N. Umeda et al., 1995)
free-running	1995	NRIFE	Japan	(Naoya Umeda et al., 1995)
free-running	1999	NRIFE	Japan	(Umeda et al., 1999)
free-running	2000	NRIFE	Japan	(Umeda and Hamamoto, 2000)
captive	2004	NRIFE	Japan	(Hashimoto et al., 2004)
captive	2008	NRIFE	Japan	(Umeda et al., 2008)
captive/static heel	2009	Osaka University	Japan	(Sadat Hosseini, 2009)
captive	2014	LHEEA	France	(Horel et al., 2014)
free-running	2014	Hokaido University	Japan	(Nakamura et al., 2014)
free-running	2017	CSSRC	China	(Gu Min et al., 2017)
free-running	2024	CSSRC	China	(Chu et al., 2024)

1.3. Knowledge gap identification

According to the contemporary knowledge related to the ship response to the encountered wave action in following seas, the surf-riding equilibrium becomes inherently dynamic and unstable in irregular wave conditions, unlike in regular waves, where the equilibrium is static. The quasi-equilibrium points in irregular seas shift continuously due to random fluctuations in wave forces, resulting in a frame of reference that is no longer inertial. This non-inertial acceleration causes the actual equilibrium to vanish, as the duration during which surf-riding conditions may persist is often insufficient to trigger full broaching or surf-riding events. Consequently, the indeterministic nature of these phenomena in irregular waves necessitates extensive global research efforts to characterize their behavior (Belenky et al., 2019, 2016).

The recent experimental advancements, such as free-running model studies in irregular following seas (Matsubara et al., 2023; Umeda et al., 2016), have further illuminated these challenges by aligning with theoretical methods for estimating surf-riding probability in irregular waves. These approaches employ deterministic surf-riding thresholds and joint probability distributions of local wave heights and periods, as originally proposed by Umeda (1990). They further demonstrated that the non-inertial frame arising from accelerating quasi-equilibrium points fundamentally alters wave celerity dynamics, reinforcing the need for probabilistic and dynamic frameworks to address the transient nature of ship-wave interactions in real-world conditions. This interdisciplinary convergence underscores the ongoing global effort to mitigate the risks associated with surf-riding and broaching in complex oceanic environments

The ship surf-riding still remains not fully explored nor understood phenomenon in ship hydrodynamics. Specifically, the actual response of a vessel sailing in bi-chromatic following wave conditions constitutes the identified knowledge gap, as the state-of-the-art theoretical predictions for the surf-riding occurrence, disappearance, or movement under bi-chromatic wave conditions have not yet been experimentally validated. Therefore, for the time being it is not fully clear whether the theoretically predicted ship behavior patterns result from the actual physics of the considered phenomena or rather from the features of the utilized differential equations 2.1 to 2.4, thus being only artifacts of those equations' solutions. The bi-chromatic waves serve here as the simplification of the irregular wave, which is modeled with just two components. Therefore, it may be considered as a handy intermediate representation between the regular and the fully irregular waves (Belenky et al., 2019, 2016; Spyrou et al., 2016). Analytical and numerical studies demonstrate that the interference of these two wave components is sufficient to trigger surf-riding conditions in ship responses, yet this phenomenon has never been observed in physical experiments. This unresolved gap motivated the research at Gdańsk Tech to investigate whether experimental results align with predictions from a simplified 1-DoF model adopting the linear Froude-Krylov theory (Spyrou, 1996b).

The consideration of the bi-chromatic waves provides the framework for understanding ship responses in following wave environments, as extensively explored by recent theoretical studies (Spyrou et al., 2018, 2016; Tigkas and Spyrou, 2023, 2021). Those investigations have yielded critical insights into the phenomena such as ship velocity oscillations during surging motions, where the ship rides with the velocity of one wave component while experiencing oscillatory behavior from the other. It is of note that such a comprehensive understanding must be contextualized against the complexities of irregular waves, where the physics of surf-riding and broaching phenomena diverges significantly from the regular wave regime. Therefore, first the experimental insight into the ship response to the simplest possible wave mimicking the physics of the fully irregular wave conditions, remains utmost essential.

1.4. Research questions

In order to address the identified research gap, this dissertation poses four research questions:

- Are the surf-riding experiments feasible in bi-chromatic following wave conditions?
- Do phenomena observed in recent numerical studies actually occur in physical experiments? Can the theoretical predictions be confirmed by the experiment, if so, only qualitatively or also quantitatively?
- Can experiments in following seas conditions be conducted in a short 40 meters towing tank?
- Can surf-riding experiments be considered scalable?

1.5. Aim and scope of the study

Considering all four formulated research questions, the main objective of this work remaining of the greatest scientific significance is to acquire results from the towing tank experiments directed to surf-riding in bi-chromatic following seas, for the sake of comparison of the theoretical predictions. Thus, thru this study the aim is to proof or deny the standing recent theory of the surf-riding phenomenon, including recreating eight predicted response types described by Warnke-Olewniczak & Krata (2024).

Additional objectives were to determine how to conduct such experiments and to ascertain whether the short towing tank available at Gdańsk Tech is sufficient to obtain meaningful qualitative results, and what is the quantitative difference in experiments conducted at the scale of 1/14 and 1/64.

The scope of this work includes:

- Experiments conducted at a scale of 1/64 in regular and bi-chromatic following waves;
- Experiments conducted at a scale of 1/14 in regular and bi-chromatic following waves;
- Comparison of experimental results: 1/64 vs. 1/14 scale;
- Comparison of experimental and theoretical results obtained for corresponding conditions.

1.6. Thesis structure

The remainder of this dissertation is organized as follows: Chapter 2 details the experimental methodology, including the ship model, towing tanks, and measurement systems, with specific focus on calm-water resistance tests, regular and bi-chromatic wave experiments conducted in 1/64 and 1/14 scale. Chapter 3 presents the comprehensive results organized by

experiment type and scale, while Chapter 4 critically discusses findings, comparing scale-dependent outcomes, quantifying uncertainties, and identifying limitations of experiments conducted. The conclusion synthesizes key insights and implications, demonstrating how this work addresses the initial knowledge gap through the conducted systematic experimental study.

This page was intentionally left blank.

2. MATERIALS & METHODS

2.1. Experimental setup

2.1.1. *The ship - A2 ITTC purse-seiner*

The ships used in the experiment were free-running models of the ITTC A2 purse-seiner (e.g., Umeda et al., 1995), additionally equipped with a “cruise control” system for the purpose of maintenance of constant setting of the shaft revolutions. Geometry used for manufacturing of the hulls is shown in Figure 2.1.

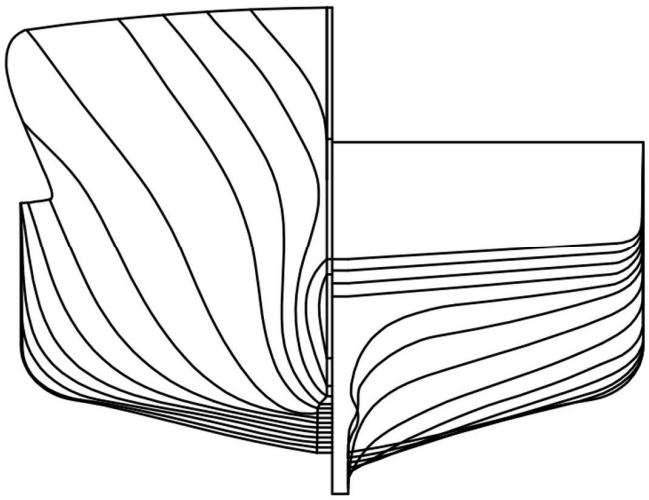

Figure 2.1 Lines plan of the ship model i.e. the ITTC A2 purse-seiner

The shape of two hulls was CNC milled in negative to achieve as close as possible similarity between the digital and physical models. As the ship models were intended to use in experiments in two towing tanks of significantly different length, two ship models were manufactured in corresponding scale, i.e. 1/64 and 1/14. Both hulls are made of glass fiber epoxy composite using vacuum lamination process. The hulls are covered with a putty, then sanded for the sake of the surface smoothness, and finally coated with a polyurethane paint. The deck of the 1/64 scale model was built with a glass fiber epoxy composite; while the deck of 1/14 scale model was made of ABS plastic with additional bulwarks welded on top.

The specification of the models shown in Figure 2.2 and Figure 2.3 are listed in Table 2.1.

Table 2.1 The principal dimensions and mass of the ship models

Shown in	Scale of the model	L_{BP} [m]	L_{OA} [m]	B [m]	d [m]	m [kg]
Figure 2.2	1/64	0.54	0.64	0.12	0.04	1.58
Figure 2.3	1/14	2.51	2.93	0.55	0.17	151.2

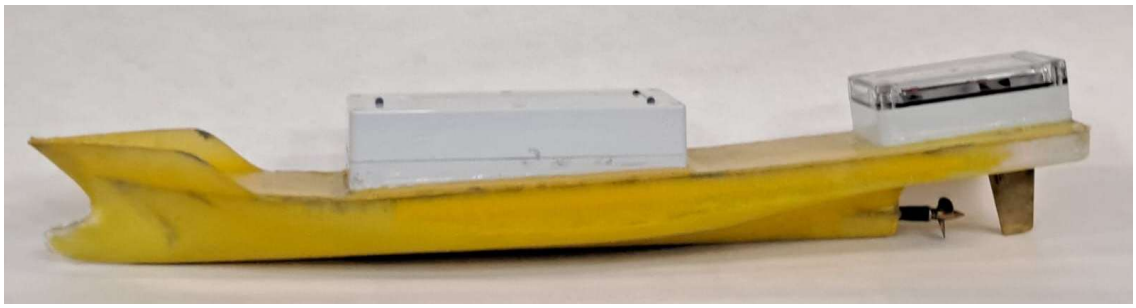

Figure 2.2 Radio-controlled self-propelled model of the ITTC A2 purse-seiner manufactured in 1/64 scale

Figure 2.3 Radio-controlled self-propelled model of the ITTC A2 purse-seiner manufactured in 1/14 scale

2.1.2. *Towing tanks*

Throughout the course of the experiments, two towing tanks were facilitated. Both of them are located in Gdańsk, Poland. First of them is the relatively short towing tank available at Gdańsk Tech. The characteristics of this facility are as follows (ITTC, 2025):

- length 40 m,
- width 4 m,
- depth 3 m,
- maximum carriage speed 2.5 m/s,
- plate type electrically driven, 8 segmented wave generator;
- equipped with Qualisys optical motion tracking system.

The second towing tank used in this study is at Maritime Advanced Research Centre, from now on, it will be referred to as CTO, from its Polish abbreviation (Centrum Techniki Okrętowej). The main characteristics of this facility, which is significantly longer, are as follows (ITTC, 2025):

- length 270 m,
- width 12 m,
- depth 6 m,
- maximum carriage speed 12 m/s,
- flap-type hydraulically driven wave generator,
- equipped with Qualisys optical motion tracking system.

Both facilities have the ability to control and record the speed of the carriage. However, in the CTO towing tank that speed varied over time since it was manually controlled by the technician in order to adjust to the instantaneous speed of the ship model. Such precautions were made due to the need for keeping the model within the Qualisys cameras field of operation.

The time allocated to measurements in the CTO towing tank was significantly constrained to only two weeks due to the schedule of the project and related financial limits. At the Gdańsk Tech towing tank, the access to the laboratory was limited only by other ongoing tasks between 7am and 3pm Monday to Friday. During the course of the work, the author was able to adapt the lab to accommodate a one-person handling of the experiment, which greatly facilitated research outside of typical working hours.

2.1.3.*Measurement systems*

The ship models position at both towing tanks were measured using Qualisys system. The system developer describes that system as follows: "*Qualisys Track Manager is a Windows-based data acquisition software with an interface that allows the user to perform 2D and 3D motion capture. QTM is designed to provide both advanced features required by technically advanced users and a simple method of application for the inexperienced user. Together with the Qualisys line of optical measurement hardware, QTM will streamline the coordination of all features in a sophisticated motion capture system and provide the possibility of rapid production of distinct and accurate 3D, 2D and 6D data. During the capture, real time 3D, 2D and 6D information is displayed allowing instant confirmation of accurate data acquisition. The individual 2D camera data is quickly processed and converted into 3D or 6D data by advanced algorithms, which are adaptable to different movement characteristics. The data can then be exported to analysis software via several external formats."*(Qualisys AB, 2013). Data acquired by Qualisys was combined with measurements from the towing tank carriage speed encoders to archive global speed of tested ship models.

A method of measurement between two used models differs in two aspects. Firstly, in the 1/14 scale model passive markers were used as seen in Figure 2.4 (grey reflective spheres), while in the 1/64 scale model I manufactured "inactivated active markers" (Qualisys AB, 2013), in a form of 3 infrared emitters mounted on top of the models' electronics box as seen in Figure 2.5. Secondly, additional passive markers on a rod were placed near the stern of the 1/14 scale model to track rudder angle.

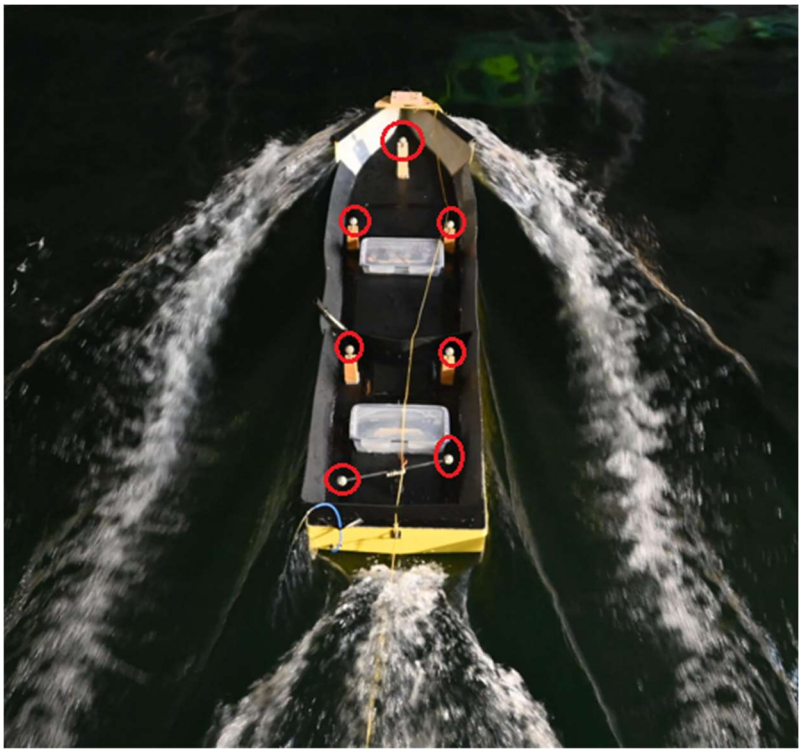

Figure 2.4 1/14 scale model with the passive markers marked with red circles

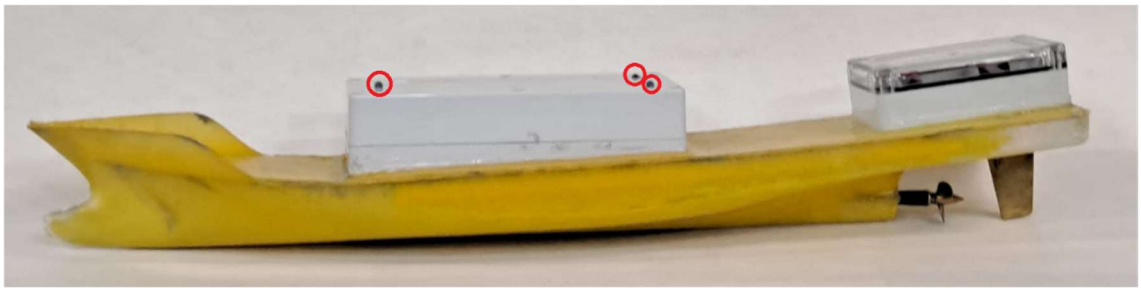

Figure 2.5 1/64 scale model with the 'inactive passive markers' marked with red circles

2.2. Experimental method

The experiment itself should produce repeatable results demonstrating phenomena that are already known in regular waves, and enable the experiment to be carried out in bi-chromatic waves, making it feasible. A method designed like this should enable the observation of phenomena related to sailing in bi-chromatic following seas and lead to a conclusion as to whether the theoretical predictions are true. To determine the qualitative and quantitative accuracy of the predictions, the experimental and numerical results must be cross-referenced. The possibility of conducting the following sea experiment should be assessed by observing the number of encounters and evaluating whether the resulting velocity graph is periodic, i.e., whether the oscillations appear to be indefinite. The scalability of the experiment should be determined by directly comparing two experiments conducted with the same methodology and assumptions, but with different scales.

One approach could be to run a large set of regular wave experiments and then try to approximate the response based on these results. However, approximating irregular wave

segments to the most similar regular wave is not simple. In order to visualize the problem, the Figures 2.6 thru 2.8 show the shapes of the following bi-chromatic encounter wave with the instantaneous amplitude and celerity plotted based on the analysis of local extremes and zero crossings, assuming a constant forward speed of the ship. In addition, matching the wave amplitude and celerity would be insufficient to determine the ship's response; its position on the wave, instantaneous speed, and acceleration would also be needed.

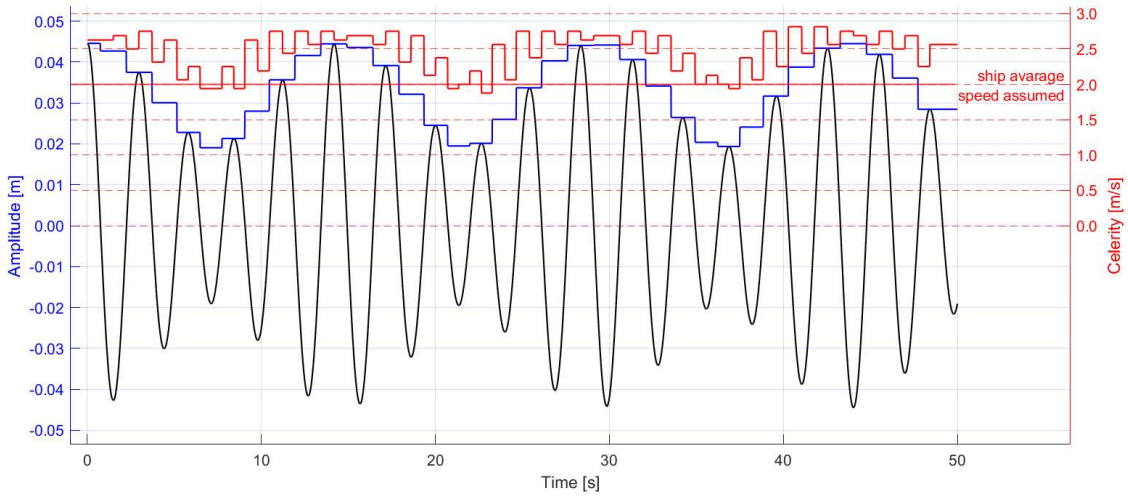

Figure 2.6 Bi-chromatic wave generated with the wave measurement results observed from the ship moving with constant speed; Case B119, f_1/f_2=1.24, A_1/A_2=2.48

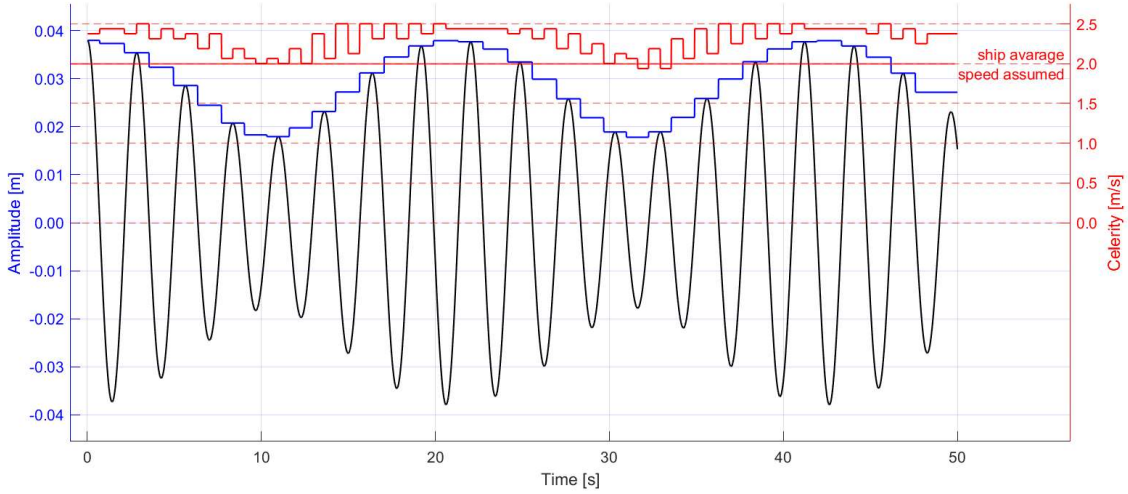

Figure 2.7 Bi-chromatic wave generated with the wave measurement results observed from the ship moving with constant speed; Case B94, f_1/f_2=1.15, A_1/A_2=2.76

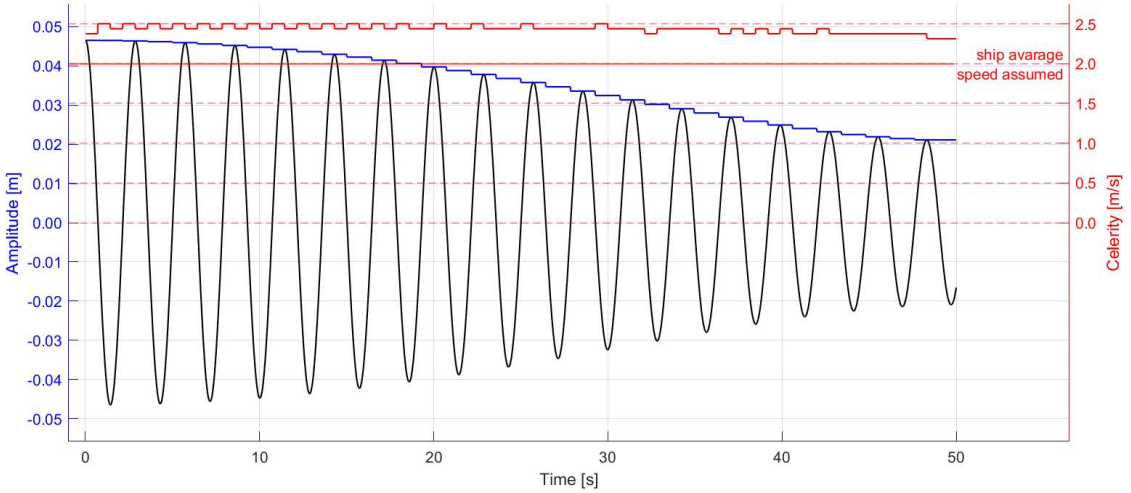

Figure 2.8 Bi-chromatic wave generated with the wave measurement results observed from the ship moving with constant speed; Case B100, f_1/f_2=1.03, A_1/A_2=2.63

Maintaining speed and acceleration when transitioning from one regular wave to another using the technique of approximating a bi-chromatic wave with a set of regular waves is simply unphysical. The inertia of a real-world ship would never allow for sudden changes in acceleration. In reality, acceleration and velocity values are continuous and do not change abruptly, as can be seen in Figure 2.9, which shows a phase-space diagram of the results acquired using the wave shown in Figure 2.7.

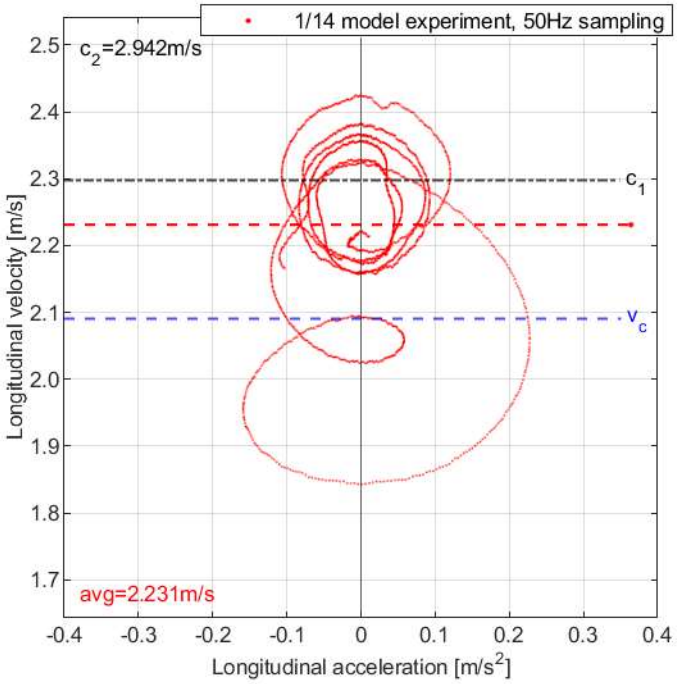

Figure 2.9 Case No. B94 Phase-space diagram; Bi-chromatic wave λ_1=3.378m; A_1=0.028m; λ_2=5.540m; A_2=0.010m; v_c=2.091m/s; T_{E1}=51.08s; T_{E2}=7.795s

The method of running an unattached, self-propelled, radio-controlled model that sails in multi-chromatic seas was designed to overcome the unphysical nature of the 'approximating by regular waves' method. The experimental work conducted in this research applies this method,

whereby the position of the ship is measured over time as it sails in following waves under specific conditions. This enables an instantaneous velocity versus time calculation.

In practice, each experimental run proceeded in the following steps:

1. Entering the run parameters in all devices.
2. Placing the ship model near the wave generator in the towing tank.
3. Starting all the measuring devices.
4. Starting the wave generator and waiting long enough so that the ship model does not overtake the wave front during the experiment.
5. Starting the towing tank carriage and the ship model.
6. Conducting the run.
7. Stopping the devices and the wave generator.

For the sake of clarity, three different prefixes were used to organize the runs in the different experiments:

- A (A1, A2, A3 etc,) – experiment conducted at Gdańsk Tech towing tank using the 1/64 scale model ship, results are presented in model scale;
- B (B1, B2, B3 etc,) – experiment conducted at CTO towing tank using the 1/14 scale model ship, results are presented in model scale;
- C (C1, C2, C3 etc,) – comparison cases of experiment conducted at Gdańsk Tech towing tank using the 1/64 scale model ship and experiments conducted at CTO towing tank using the 1/14 scale model ship, results are presented in 1/64 model scale.

The cases are numbered in chronological order; therefore, it may seem chaotic occasionally. However, renumbering all the cases could lead to mistakes during postprocessing and reporting. Therefore, I decided to keep the numbering as being more convenient for me. This, does not affect the reported results by no means.

2.2.1. *Measurements of ship motion*

The main measurements were taken with the Qualisys system. The process of tracking identified 3D trajectories of markers using 2D data (Qualisys AB, 2013). The markers were placed around the deck of each model. The model's position captured by the Qualisys system was combined with the known speed of the towing tank carriage in order to obtain the forward speed of the ship model in time in global coordinates of the towing tank. Four Qualisys cameras positioned at different angles are shown in Figure 2.10.

Figure 2.10 Gdańsk Tech Towing Tank with QualiSys cameras fitted on carriage

Thru all the experiments, the methodology was the same. A visualization of the experimental setup in the Gdańsk Tech towing tank is shown in Figure 2.11. In the aforementioned visualization can be seen a wave generator in red, a yellow trolley with Qualisys cameras mounted on top and a yellow model moving in following seas towards the towing tank carriage. For the CTO towing tank, the experimental setup differed only with respect to the model location since it sailed in front of the moving carriage, which followed.

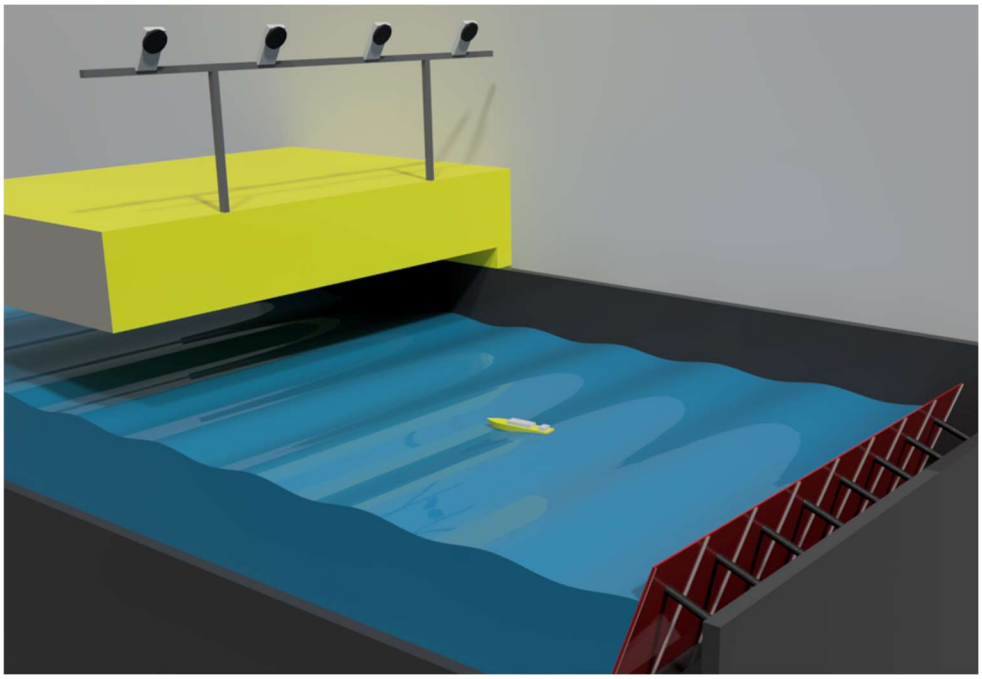

Figure 2.11 Visualization of the experimental setup in the Gdańsk Tech towing tank

2.2.2. *Calm water tests – resistance and propulsion*

The resistance of each hull was measured as a function of speed using a dynamometer. During these measurements, the propeller was replaced with a sleeve. The thrust was measured

as the longitudinal force on a dynamometer mounted in the hull as a function of forward speed and the propeller revolutions. The hull resistance corresponding to the forward speed was subtracted from this measurement resulting in the thrust matrix.

Another one of the parameters set in the experiment is the commanded speed of the model, which is meant to be the speed that the ship model maintains in calm water at a given propulsion setting. To determine the value of the commanded speed as a function of the motor setting, a series of speed measurements were carried out on calm water for each model. The Figure 2.12 shows a frame from the typical calibration recording. The ship position was tracked while the speed setting remained constant. By converting position record to velocity and averaging the results, we determined the commanded speed on calm water. This procedure was repeated whenever thrust or resistance characteristics might have changed.

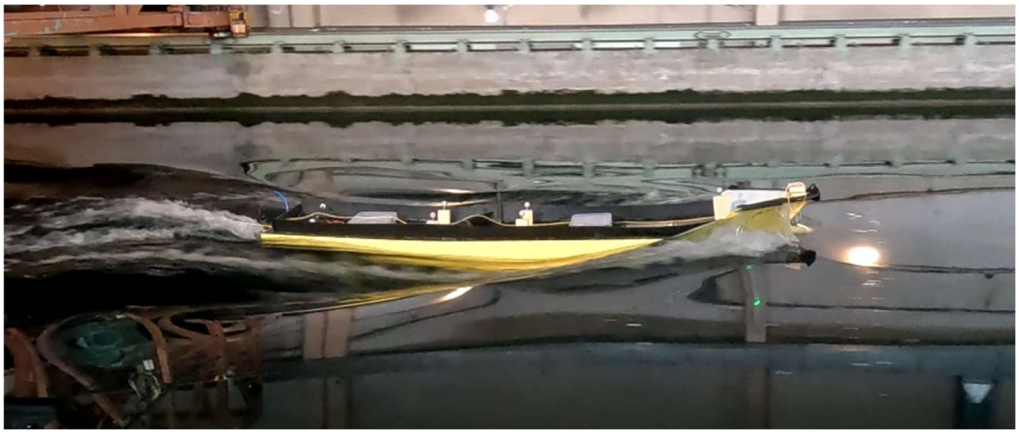

Figure 2.12 Frame of the recording of the calm water speed calibration in the CTO towing tank

With this data it was possible to pick as close as possible throttle setting to the assumed commanded speed. In addition, to provide data for the simulation work, resistance as a function of speed and thrust as a function of velocity and shaft revolutions were determined.

2.2.3.*Experiments in regular wave conditions*

The following part of the experiment was conducted as a proof of feasibility of the experimental setup. Since the behavior of a ship on regular waves is known and predictable, it can be determined whether the results align with the established theory. Attention was drawn to the occurrence of three characteristic ship responses (surging, high-runs, surf-riding) and the surf-riding velocity threshold. These experiments were carried out in regular following waves, while the ship model commanded speed was kept constant. An instantaneous velocity vs time measurement was acquired. The cases presented in the text of this dissertation are shown in Table 2.2, while the remaining cases shown only in Appendix A and Appendix B are presented in Table 2.3.

Table 2.2 Regular wave cases presented in results section

Case No.	f [Hz]	A [cm]	λ [m]	c [m/s]	v_c [m/s]
A10	1.50	1.00	0.694	1.041	0.756
A11	1.50	1.00	0.694	1.041	0.847
A12	1.50	1.00	0.694	1.041	0.907
A13	1.50	1.00	0.694	1.041	0.934
A14	1.50	1.00	0.694	1.041	0.960
A15	1.50	1.00	0.694	1.041	1.006
B78	0.641	2.92	3.802	2.437	2.074
B79	0.641	2.99	3.802	2.437	2.108
B80	0.641	2.98	3.802	2.437	2.126
B82	0.641	2.99	3.802	2.437	2.161
B87	0.641	3.04	3.802	2.437	2.161
B88	0.641	3.11	3.802	2.437	2.178

Table 2.3 Regular wave cases presented only in Appendix A and Appendix B

Case No.	f [Hz]	A [cm]	λ [m]	c [m/s]	v_c [m/s]
B11	0.734	2.11	2.899	2.128	1.915
B12	0.734	2.47	2.899	2.128	1.996
B13	0.641	1.87	3.802	2.437	1.815
B14	0.641	1.88	3.802	2.437	1.915
B15	0.641	1.85	3.802	2.437	1.996
B16	0.641	1.93	3.802	2.437	2.074
B17	0.641	1.99	3.802	2.437	2.161
B81	0.641	3.48	3.802	2.437	2.143
B91	0.641	2.12	3.802	2.437	2.196
B92	0.641	2.07	3.802	2.437	2.215
B154	0.641	3.38	3.802	2.437	2.178

2.2.4. *Experiments in bi-chromatic wave conditions*

Unlike the experiments with regular waves, where results are predictable and prediction methods have been validated, the results from bi-chromatic wave experiments couldn't be cross-referenced. This is the main focus of the study. It consists of experiments conducted at a 1/64 scale at Gdańsk Tech towing tank and at a 1/14 scale at CTO towing tanks using bi-chromatic following waves. The experimental work conducted in part of the study involves running the ship model through waves under specific conditions in order to measure its position over time, which enables an instantaneous velocity vs time calculation. This corresponds to the predictions that can be made using the mathematical model of the ship's response. Due to the use of numerical modeling results, these studies should be referred to as simulation-guided experiments. Therefore, it was feasible to make direct comparisons between the experimental outcome and the outcome of the calculations, which was made for the 1/64 scale model ship experiment (Warnke-Olewniczak and Krata, 2024) for parameter set as shown in Table 2.4. This purpose

required arranging a relevant experimental setup and preparing the testing procedures, as well as predefining a set of scenarios for the examination.

Table 2.4 Bi-chromatic wave cases conducted at a scale of 1/64

Case No.	A_1 [cm]	λ_1 [m]	c_1 [m/s]	A_2 [cm]	λ_2 [m]	c_2 [m/s]	v_c [m/s]
A1	0.80	0.560	0.935	1.00	0.694	1.041	0.743
A2	0.80	0.560	0.935	1.00	0.694	1.041	0.847
A3	1.60	0.560	0.935	0.80	1.562	1.562	0.847
A4	1.60	0.560	0.935	0.80	1.562	1.562	1.020
A5	0.80	0.560	0.935	3.90	1.562	1.562	1.124
A6	1.00	0.560	0.935	6.00	1.562	1.562	0.960
A7	0.80	0.560	0.935	2.60	1.050	1.280	1.020
A8	0.80	0.560	0.935	0.40	0.753	1.085	1.124
A9	1.00	0.560	0.935	3.50	1.562	1.562	1.034

Cases conducted in bi-chromatic following seas at a 1/14 scale are presented as four separate experiments with different goals in mind. The cases shown in Table 2.5 are selected to analyze what happens when the commanded speed is changed for the three different bi-chromatic waves. Table 2.6 shows cases used to determine the influence of the secondary wave amplitude on the ship's response type. In those cases, the commanded speed was first determined experimentally by establishing the surf-riding threshold for the primary wave. Three waves with different frequencies and increasing amplitude with each successive cycle were used as the secondary waves, while the primary wave remained unchanged. The cases presented in Table 2.7 were used to estimate the sensitivity of the phenomenon to a slight change in the specified parameters. Table 2.8 presents the cases used to analyze repeatability of the results and how the ship’s response changes when the ship commanded speed is changed; the wave parameters were not changed between these cases.

Table 2.5 The bi-chromatic wave cases conducted at a scale of 1/14 with varying commanded speeds

Case No.	A_1 [cm]	λ_1 [m]	c_1 [m/s]	A_2 [cm]	λ_2 [m]	c_2 [m/s]	v_c [m/s]
B29	2.97	2.899	2.128	1.88	7.102	3.331	1.638
B30	2.97	2.899	2.128	1.85	7.102	3.331	1.703
B31	2.96	2.899	2.128	1.98	7.102	3.331	1.879
B38	3.11	2.777	2.083	2.17	7.102	3.331	1.996
B40	2.01	2.899	2.128	1.39	3.300	2.270	1.557
B41	2.08	2.899	2.128	1.84	3.300	2.270	1.638
B42	2.07	2.899	2.128	1.82	3.300	2.270	1.759
B43	1.81	2.899	2.128	1.45	3.300	2.270	1.815
B44	2.08	2.899	2.128	1.75	3.300	2.270	1.860
B45	1.99	2.899	2.128	1.41	3.300	2.270	1.996
B47	2.27	2.899	2.128	0.92	4.676	2.703	1.557
B48	2.91	2.837	2.105	0.77	4.676	2.703	1.703
B49	2.61	2.899	2.128	0.88	4.676	2.703	1.897

Table 2.6 The bi-chromatic wave cases conducted at a scale of 1/14 with varying secondary wave amplitude

Case No.	A_1 [cm]	λ_1 [m]	c_1 [m/s]	A_2 [cm]	λ_2 [m]	c_2 [m/s]	v_c [m/s]
B99	2.51	3.802	2.437	0.74	4.212	2.565	2.178
B129	3.22	3.802	2.437	0.99	4.212	2.565	2.178
B102	2.61	3.802	2.437	1.08	4.212	2.565	2.178
B124	3.40	3.802	2.437	0.96	4.212	2.565	2.178
B104	3.16	3.802	2.437	1.62	4.212	2.565	2.178
B132	3.20	3.802	2.437	0.62	5.867	3.027	2.178
B106	3.05	3.802	2.437	0.81	5.867	3.027	2.178
B137	3.21	3.802	2.437	0.79	5.867	3.027	2.178
B108	3.06	3.802	2.437	1.06	5.867	3.027	2.178
B121	3.14	3.802	2.437	1.46	5.867	3.027	2.178
B110	3.19	3.802	2.437	1.63	5.867	3.027	2.178
B139	3.11	3.802	2.437	0.63	7.888	3.510	2.178
B112	3.15	3.802	2.437	0.74	7.888	3.510	2.178
B135	3.06	3.802	2.437	0.94	7.888	3.510	2.178
B114	3.15	3.802	2.437	1.09	7.888	3.510	2.178
B119	3.18	3.802	2.437	1.28	7.888	3.510	2.178
B117	3.04	3.802	2.437	1.49	7.888	3.510	2.178

Table 2.7 The bi-chromatic wave cases conducted at a scale of 1/14 conducted in similar conditions

Case No.	A_1 [cm]	λ_1 [m]	c_1 [m/s]	A_2 [cm]	λ_2 [m]	c_2 [m/s]	v_c [m/s]
B175	0.94	2.837	2.105	4.50	3.090	2.197	1.839
B176	0.81	2.837	2.105	4.23	3.090	2.197	1.915
B177	0.50	2.837	2.105	4.56	3.090	2.197	1.915

Table 2.8 The bi-chromatic wave cases conducted at a scale of 1/14 with varying commanded speeds while keeping the same wave conditions

Case No.	A_1 [cm]	λ_1 [m]	c_1 [m/s]	A_2 [cm]	λ_2 [m]	c_2 [m/s]	v_c [m/s]
B183	0.94	2.956	2.149	4.92	3.300	2.270	1.980
B184	0.92	2.956	2.149	5.07	3.300	2.270	1.980
B185	0.61	2.956	2.149	4.99	3.300	2.270	1.915
B186	0.90	2.956	2.149	4.88	3.300	2.270	1.915
B187	0.67	2.956	2.149	4.98	3.300	2.270	1.915
B188	0.58	2.956	2.149	5.04	3.300	2.270	1.839
B189	0.85	2.956	2.149	5.08	3.300	2.270	1.839
B190	0.69	2.956	2.149	5.10	3.300	2.270	1.730
B191	0.84	2.956	2.149	5.04	3.300	2.270	1.730

All cases conducted at a scale of 1/14 are listed in Appendix A.

2.2.5. *Comparative evaluation of the scale effect*

This section presents the cases used for comparative analysis of two similar experiments conducted at different scales. Two sets of parameters were examined to assess feasibility across scales. All dimensions were scaled linearly, and square root scaling was applied to time. The Froude number was kept constant, but it was not possible to maintain the Reynolds number. The cases conducted in this part of the study are listed in Table 2.9.

Table 2.9 Cases used in comparison of the 1/14 and the 1/64 scale ship experiments

Case No.	A_1 [cm]	λ_1 [m]	c_1 [m/s]	A_2 [cm]	λ_2 [m]	c_2 [m/s]	v_c [m/s]
C1	0.57	0.875	1.169	0.42	1.781	1.668	1.02
C2	0.65	0.832	1.140	0.32	1.726	1.642	1.02
C3	0.13	0.621	0.985	1.00	0.676	1.028	0.86
C4	0.19	0.621	0.985	0.96	0.676	1.028	0.86
C5	0.21	0.621	0.985	0.98	0.676	1.028	0.86
C6	0.21	0.647	1.005	0.97	0.722	1.062	0.93
C7	0.13	0.647	1.005	1.09	0.722	1.062	0.93
C8	0.21	0.647	1.005	1.08	0.722	1.062	0.93
C9	0.13	0.647	1.005	1.09	0.722	1.062	0.90
C10	0.20	0.647	1.005	1.07	0.722	1.062	0.90
C11	0.13	0.647	1.005	1.10	0.722	1.062	0.86
C12	0.19	0.647	1.005	1.11	0.722	1.062	0.86
C13	0.15	0.647	1.005	1.12	0.722	1.062	0.81
C14	0.18	0.647	1.005	1.10	0.722	1.062	0.81

This page was intentionally left blank.

3. RESULTS

This chapter presents the results obtained in all experimental campaigns. In accordance with the research method described in Chapter 0, individual parts of the research were carried out according to the assumed scenarios. For certainty, some cases were examined 2-3 times, but it was not possible to repeat each scenario multiple times due to practical limitations in terms of time and budget.

The results are presented in individual subsections in the order in which the experiments were described in Chapter 0, which presents the method used. For the sake of clarity and fluidity of the text, the results of the 1/14 scale experiment obtained for selected cases are presented graphically, while the complete set of results is documented and presented in Appendix B.

3.1. Results of calm water experiments

3.1.1. *Results of calm water experiment at a scale of 1/64*

In accordance with the method described in the Chapter 2.2.2, a series of measurements was carried out for the 1/64 scale model in the Gdańsk Tech towing tank. The thrust and resistance results for the 1/64 scale model are shown in Table 3.1, the results of the commanded speed measurements of the same ship model are shown in Table 3.2.

Table 3.1 Thrust and resistance of the 1/64 scale ship model

Carriage speed [m/s]	Speed setting [-]						Resistance [N]
	10	20	30	35	40	50	
	Thrust [N]						
0.7	0	0.27	0.74	-	-	-	0.21
0.9	-	0.23	0.69	1.03	1.36	-	0.50
1	-	-	0.67	0.95	1.32	2.19	0.77
1.1	-	-	0.59	0.89	1.25	2.09	1.05
1.3	-	-	-	0.79	1.14	2.03	1.51

Table 3.2 Results of commanded speed measurements for the 1/64 scale model ship

Throttle setting [-]	Measured commanded speed [m/s]
20	0.731
30	0.946
35	1.013
40	1.095
45	1.165
50	1.313

3.1.2. *Results of calm water experiment at a scale of 1/14*

Following the same method as for the 1/64 scale model, a series of measurements was carried out for the 1/14 scale model in the CTO towing tank. The thrust and resistance results for the 1/14 scale model are shown in Table 3.3, the results of commanded speed measurements for the same ship model are shown in Table 3.4.

Table 3.3 Thrust and resistance of the 1/14 scale ship model

Carriage speed [m/s]	Speed setting [-]						Resistance [N]
	20	40	60	70	80	90	
	Thrust [N]						
1	-0.75	12.47	45.34	69.85	-	-	5.60
1.4	-5.23	6.66	36.42	59.76	88.27	-	13.28
1.6	-	4.40	30.67	51.89	78.48	-	23.57
1.8	-	-	27.18	50.00	76.83	106.16	35.70
1.9	-	-	24.84	47.17	72.30	103.97	43.00
2	-	-	-	43.52	69.76	100.47	53.42
2.1	-	-	-	-	68.77	94.29	65.44
2.2	-	-	-	-	66.27	91.55	85.38

Table 3.4 Results of commanded speed measurements for the 1/14 scale ship model

Throttle setting [-]	Measured commanded speed [m/s]
20	0.581
40	1.256
50	1.455
60	1.678
70	1.915
80	2.074
90	2.245
100	2.306

The results of thrust and resistance were obtained for both models and served as the input data for case preselection. The speed versus throttle setting curve was necessary for further experiments and was used to set the commanded speed. This is a key input parameter for all wave tests, both regular and irregular. Therefore, the model operator must know which throttle setting to use to match a specific commanded speed value.

3.2. Results of regular wave experiments

The following part of the experiment was conducted as a proof of feasibility of the experimental setup. Due to the fact that the basis for classification of the ship response mode when surf-riding is the instantaneous speed developing in the time domain, the data presented on the graphs consists of the model's longitudinal velocity versus time. In case of the 1/64 model, it is marked as a bold blue line, and in case of the 1/14 model as a bold red line, while the commanded speed v_c (dashed green line), the regular wave celerity c (dashed black dotted line) and the average speed of the ship model marked with dashed line same color as velocity plot.

3.2.1. *Results of regular wave experiment at a scale of 1/64*

Figure 3.1 thru Figure 3.6 present the results of the runs conducted in regular waves with the amplitude of A=0.010 m, the length of λ=0.694 m, thus the corresponding celerity of c=1.041 m/s. The ship model commanded speed was set according to the scenarios shown in Table 2.2.

Figure 3.1 reveals regular, symmetric surging with the commanded speed set to v_c=0.756 m/s, and the average velocity very close to the calm water speed. While increasing the commanded speed to v_c=0.847 m/s, as demonstrated in Figure 3.2, surging becomes asymmetric. However, the attraction to the wave celerity does not noticeably influence the average speed, as it remains close to the commanded speed.

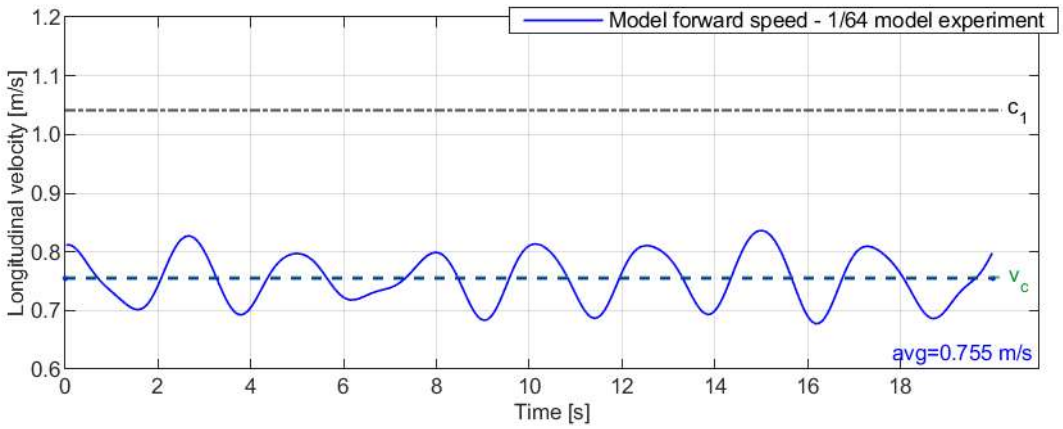

Figure 3.1 Case No. A10 Regular wave; λ=0.694m; c=1.041m/s; A=0.010m; v_c=0.756m/s; Surging

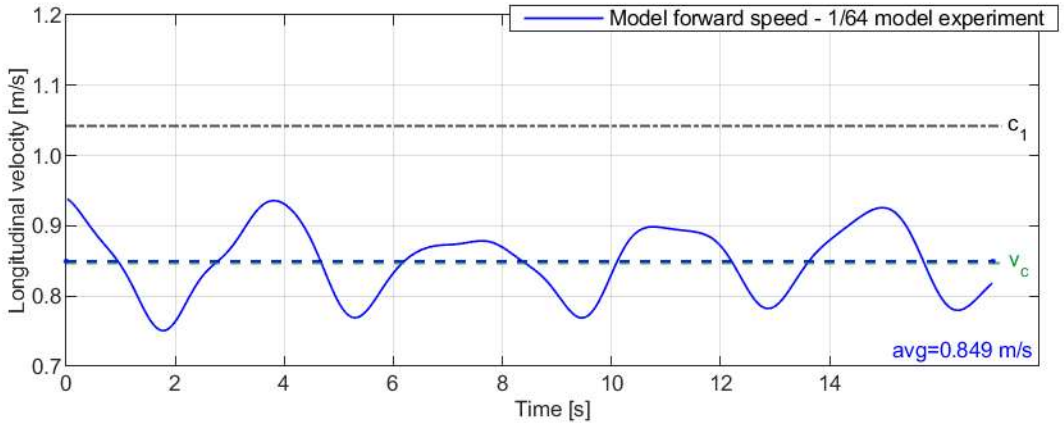

Figure 3.2 Case No. A11 Regular wave; λ=0.694m; c=1.041m/s; A=0.010m; v_c=0.847m/s; Asymmetric surging

A significant attraction to surf-riding conditions has become visible in Figure 3.3 and Figure 3.4, while the commanded speeds were increased to v_c=0.907 m/s and then up to v_c=0.934 m/s. As a result, not only the instances of higher velocity response lasted longer, but also the average speed noticeably increased above the value of the commanded speed.

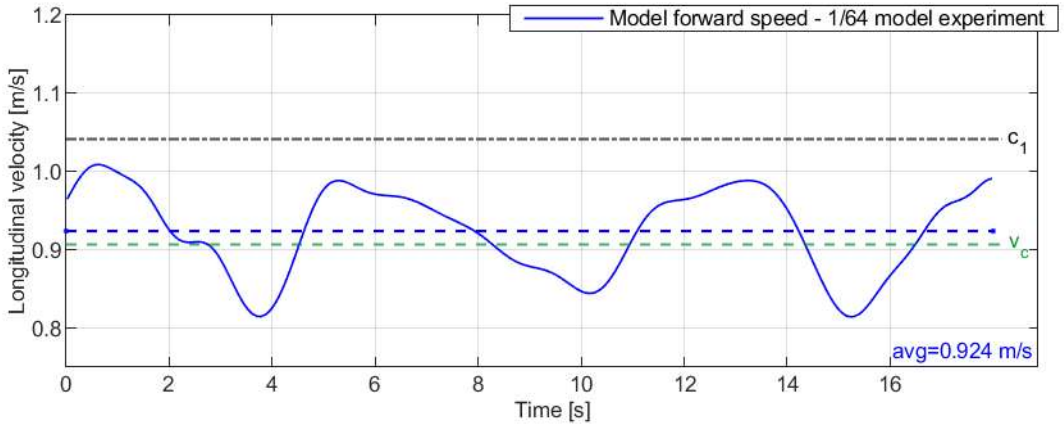

Figure 3.3 Case No. A12 Regular wave; λ=0.694m; c=1.041m/s; A=0.010m; v_c=0.907m/s; Asymmetric surging

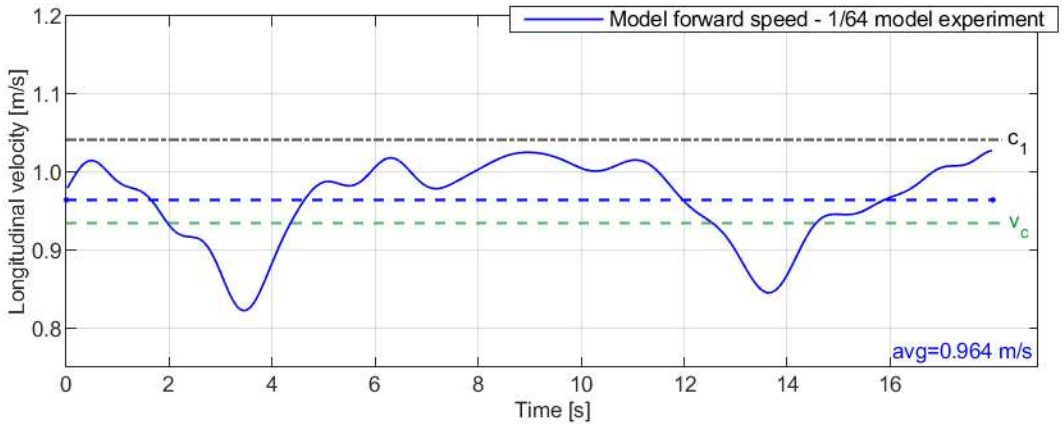

Figure 3.4 Case No. A13 Regular wave; λ=0.694m; c=1.041m/s; A=0.010m; v_c=0.934m/s; High-runs

Figure 3.5 and Figure 3.6 present surf-riding in regular waves. The wave's surf-riding threshold was indisputably achieved at the commanded speed of v_c=0.960 m/s. The ship model was captured by the wave after a brief period. Once the commanded speed rose up to v_c=1.006 m/s, the surf-riding state became more stable, generating lower amplitude of oscillations around the wave celerity.

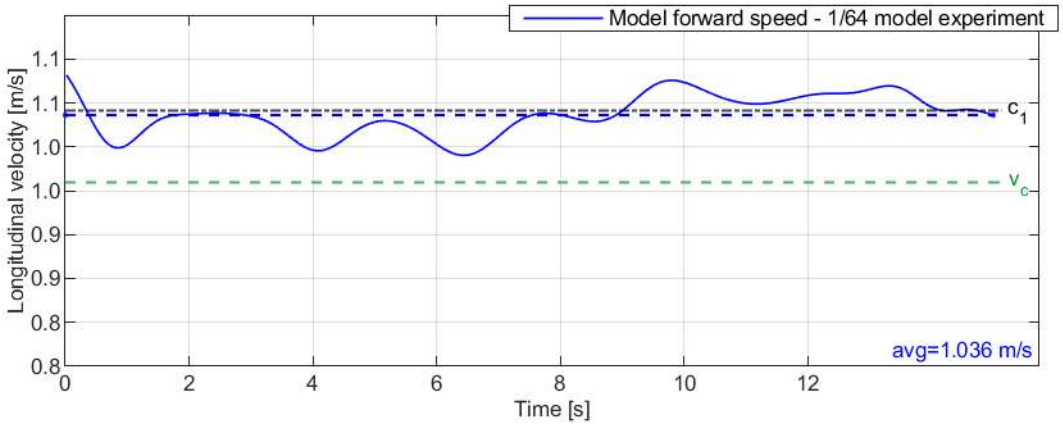

Figure 3.5 Case No. A14 Regular wave; λ=0.694m; c=1.041m/s; A=0.010m; v_c=0.96m/s; Surf-riding

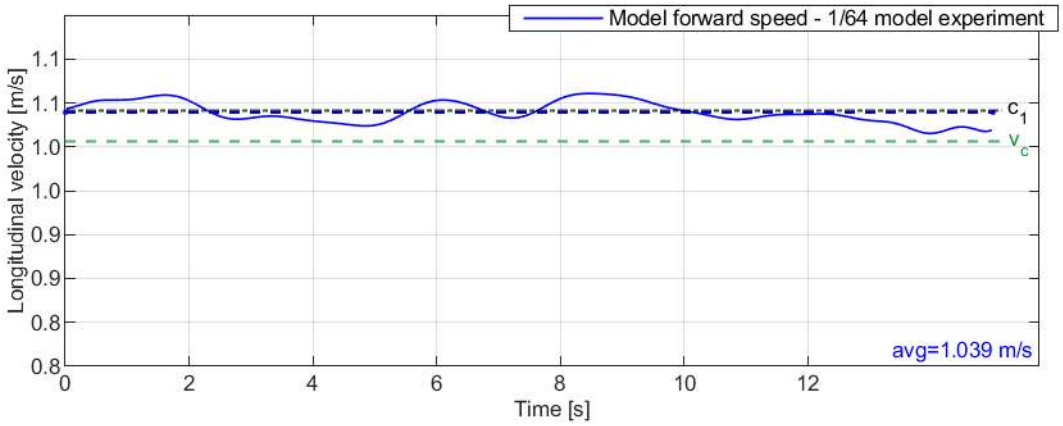

Figure 3.6 Case No. A15 Regular wave; λ=0.694m; c=1.041m/s; A=0.010m; v_c=1.006m/s; Surf-riding

3.2.2.*Results of regular wave experiment at a scale of 1/14*

Figure 3.7 to Figure 3.12 present a sequence of the results obtained for the runs conducted in regular waves with the amplitude of A≈0.03 m, the length of λ=3.802 m, and the celerity of c=2.437 m/s. The varying parameter was the ship model commanded speed, which was set from the value v_c=2.074 m/s up to v_c=2.178 m/s, according to the scenarios presented in Table 2.2.

Figure 3.7 shows a regular, asymmetric surging with the commanded speed set to v_c=2.074 m/s, and the average velocity above the calm water speed. While increasing the commanded speed to v_c=2.108 m/s, as shown in Figure 3.8, high-runs occur with clear attraction to wave celerity. In Figure 3.9 increased commanded speed to v_c=2.126 m/s does not yet change the response type. However, high-runs become longer.

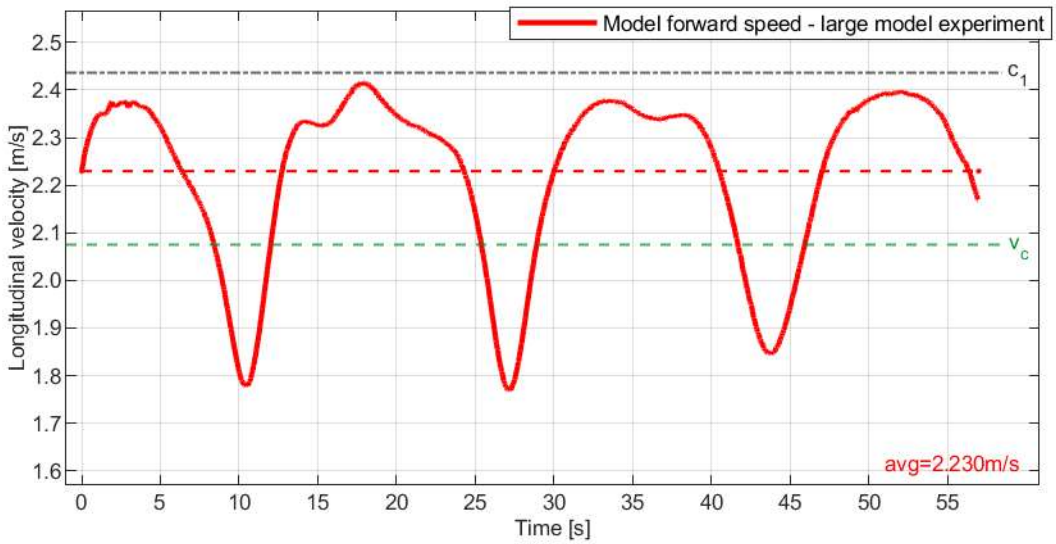

Figure 3.7 Case No. B78 Regular wave; λ_1=3.802m; c_1=2.437m/s; A_1=0.029m; v_c=2.074m/s; T_{E1}=18.34s; Asymmetric surging

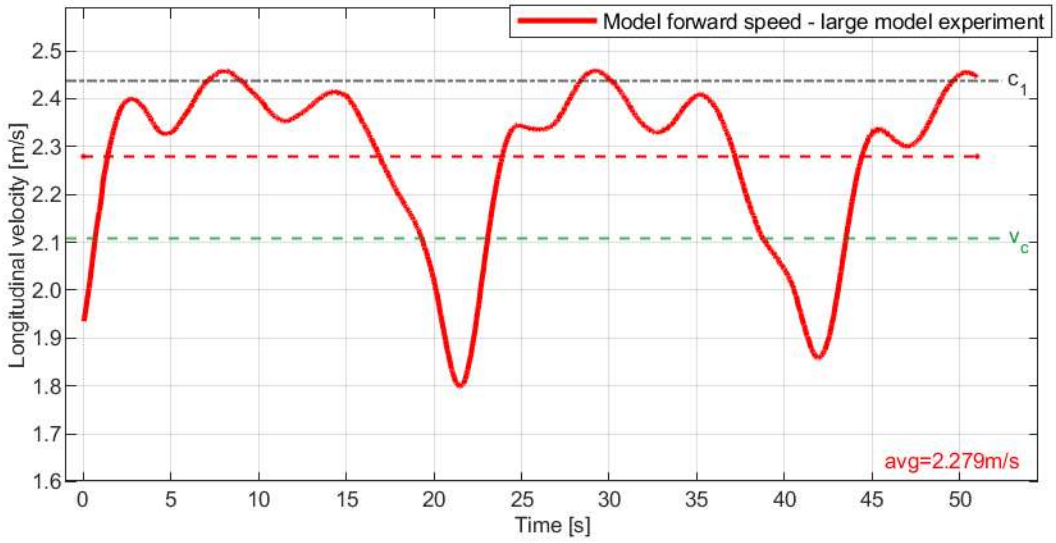

Figure 3.8 Case No. B79 Regular wave; λ_1=3.802m; c_1=2.437m/s; A_1=0.030m; v_c=2.108m/s; T_{E1}=24.12s; High-runs

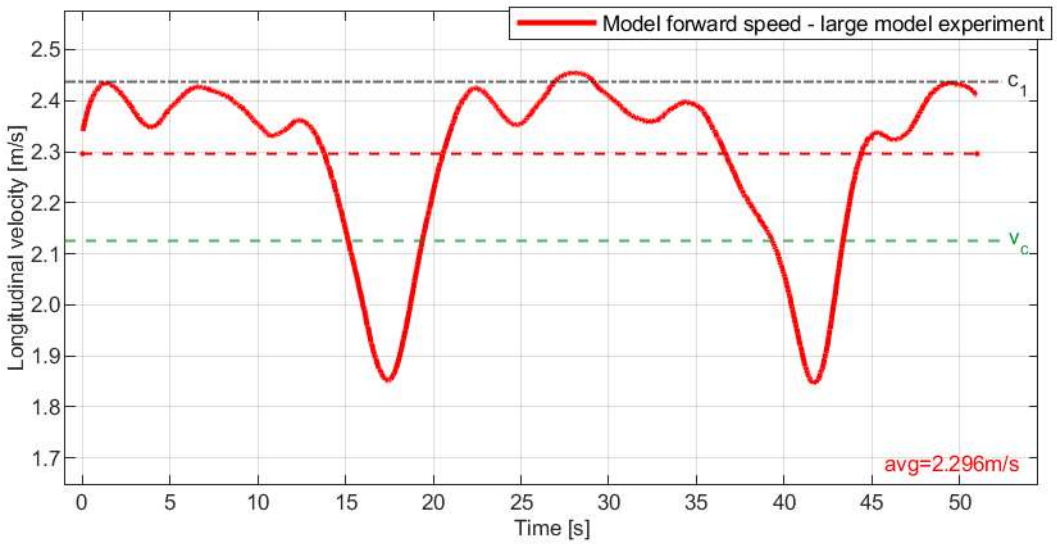

Figure 3.9 Case No. B80 Regular wave; λ_1=3.802m; c_1=2.437m/s; A_1=0.030m; v_c=2.126m/s; T_{E1}=26.97s; High-runs

While the ship commanded speed was increased to v_c=2.161 m/s, as shown in Figure 3.10 and Figure 3.11, it appears that the ship was surf-riding for 25 seconds, then fell out of the wave close to the end of the run. These two runs can be described as high-runs or surf-riding depending on selected time frame.

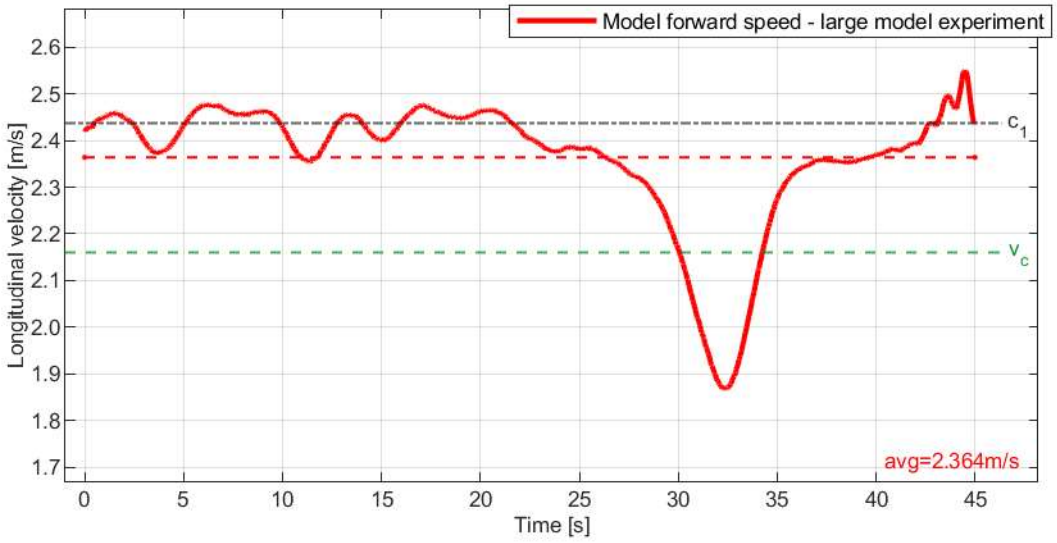

Figure 3.10 Case No. B82 Regular wave; λ_1=3.802m; c_1=2.437m/s; A_1=0.030m; v_c=2.161m/s; T_{E1}=52.07s; High-runs

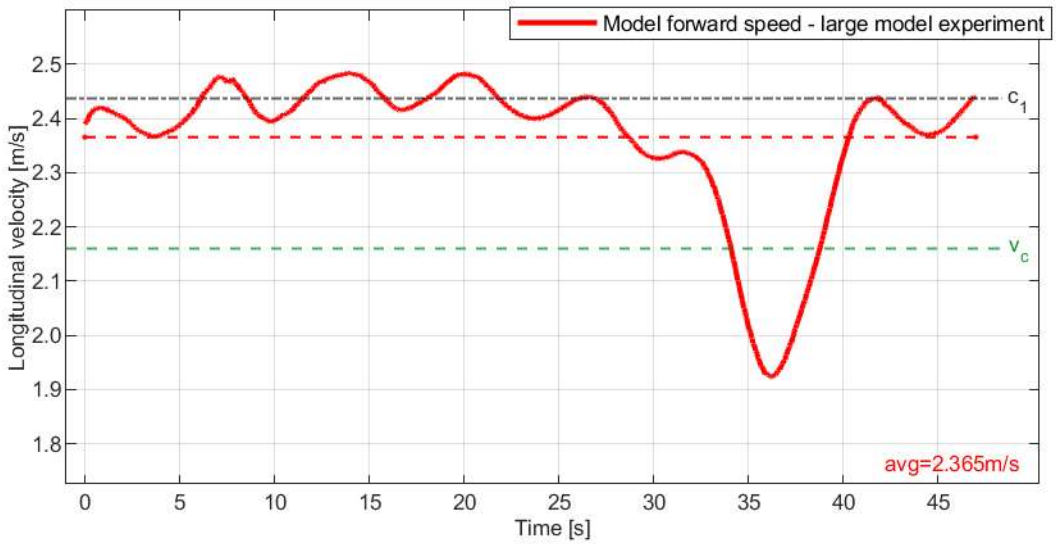

Figure 3.11 Case No. B87 Regular wave; λ_1=3.802m; c_1=2.437m/s; A_1=0.030m; v_c=2.161m/s; T_{E1}=53.19s; High-runs

In Figure 3.12 where commanded speed was increased to v_c=2.178 m/s, the ship surfed thru the whole length of the towing tank. Clear attraction to the wave celerity was observed. Average ship velocity was observed to be very close to wave celerity.

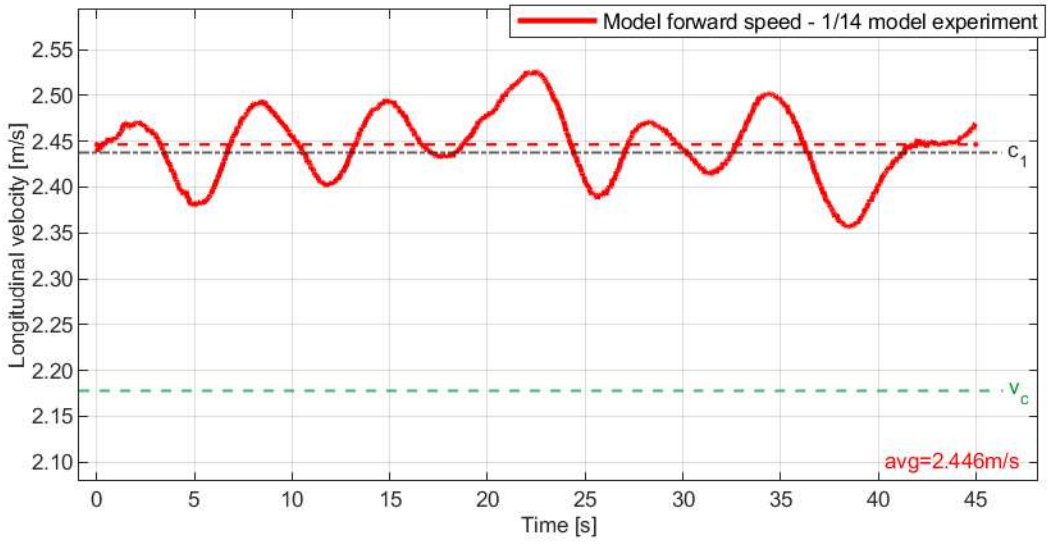

Figure 3.12 Case No. B88 Regular wave; λ_1=3.802m; c_1=2.437m/s; A_1=0.031m; v_c=2.178m/s; Surf-riding

3.3. Results of bi-chromatic wave experiments

3.3.1. *Results of bi-chromatic wave experiment at a scale of 1/64*

This part of the study aims to reproduce 8 characteristic response patterns to various bi-chromatic following waves, which were identified on the theoretical basis in recent works (Warnke-Olewniczak and Krata, 2024). The aforementioned responses include the following:

A1. Beating oscillations in surge;
A2. High-runs on primary wave;
A3. Surf-riding on primary wave;
A4. Low runs on primary wave;
A5. Surging due to attraction to secondary wave;
A6. High-runs on secondary wave;
A7. Surf-riding on secondary wave;
A8. Low runs on secondary wave.

The values of the governing variables for our experiment were taken directly from the conducted simulations (Warnke-Olewniczak and Krata, 2024). However, for the surging due to attraction to secondary wave, because of significant difference in the results the exploration of parameters values was carried out and with minor alterations for the sake of searching for a corresponding response. Case with adjusted parameters is assigned case number A9. Each of the cases presented in this subsection was carried out in accordance with the scenarios presented in Table 2.4.

Each case presented in the sequence of plots shown in Figure 3.13 thru Figure 3.21 consists of three side by side graphs representing three different realizations recorded with the same input parameters, i.e., identical wave frequencies and amplitudes as well as the same propeller revolutions. Scale on vertical axis is the same thru all three runs for each case. The data presented on the graphs consists of the model's longitudinal velocity in time as a bold blue line, the commanded speed v_c (dashed green line), the two wave components celerities c_1 and c_2 (dashed black dotted lines) as well as the average speed of the ship model marked with a dashed line same color as velocity plot. The results of calculations for each case are plotted as black dashed lines.

In Figure 3.13, the phenomenon of *beating surging* can be observed. In this case, the ship's velocity was oscillating around the average speed, which was closely matching with the commanded speed. This response is also recognized by the sinusoidal envelope of the ship velocity graph. While the commanded speed was increased from v_c=0.743 m/s up to v_c=0.847 m/s, the response type changed to *high-runs on primary wave* as shown in Figure 3.14. In this case the ship is strongly attracted to the primary wave, yet surf-riding is not occurring. The average speed falls between the speed of calm water and the primary wave celerity.

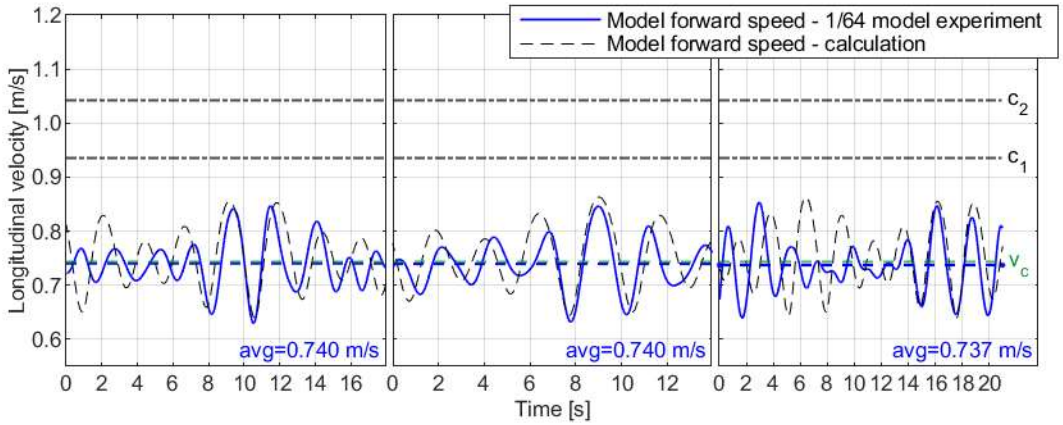

Figure 3.13 Case No. A1 Bi-chromatic wave; λ_1=0.560m; c_1=0.935m/s; A_1=0.008m; λ_2=0.694m; c_2=1.041m/s; A_2=0.010m; v_c=0.743m/s; Beating surging

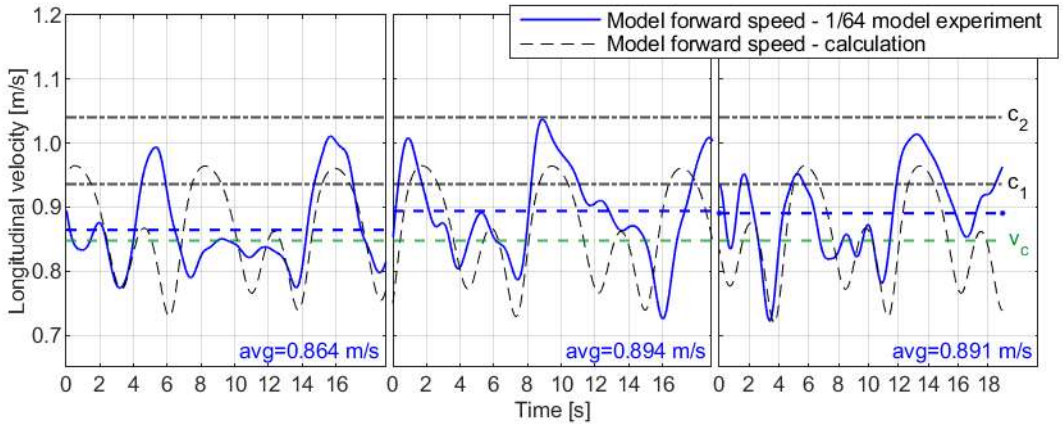

Figure 3.14 Case No. A2 Bi-chromatic wave; λ_1=0.560m; c_1=0.935m/s; A_1=0.008m; λ_2=0.694m; c_2=1.041m/s; A_2=0.010m; v_c=0.847m/s; High-runs on primary wave

Surf-riding on primary wave behavior was observed in Figure 3.15. The difference between the primary wave celerity and the average speed is minimal. The strong characteristic for this phenomenon is the attraction to primary wave with regular velocity oscillations around its celerity.

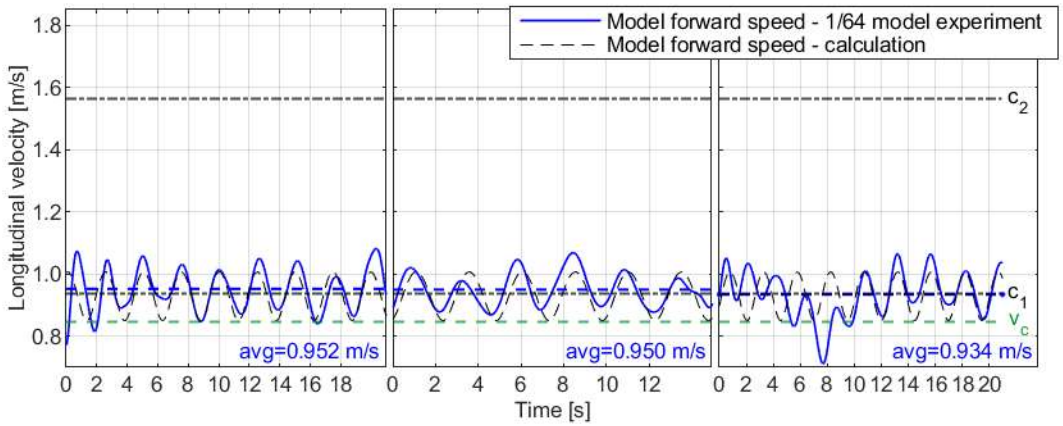

Figure 3.15 Case No. A3 Bi-chromatic wave; λ_1=0.560m; c_1=0.935m/s; A_1=0.016m; λ_2=1.562m; c_2=1.562m/s; A_2=0.008m; v_c=0.847m/s; Surf-riding on primary wave

In Figure 3.16 it can be observed that after increasing the commanded speed from the value below the primary wave celerity v_c=0.847 m/s to above the primary wave celerity v_c=1.020 m/s, slight differences had occurred. The response characteristics, such as a high-velocity peak occurring every third speed oscillation, indicate the occurrence of *low runs on primary wave*. However, only once in three runs was it observed that the average speed was noticeably below the commanded speed, therefore another characteristic of the phenomenon is not strongly evident.

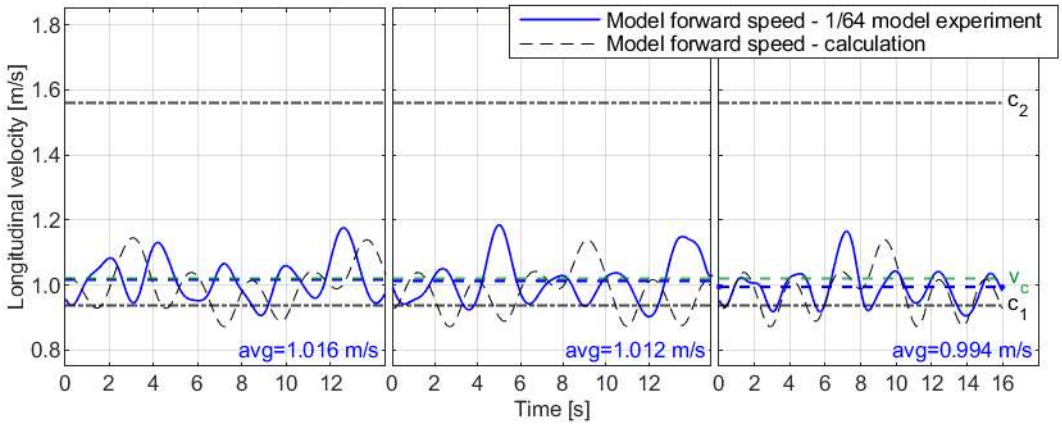

Figure 3.16 Case No. A4 Bi-chromatic wave; λ_1=0.560m; c_1=0.935m/s; A_1=0.016m; λ_2=1.562m; c_2=1.562m/s; A_2=0.008m; v_c=1.02m/s; Low-runs on primary wave

Figure 3.17 represents an attempt to reproduce *surging due to attraction to secondary wave* utilizing original parameters used by (Warnke-Olewniczak and Krata, 2024). However, the original parameters resulted in *surf-riding on secondary wave* being observed.

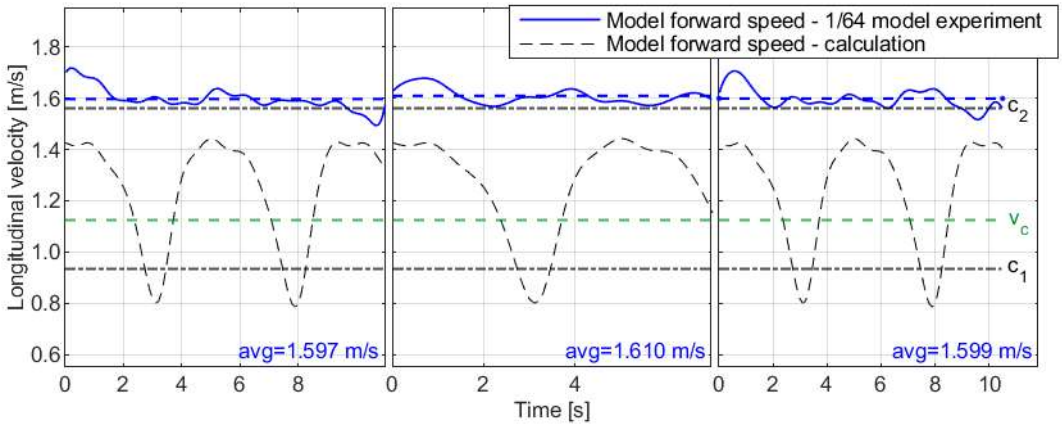

Figure 3.17 Case No. A5 Bi-chromatic wave; λ_1=0.560m; c_1=0.935m/s; A_1=0.008m; λ_2=1.562m; c_2=1.562m/s; A_2=0.039m; v_c=1.124m/s; Surf-riding on secondary wave

Figure 3.18 shows the response type called *high-runs on secondary wave*, which has noticeable similarities to the previous case. The reason for this outcome lies in the difficulties in overcoming the wave blocking. Despite the attempts to adjust the parameters (alteration vs. the theoretical predictions), no results matching the calculations more accurately were achieved.

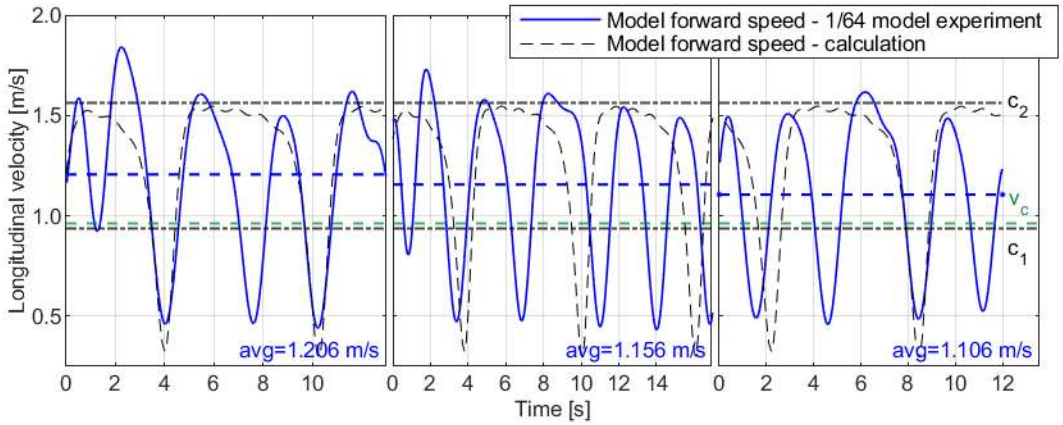

Figure 3.18 Case No. A6 Bi-chromatic wave; λ_1=0.560m; c_1=0.935m/s; A_1=0.010m; λ_2=1.562m; c_2=1.562m/s; A_2=0.060m; v_c=0.96m/s; High-runs on secondary wave

Figure 3.19 presents the occurrence of *surf-riding on secondary wave*. Given attempts show clear attraction to the second wave celerity with the velocity oscillations resulting from the primary wave. This result proves the occurrence of the phenomenon. In accordance with the predictions, the vessel's average speed during measurements has reached sufficient proximity to wave celerity to be described as surf-riding.

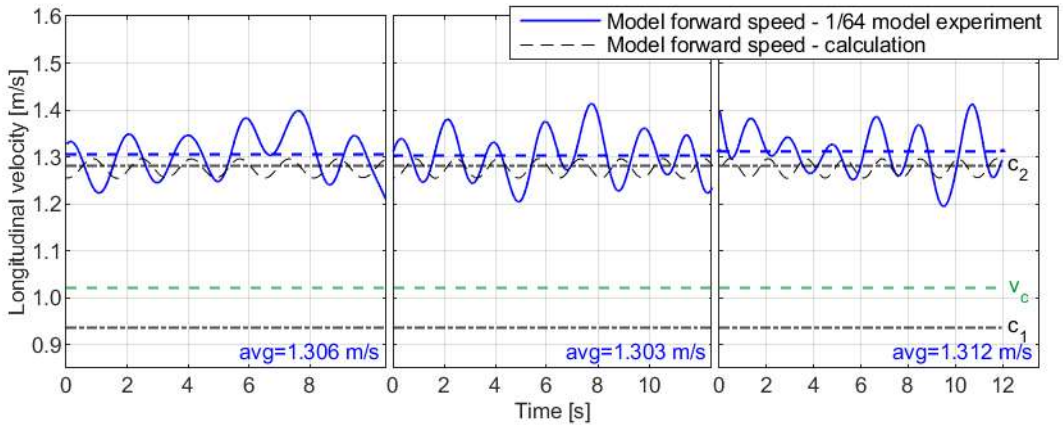

Figure 3.19 Case No. A7 Bi-chromatic wave; λ_1=0.560m; c_1=0.935m/s; A_1=0.008m; λ_2=1.050m; c_2=1.280m/s; A_2=0.026m; v_c=1.02m/s; Surf-riding on secondary wave

Shown in Figure 3.20 was case related to *low runs on secondary wave*. With the commanded speed set above both waves' celerities, surging at two frequencies was observed. Both waves generated oscillations around the average speed. However, in none of the three cases noticeable average speed decrease was observed.

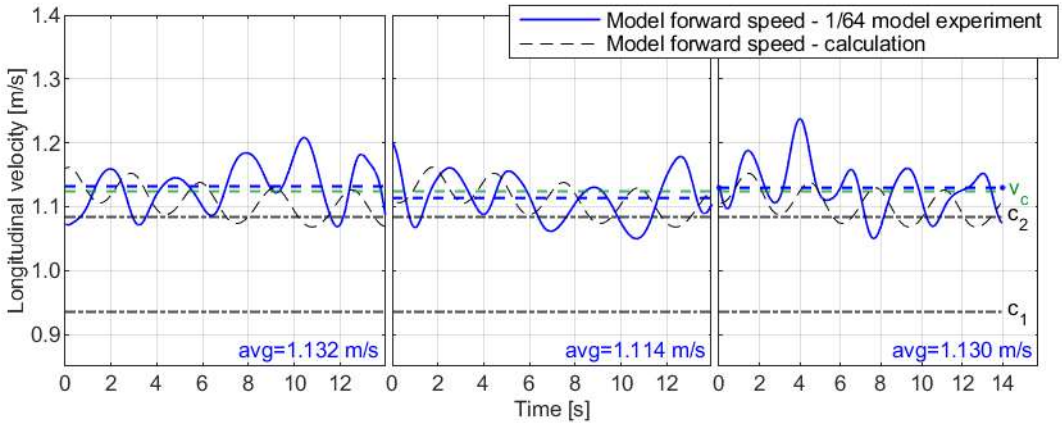

Figure 3.20 Case No. A8 Bi-chromatic wave; λ_1=0.560m; c_1=0.935m/s; A_1=0.008m; λ_2=0.753m; c_2=1.085m/s; A_2=0.004m; v_c=1.124m/s; Surging

Considering the exploration of the response modes as the primary focus of this study, the input parameters of the case A5 shown in Figure 3.17 were gradually altered until *surging due to attraction to secondary wave* was observed as represented in Figure 3.21. This case is characterized by significant velocity oscillations, where the ship does not accelerate above the second wave celerity.

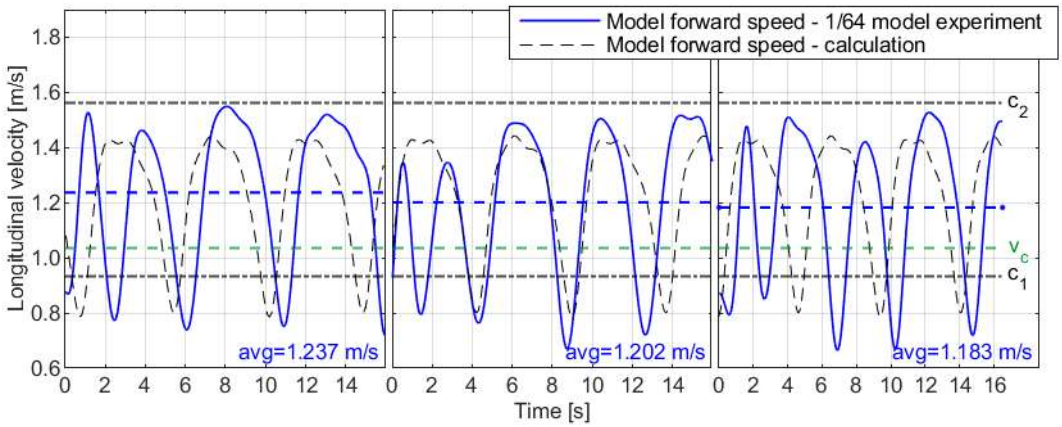

Figure 3.21 Case No. A9 Bi-chromatic wave; λ_1=0.560m; c_1=0.935m/s; A_1=0.010m; λ_2=1.562m; c_2=1.562m/s; A_2=0.035m; v_c=1.034m/s; Surging due to attraction to secondary wave

3.3.2. *Results of bi-chromatic wave experiment at a scale of 1/14*

The data presented on the graphs consists of the model's longitudinal velocity in time plotted as a bold red line, the commanded speed v_c (dashed green line), the two wave components celerities c_1 and c_2 (dashed black dotted lines) as well as the average speed of the ship model marked with a dashed line the same color as velocity plot. Each of the cases presented in this subsection was carried out in accordance with the scenarios presented in Table 2.5, Table 2.6, Table 2.7 and Table 2.8.

The cases presented in Table 2.5 shown in Figure 3.22 thru Figure 3.35 illustrate the change in the model response as the commanded speed increases for three different bi-chromatic waves.

First set of runs was conducted using a wave with the following parameters: $\lambda_1 \approx 2.90$ m, $A_1 \approx 0.030$ m, $\lambda_2 \approx 7.10$ m, $A_2 \approx 0.020$ m. Case B29 shown in Figure 3.22 presents *beating surging* with a very short period of the beats. While the commanded speed was increased from $v_c = 1.638$ m/s to $v_c = 1.703$ m/s in case B30 shown in Figure 3.23 *high-runs on primary wave* type response starts occurring. Main characteristic of the increased average model velocity helps to clearly categorize this case.

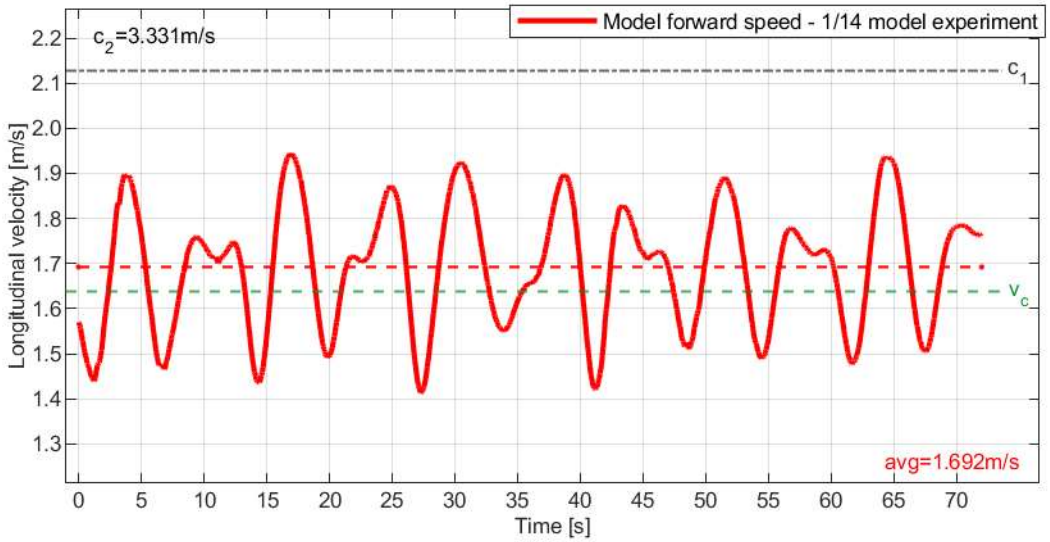

Figure 3.22 Case No. B29 Bi-chromatic wave; $\lambda_1 = 2.899$m; $c_1 = 2.128$m/s; $A_1 = 0.030$m; $\lambda_2 = 7.102$m; $c_2 = 3.331$m/s; $A_2 = 0.019$m; $v_c = 1.638$m/s; $T_{E1} = 6.655$s; $T_{E2} = 4.335$s; Beating surging

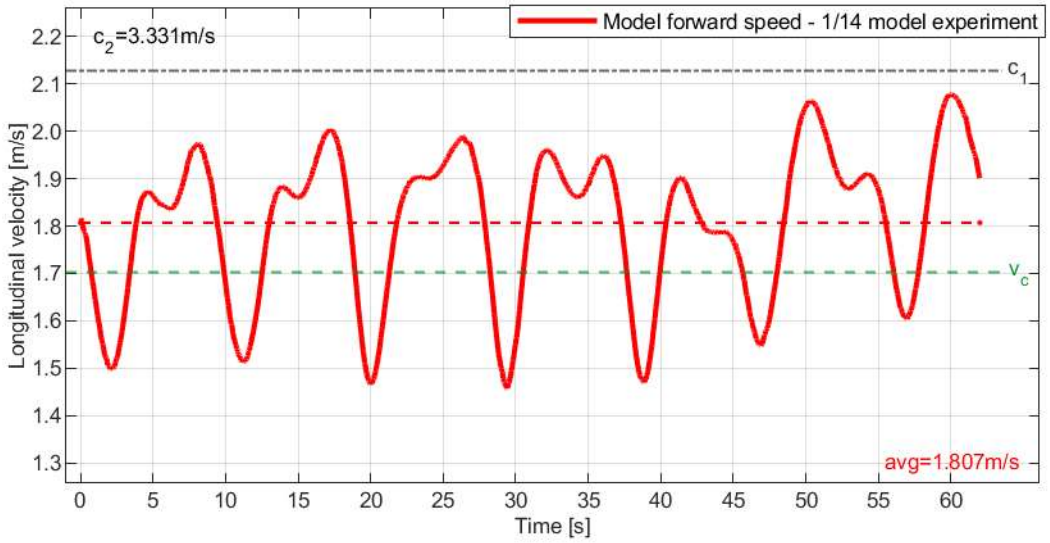

Figure 3.23 Case No. B30 Bi-chromatic wave; $\lambda_1 = 2.899$m; $c_1 = 2.128$m/s; $A_1 = 0.030$m; $\lambda_2 = 7.102$m; $c_2 = 3.331$m/s; $A_2 = 0.019$m; $v_c = 1.703$m/s; $T_{E1} = 9.028$s; $T_{E2} = 4.661$s; High-runs on primary wave

Further increase of the commanded speed up to $v_c = 1.879$ m/s results in *surf-riding on primary wave* as shown in Figure 3.24. Clear attraction to the primary wave celerity is observed as well as oscillations of period close to the encounter period of the secondary wave.

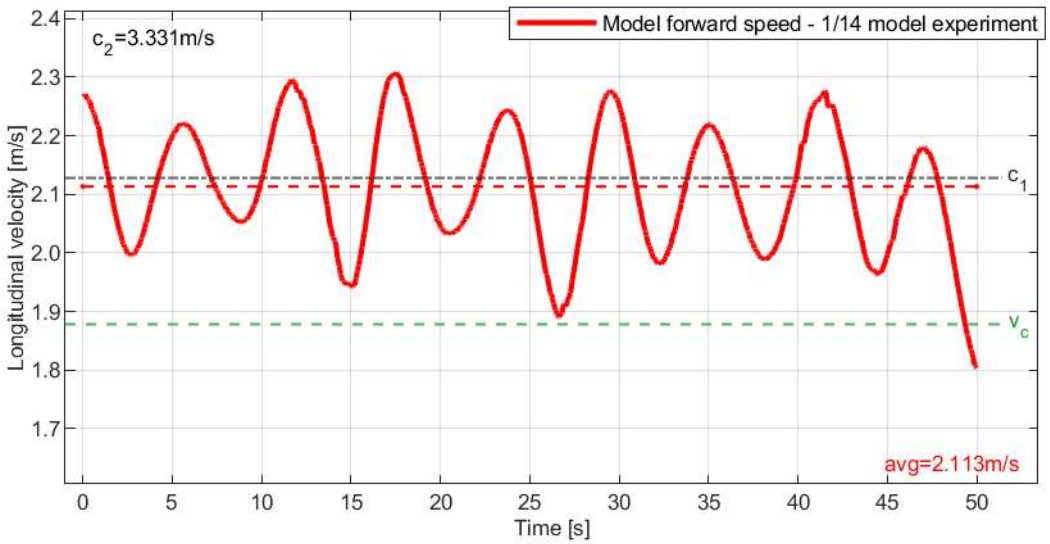

Figure 3.24 Case No. B31 Bi-chromatic wave; λ_1=2.899m; c_1=2.128m/s; A_1=0.030m; λ_2=7.102m; c_2=3.331m/s; A_2=0.020m; v_c=1.879m/s; T_{E1}=193.8s; T_{E2}=5.833s; Surf-riding on primary wave

Increasing the commanded speed once more up to v_c=1.996 m/s does not change the response type as shown in Figure 3.25. However, wave blocking start to occur, eventually resulting in the water on deck as shown in Figure 3.26.

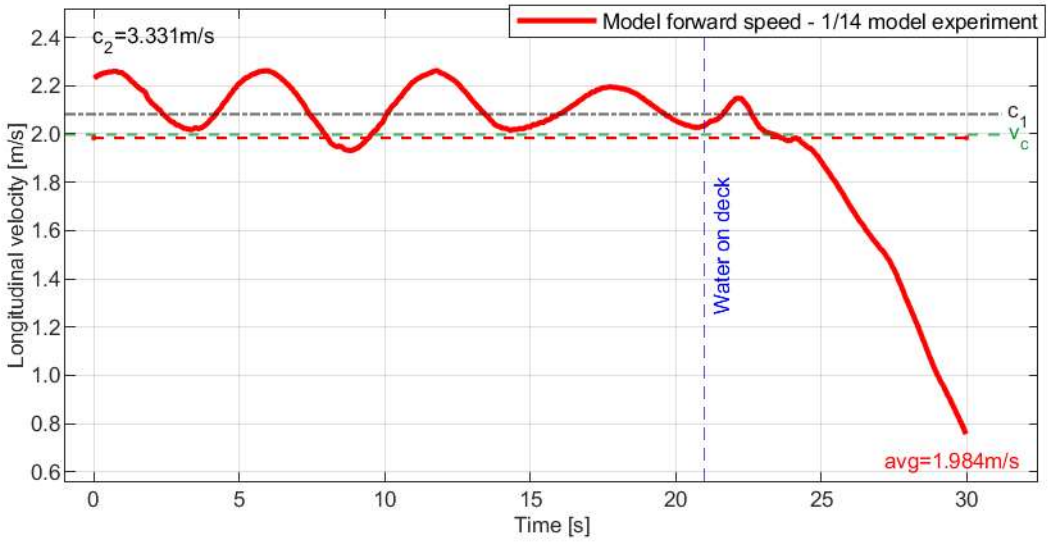

Figure 3.25 Case No. B38 Bi-chromatic wave; λ_1=2.777m; c_1=2.083m/s; A_1=0.031m; λ_2=7.102m; c_2=3.331m/s; A_2=0.022m; v_c=1.996m/s; T_{E1}=28.08s; T_{E2}=5.273s; Surf-riding on primary wave

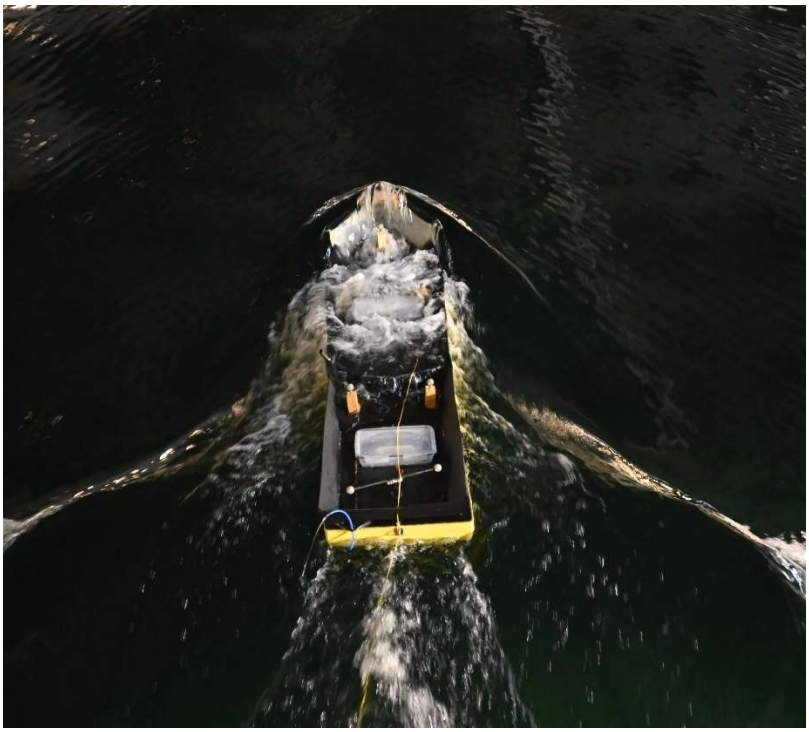

Figure 3.26 Water on deck as a result of wave blocking in case B38

The second set of runs was conducted using a wave with the following parameters: $\lambda_1 \approx 2.90$ m, $A_1 \approx 0.020$ m, $\lambda_2 \approx 3.30$ m, $A_2 \approx 0.017$ m. Case B40 shown in Figure 3.27 presents *beating surging* with long period of beats. While the commanded speed was increased from $v_c = 1.557$ m/s to $v_c = 1.638$ m/s in case B41 shown in Figure 3.28 the amplitude of velocity oscillations increased, while not changing the response type.

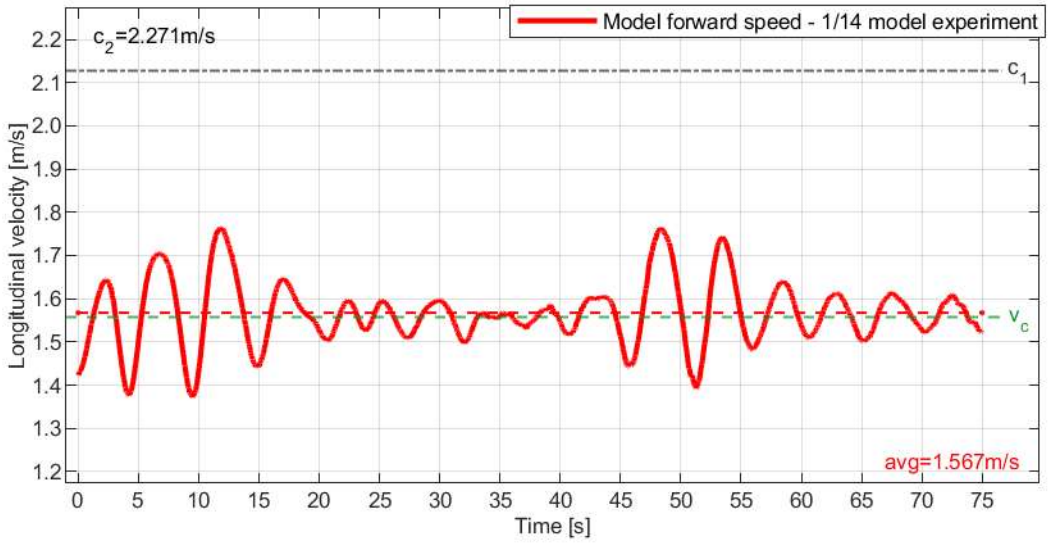

Figure 3.27 Case No. B40 Bi-chromatic wave; $\lambda_1 = 2.899$m; $c_1 = 2.128$m/s; $A_1 = 0.020$m; $\lambda_2 = 3.300$m; $c_2 = 2.271$m/s; $A_2 = 0.014$m; $v_c = 1.557$m/s; $T_{E1} = 5.17$s; $T_{E2} = 4.694$s; Beating surging

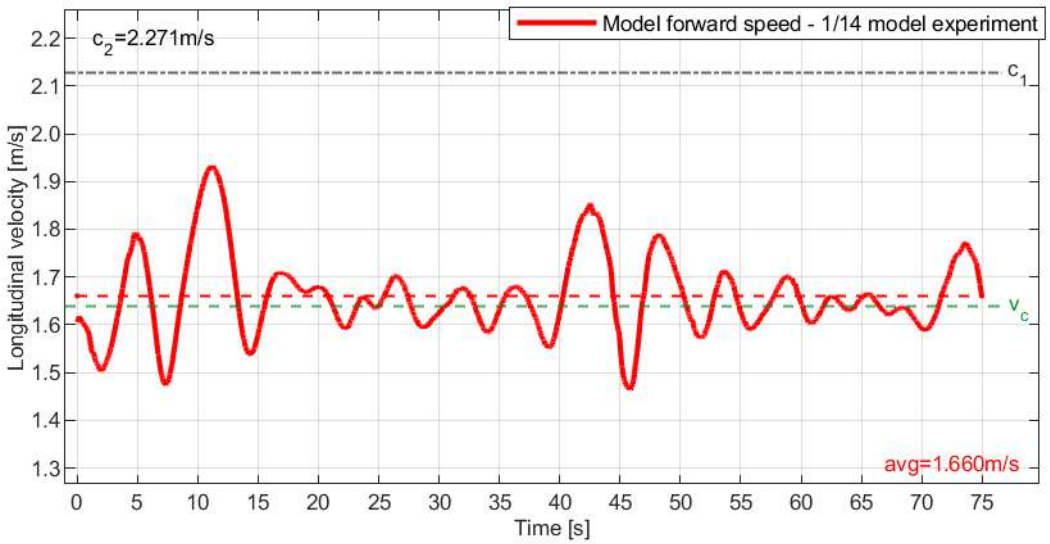

Figure 3.28 Case No. B41 Bi-chromatic wave; λ_1=2.899m; c_1=2.128m/s; A_1=0.021m; λ_2=3.300m; c_2=2.271m/s; A_2=0.018m; v_c=1.638m/s; T_{E1}=6.197s; T_{E2}=5.409s; Beating surging

Further increase of the commanded speed resulted in *high-runs on primary wave*. In case B42 shown in Figure 3.29 the commanded speed was v_c=1.759 m/s, in case B43 shown in Figure 3.30 v_c=1.815 m/s, in case B44 shown in Figure 3.31 v_c=1.860 m/s. In these cases, a slight increase in the average model velocity relative to the commanded speed was observed.

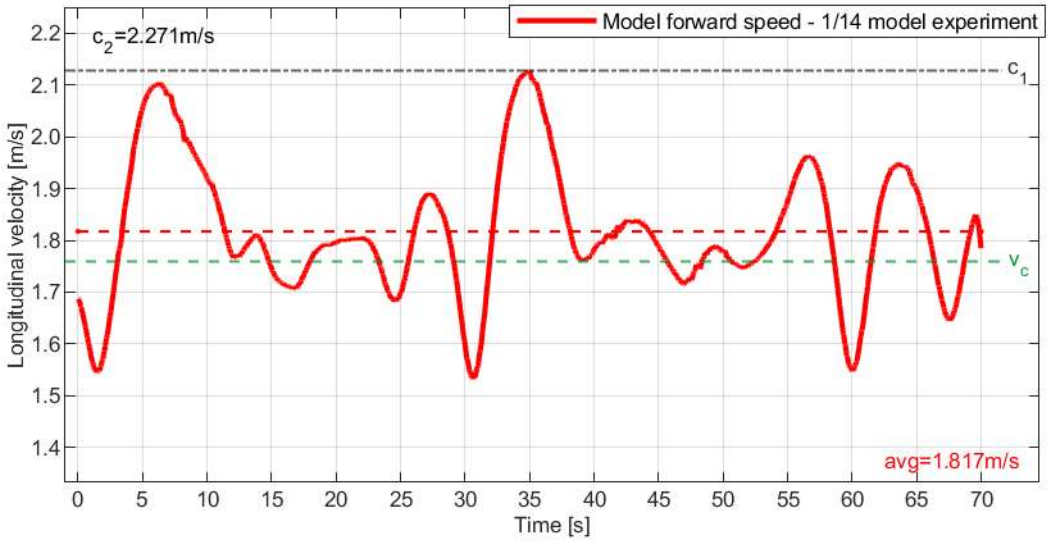

Figure 3.29 Case No. B42 Bi-chromatic wave; λ_1=2.899m; c_1=2.128m/s; A_1=0.021m; λ_2=3.300m; c_2=2.271m/s; A_2=0.018m; v_c=1.759m/s; T_{E1}=9.323s; T_{E2}=7.28s; High-runs on primary wave

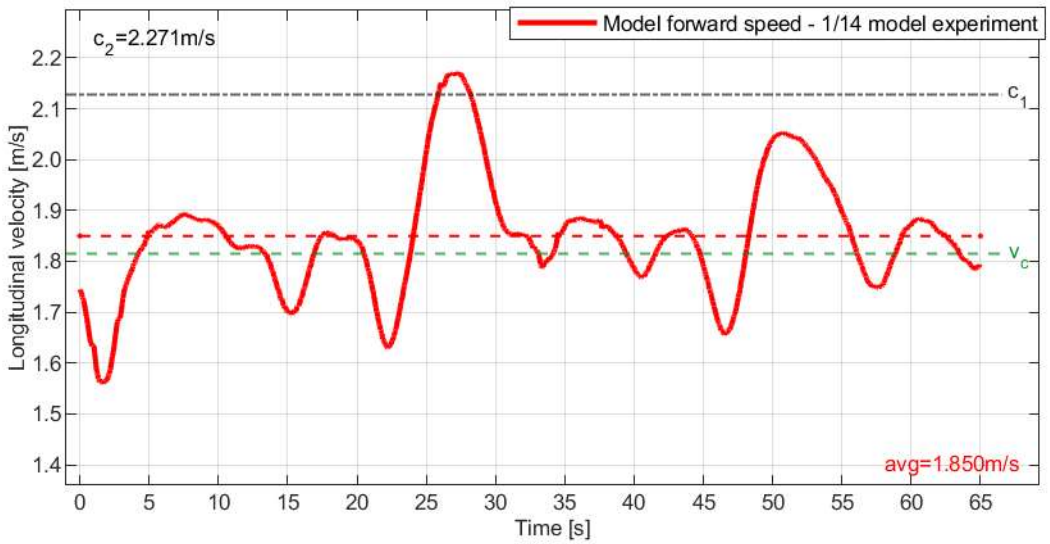

Figure 3.30 Case No. B43 Bi-chromatic wave; λ_1=2.899m; c_1=2.128m/s; A_1=0.018m; λ_2=3.300m; c_2=2.271m/s; A_2=0.014m; v_c=1.815m/s; T_{E1}=10.41s; T_{E2}=7.844s; High-runs on primary wave

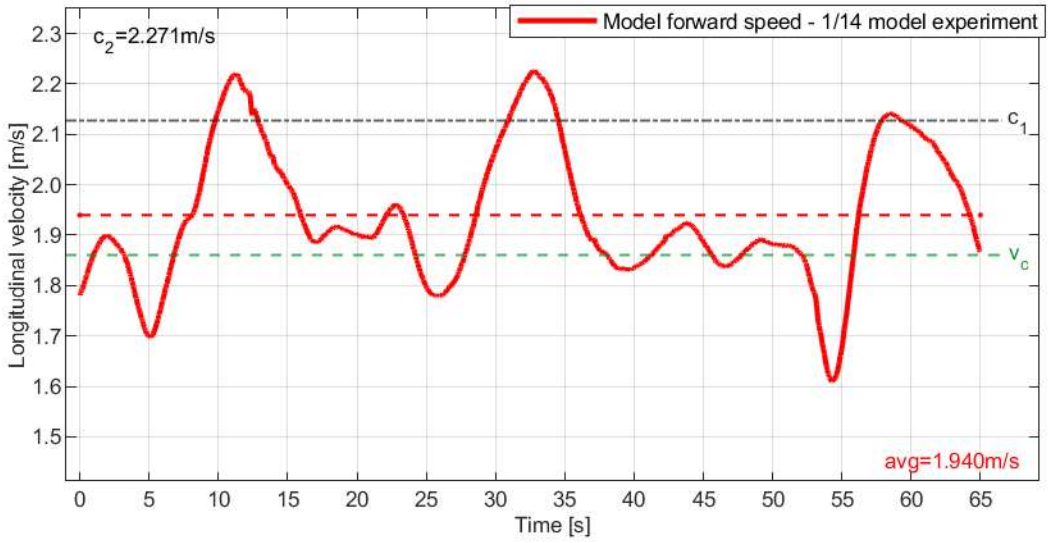

Figure 3.31 Case No. B44 Bi-chromatic wave; λ_1=2.899m; c_1=2.128m/s; A_1=0.021m; λ_2=3.300m; c_2=2.271m/s; A_2=0.018m; v_c=1.860m/s; T_{E1}=15.38s; T_{E2}=9.977s; High-runs on primary wave

In case B45 the commanded speed was increased up to v_c=1.996 m/s. This case is challenging to categorize as no recognizable pattern was observed. However, in the time frame of 20-26 s specific type of high-run was observed tentatively referred in this work as „trebuchet", which is further described and discussed in the main findings subsection.

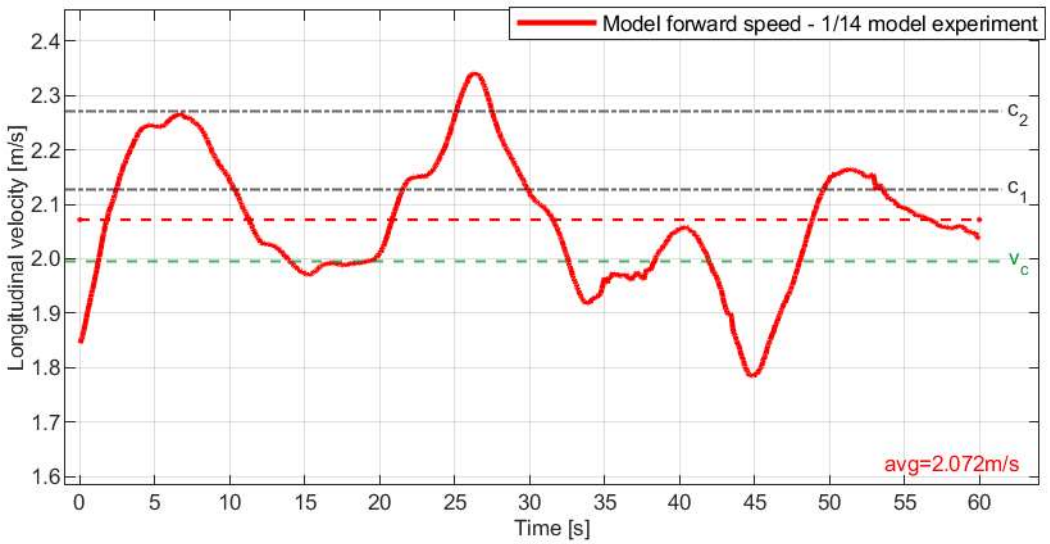

Figure 3.32 Case No. B45 Bi-chromatic wave; λ_1=2.899m; c_1=2.128m/s; A_1=0.020m; λ_2=3.300m; c_2=2.271m/s; A_2=0.014m; v_c=1.996m/s; T_{E1}=51.31s; T_{E2}=16.6s; Trebuchet

The third set of runs was conducted using a wave with the following parameters: $\lambda_1 \approx 2.90$ m, $A_1 \approx 0.027$ m, $\lambda_2 \approx 4.68$ m, $A_2 \approx 0.009$ m. Case B47 shown in Figure 3.33 is categorized as *beating surging*. Increase in the commanded speed from v_c=1.557 m/s to v_c=1.703 m/s in case B48 shown in Figure 3.34 a response similar to *asymmetric surging* occurs. This type of the response is more often associated with the phenomena occurring in the regular waves. However, the irregularity of velocity graph suggests that the secondary wave is present.

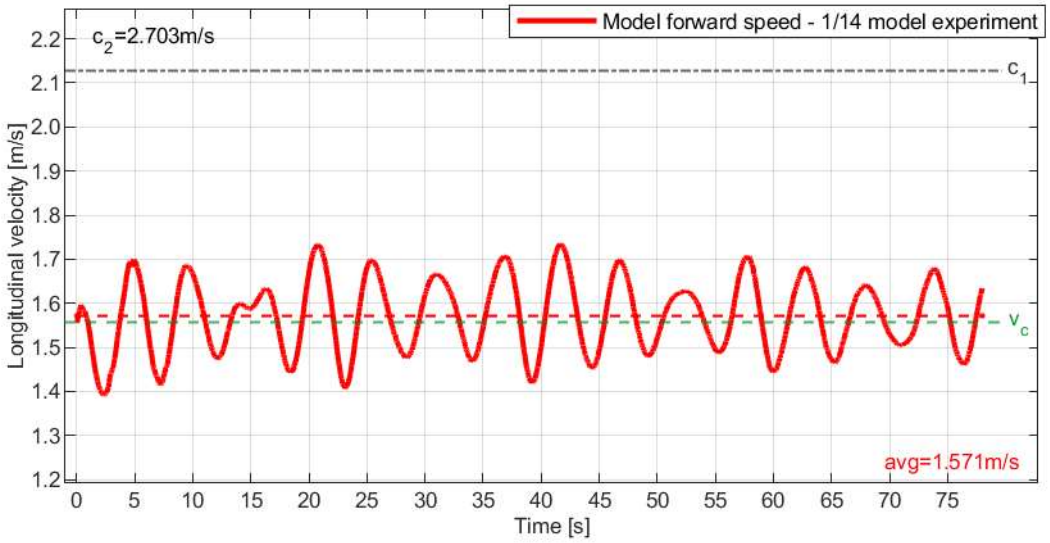

Figure 3.33 Case No. B47 Bi-chromatic wave; λ_1=2.899m; c_1=2.128m/s; A_1=0.023m; λ_2=4.676m; c_2=2.703m/s; A_2=0.009m; v_c=1.557m/s; T_{E1}=5.208s; T_{E2}=4.134s; Beating surging

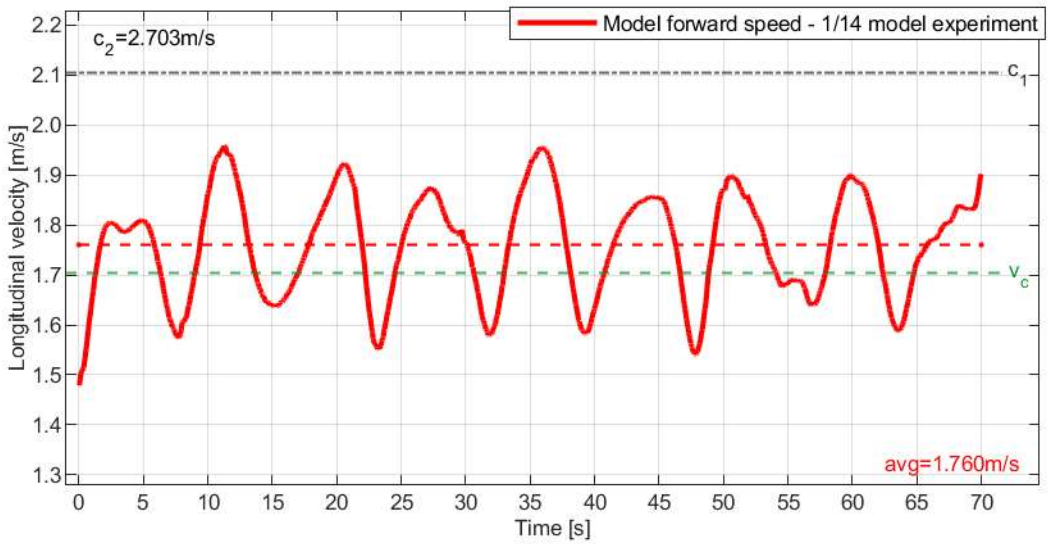

Figure 3.34 Case No. B48 Bi-chromatic wave; λ_1=2.837m; c_1=2.105m/s; A_1=0.029m; λ_2=4.676m; c_2=2.703m/s; A_2=0.008m; v_c=1.703m/s; T_{E1}=8.224s; T_{E2}=4.962s; Asymetric surging

Further increase of the commanded speed up to v_c=1.897 m/s results in *surf-riding on primary wave* as shown in Figure 3.35. Clear attraction to the primary wave celerity is observed as well as oscillations of period close to the encounter period of the secondary wave.

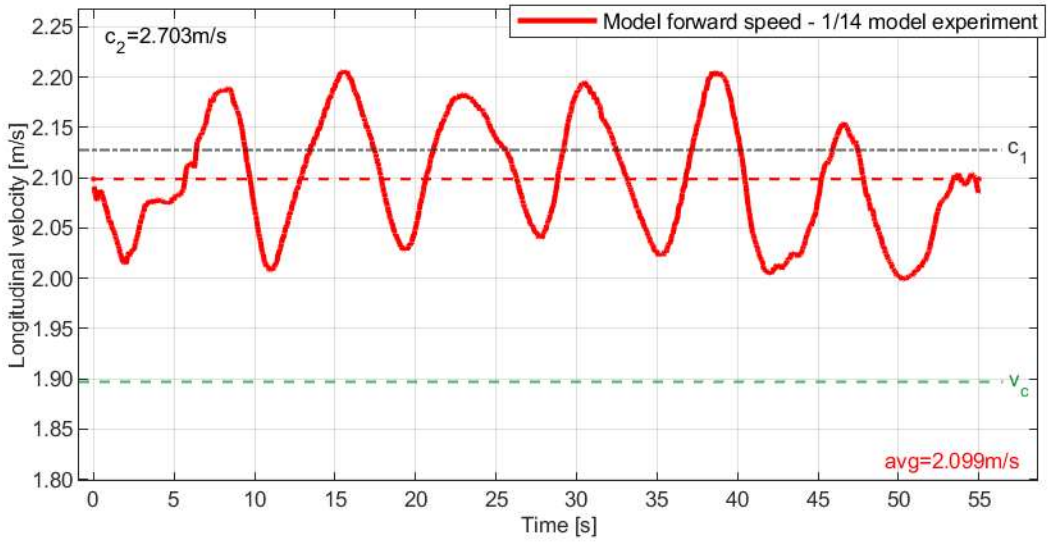

Figure 3.35 Case No. B49 Bi-chromatic wave; λ_1=2.899m; c_1=2.128m/s; A_1=0.026m; λ_2=4.676m; c_2=2.703m/s; A_2=0.009m; v_c=1.897m/s; T_{E1}=98.41s; T_{E2}=7.743s; Surf-riding on primary wave

Other three experiments were carried out with aim to determine the influence of the secondary wave on *surf-riding in regular waves*. First the surf-riding commanded speed threshold v_c=2.178 m/s was determined using the regular wave λ_1≈3.80 m, A_1≈0.030 m as presented in section 3.2.2. The results of the above experiment for the parameters shown in Table 2.6 are shown in Figure 3.36 thru Figure 3.52

The cases shown in Figure 3.36 thru Figure 3.40 were carried out using the secondary wave with a length of λ_2≈4.21 m. Cases B99 shown in Figure 3.36, B129 shown in Figure 3.37,

B102 shown in Figure 3.38 and case B124 shown in Figure 3.39; were not categorized as no response type was recognized. These results indicate complexity of phenomena occurring while sailing in a bi-chromatic following seas, and are shown because they are among the most interesting results from this experimental study.

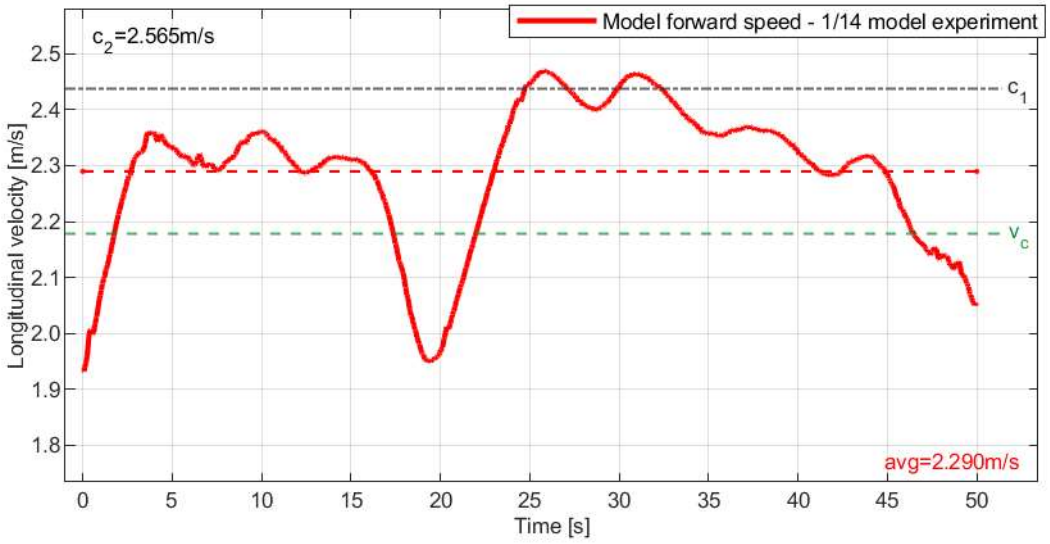

Figure 3.36 Case No. B99 Bi-chromatic wave; λ_1=3.802m; c_1=2.437m/s; A_1=0.025m; λ_2=4.212m; c_2=2.565m/s; A_2=0.007m; v_c=2.178m/s; T_{E1}=25.82s; T_{E2}=15.3s; Uncertain case

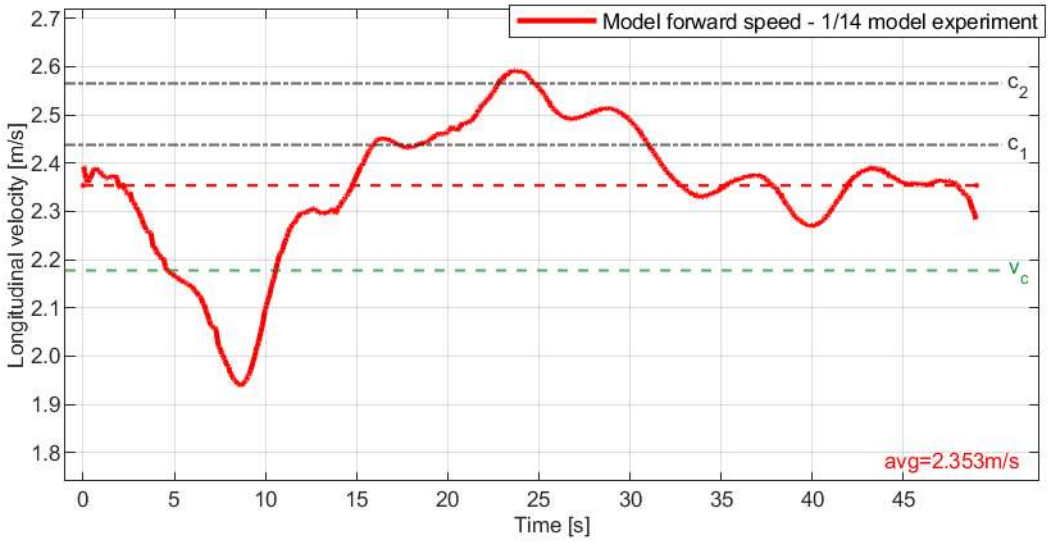

Figure 3.37 Case No. B129 Bi-chromatic wave; λ_1=3.802m; c_1=2.437m/s; A_1=0.032m; λ_2=4.212m; c_2=2.565m/s; A_2=0.010m; v_c=2.178m/s; T_{E1}=45.52s; T_{E2}=19.91s; Uncertain case

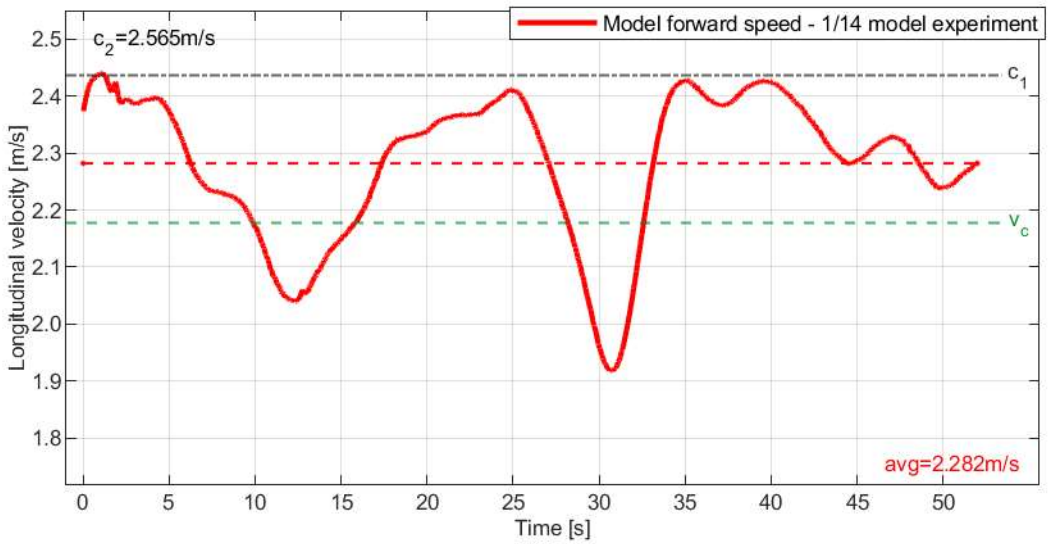

Figure 3.38 Case No. B102 Bi-chromatic wave; λ_1=3.802m; c_1=2.437m/s; A_1=0.026m; λ_2=4.212m; c_2=2.565m/s; A_2=0.011m; v_c=2.178m/s; T_{E1}=24.55s; T_{E2}=14.89s; Uncertain case

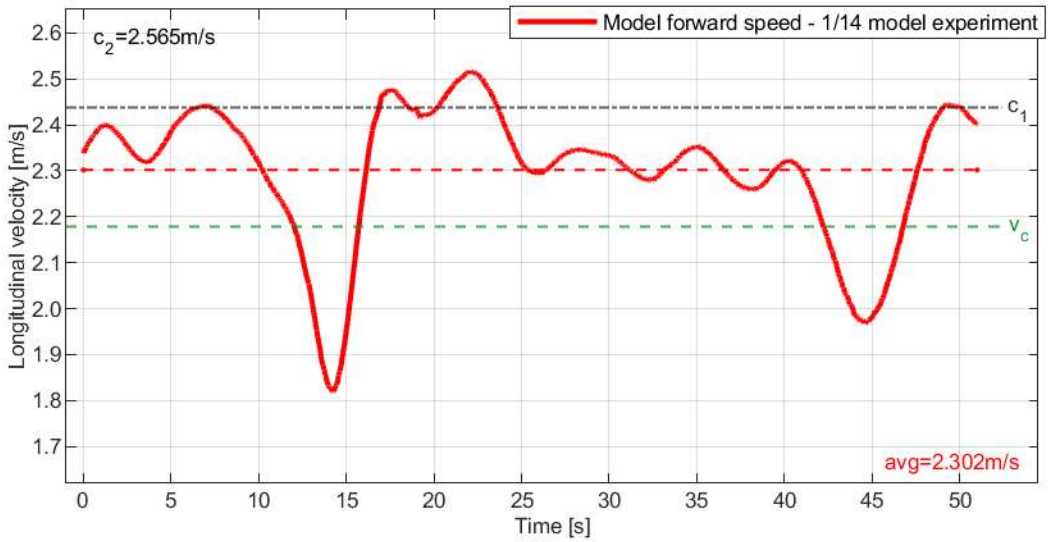

Figure 3.39 Case No. B124 Bi-chromatic wave; λ_1=3.802m; c_1=2.437m/s; A_1=0.034m; λ_2=4.212m; c_2=2.565m/s; A_2=0.010m; v_c=2.178m/s; T_{E1}=28.17s; T_{E2}=16.01s; Uncertain case

In case B104 shown in Figure 3.40 the ship model was subjected to the similar bi-chromatic following wave as in cases B99, B129, B102 and B124; where the amplitude of the secondary wave was A_2=0.016 m. In this case, between 19 and 34 seconds, another example of the “trebuchet” type response is observed, further described and discussed in the main findings subsection.

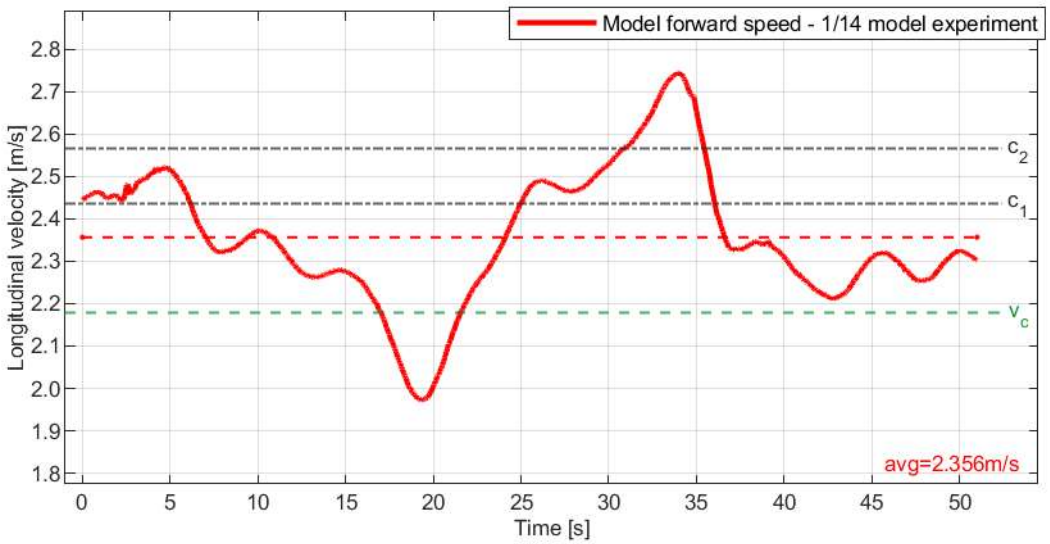

Figure 3.40 Case No. B104 Bi-chromatic wave; λ_1=3.802m; c_1=2.437m/s; A_1=0.032m; λ_2=4.212m; c_2=2.565m/s; A_2=0.016m; v_c=2.178m/s; T_{E1}=47.2s; T_{E2}=20.19s; Trebuchet

Cases shown in Figure 3.41 thru Figure 3.46 were carried out using a secondary wave with the length of $\lambda_2 \approx 5.87$ m. All of these cases show *oscillatory surf-riding on primary wave* type response. The amplitude ranging, from A_2=0.006m up to A_2=0.016m, seems to only influence the amplitude of oscillations around the primary wave celerity.

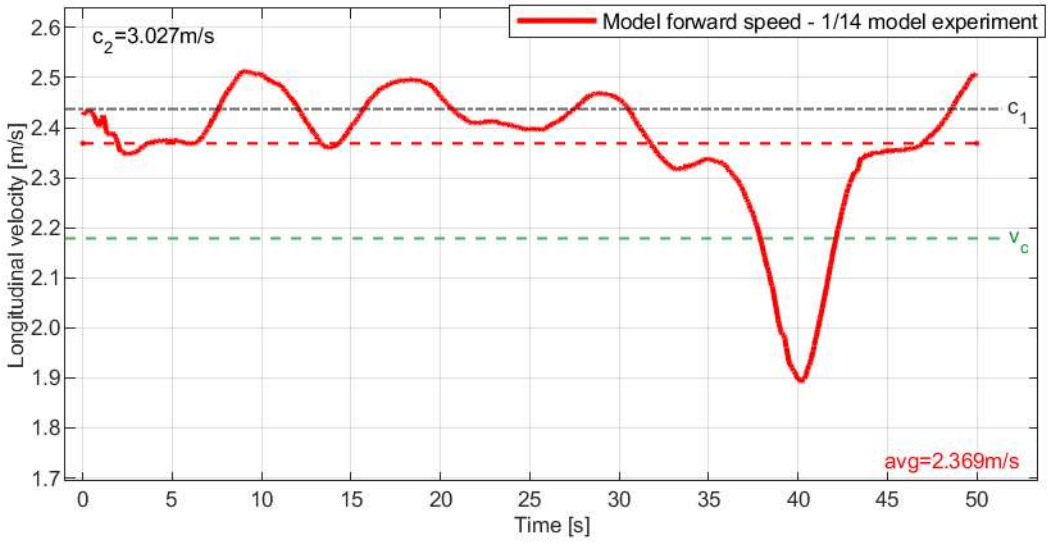

Figure 3.41 Case No. B132 Bi-chromatic wave; λ_1=3.802m; c_1=2.437m/s; A_1=0.032m; λ_2=5.867m; c_2=3.027m/s; A_2=0.006m; v_c=2.178m/s; T_{E1}=55.6s; T_{E2}=8.906s; Oscillatory surf-riding on primary wave

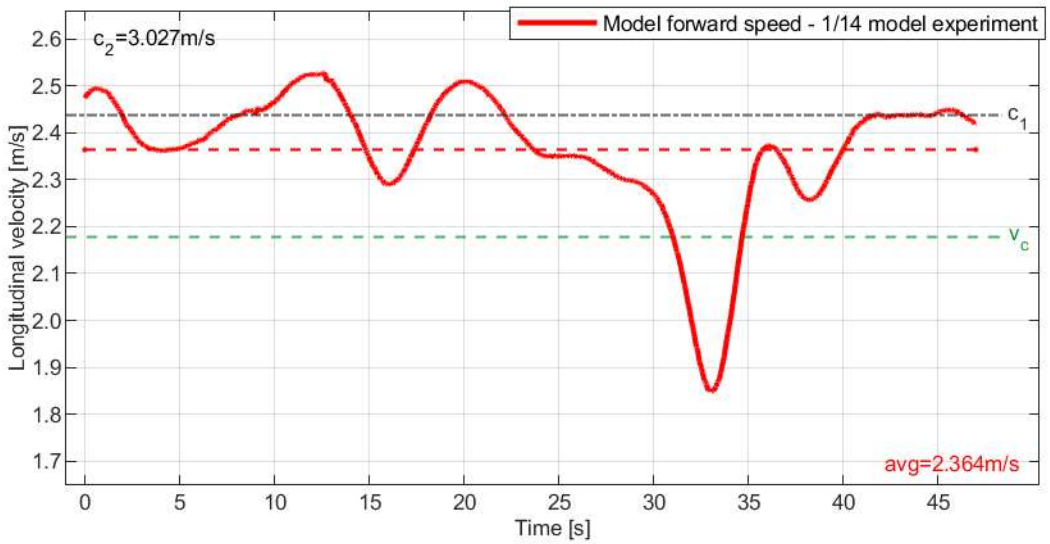

Figure 3.42 Case No. B106 Bi-chromatic wave; λ_1=3.802m; c_1=2.437m/s; A_1=0.030m; λ_2=5.867m; c_2=3.027m/s; A_2=0.008m; v_c=2.178m/s; T_{E1}=52.08s; T_{E2}=8.844s; Oscillatory surf-riding on primary wave

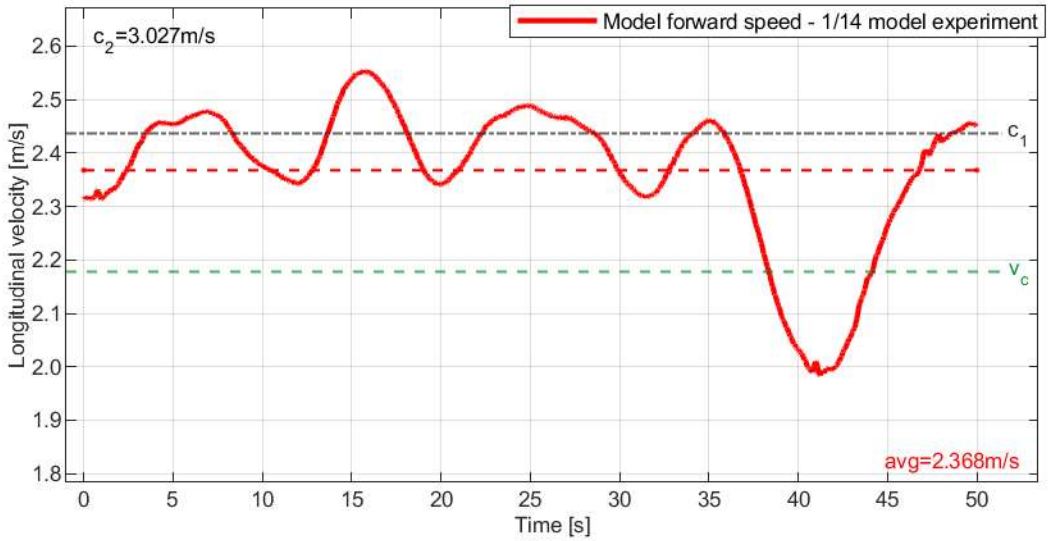

Figure 3.43 Case No. B137 Bi-chromatic wave; λ_1=3.802m; c_1=2.437m/s; A_1=0.032m; λ_2=5.867m; c_2=3.027m/s; A_2=0.008m; v_c=2.178m/s; T_{E1}=54.98s; T_{E2}=8.896s; Oscillatory surf-riding on primary wave

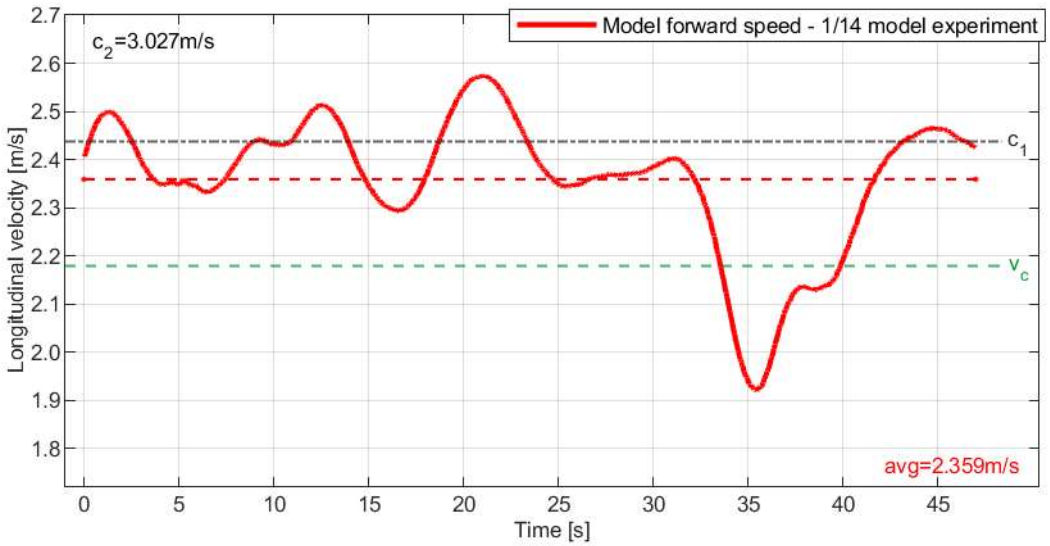

Figure 3.44 Case No. B108 Bi-chromatic wave; λ_1=3.802m; c_1=2.437m/s; A_1=0.031m; λ_2=5.867m; c_2=3.027m/s; A_2=0.011m; v_c=2.178m/s; T_{E1}=48.83s; T_{E2}=8.78s; Oscillatory surf-riding on primary wave

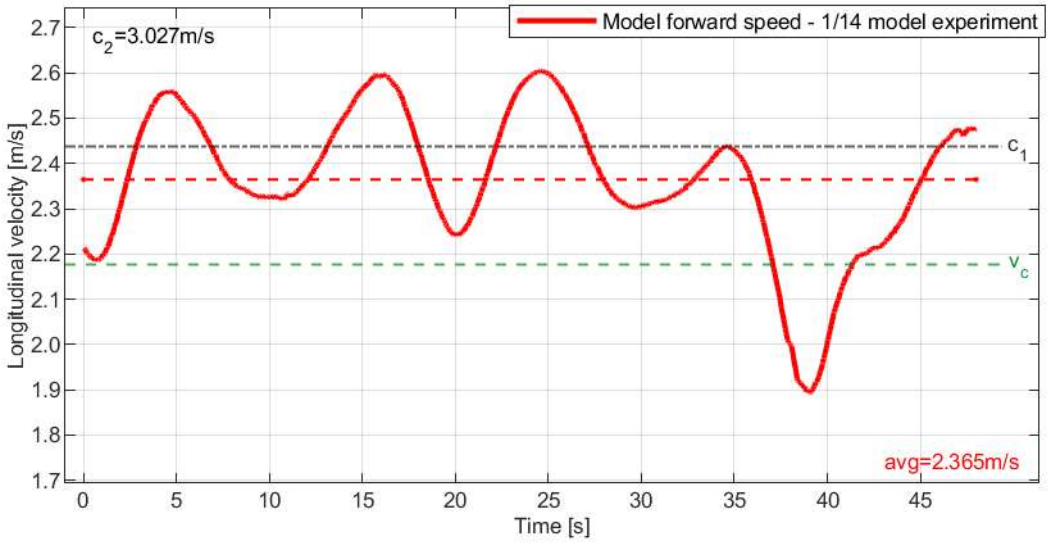

Figure 3.45 Case No. B121 Bi-chromatic wave; λ_1=3.802m; c_1=2.437m/s; A_1=0.031m; λ_2=5.867m; c_2=3.027m/s; A_2=0.015m; v_c=2.178m/s; T_{E1}=52.48s; T_{E2}=8.852s; Oscillatory surf-riding on primary wave

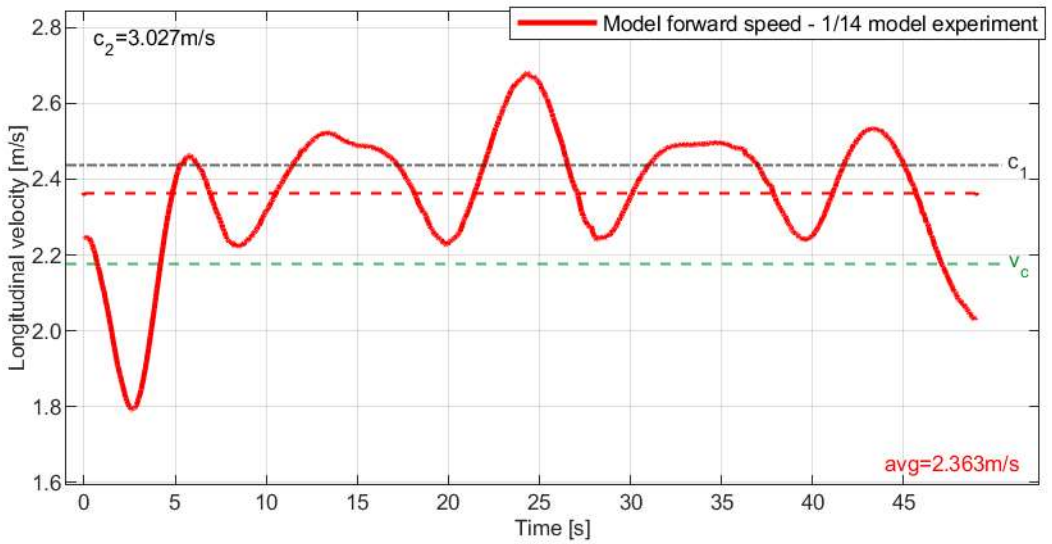

Figure 3.46 Case No. B110 Bi-chromatic wave; λ_1=3.802m; c_1=2.437m/s; A_1=0.032m; λ_2=5.867m; c_2=3.027m/s; A_2=0.016m; v_c=2.178m/s; T_{E1}=51.13s; T_{E2}=8.826s; Oscillatory surf-riding on primary wave

The cases shown in Figure 3.47 thru Figure 3.52 were carried out using the secondary wave with the length of $\lambda_2 \approx 7.89$ m. All of these cases show *oscillatory surf-riding on primary wave* type response. The amplitude ranging, from A_2=0.006m up to A_2=0.015m, seems to only influence the amplitude of oscillations around the primary wave celerity, similar to the results shown above in Figures 3.41 to 3.46

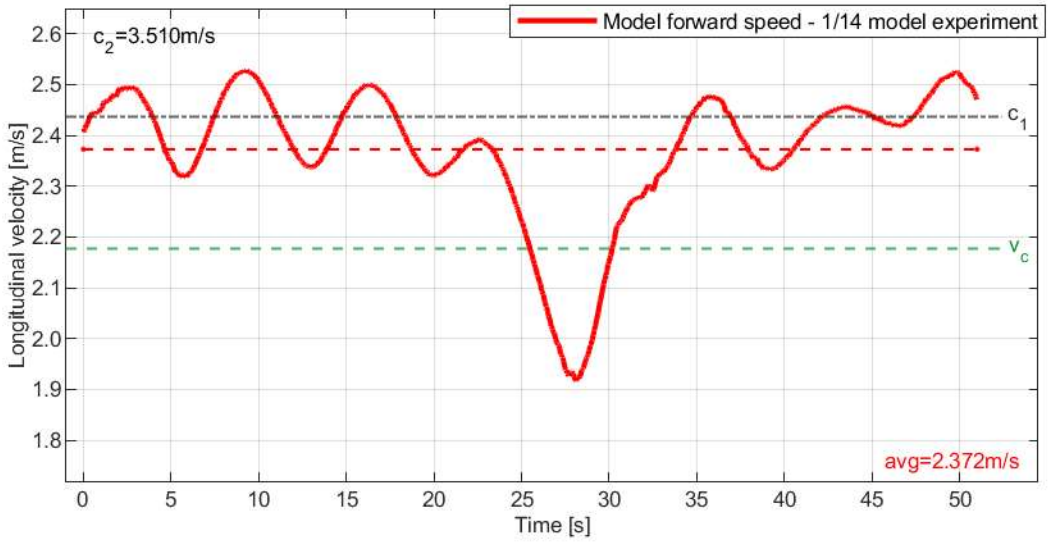

Figure 3.47 Case No. B139 Bi-chromatic wave; λ_1=3.802m; c_1=2.437m/s; A_1=0.031m; λ_2=7.888m; c_2=3.510m/s; A_2=0.006m; v_c=2.178m/s; T_{E1}=58.96s; T_{E2}=6.933s; Oscillatory surf-riding on primary wave

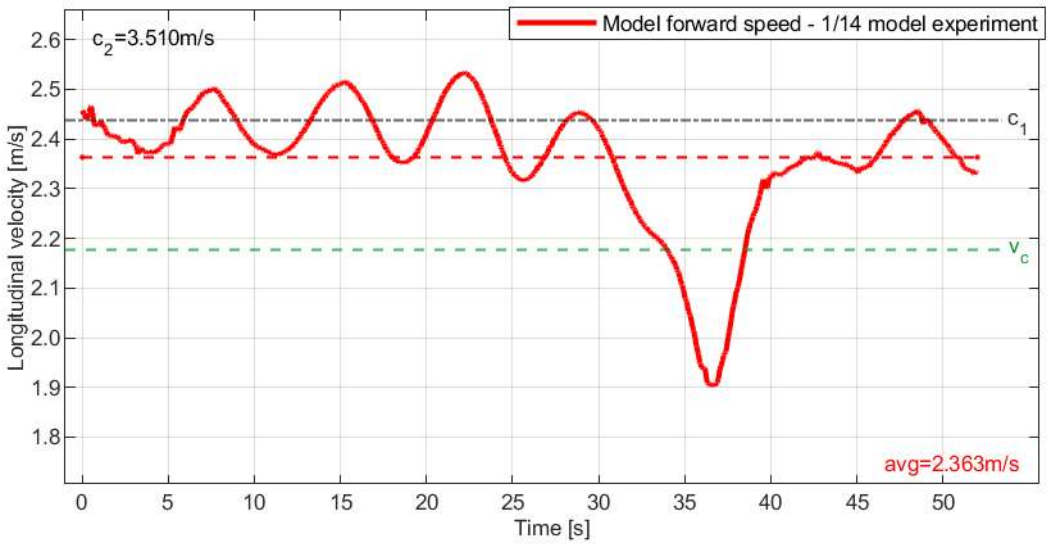

Figure 3.48 Case No. B112 Bi-chromatic wave; λ_1=3.802m; c_1=2.437m/s; A_1=0.032m; λ_2=7.888m; c_2=3.510m/s; A_2=0.007m; v_c=2.178m/s; T_{E1}=51.6s; T_{E2}=6.877s; Oscillatory surf-riding on primary wave

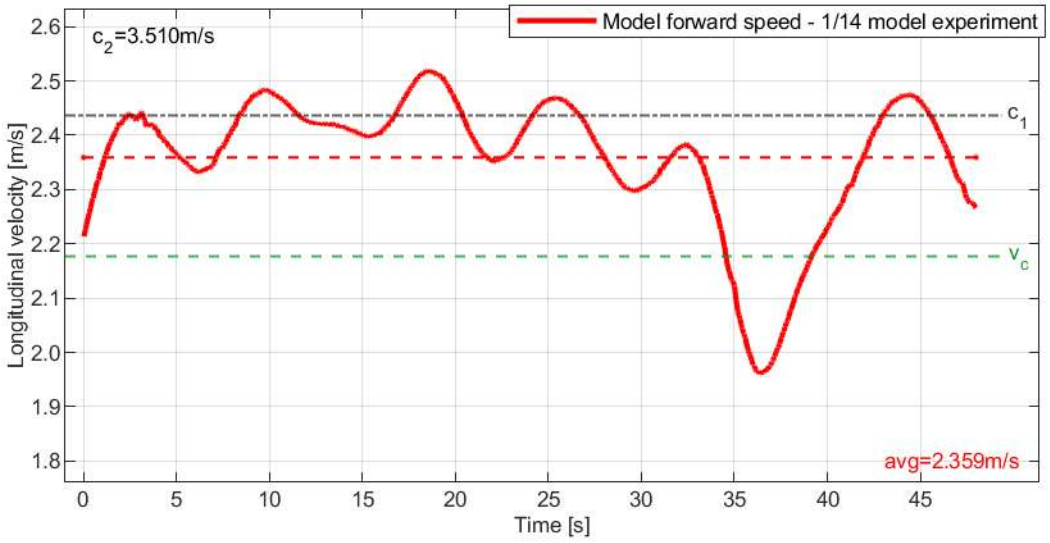

Figure 3.49 Case No. B135 Bi-chromatic wave; λ_1=3.802m; c_1=2.437m/s; A_1=0.031m; λ_2=7.888m; c_2=3.510m/s; A_2=0.009m; v_c=2.178m/s; T_{E1}=48.72s; T_{E2}=6.851s; Oscillatory surf-riding on primary wave

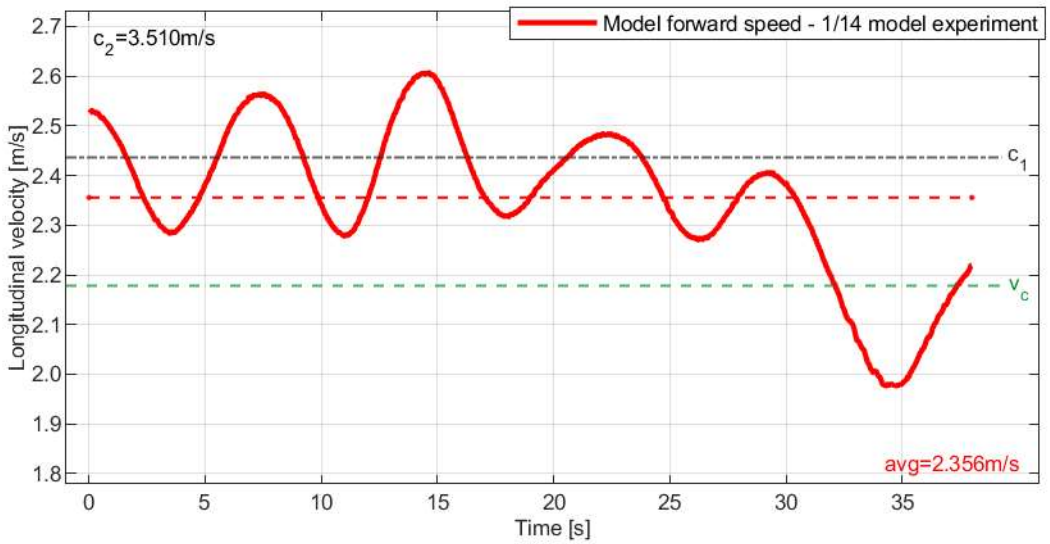

Figure 3.50 Case No. B114 Bi-chromatic wave; λ_1=3.802m; c_1=2.437m/s; A_1=0.032m; λ_2=7.888m; c_2=3.510m/s; A_2=0.011m; v_c=2.178m/s; T_{E1}=46.78s; T_{E2}=6.832s; Oscillatory surf-riding on primary wave

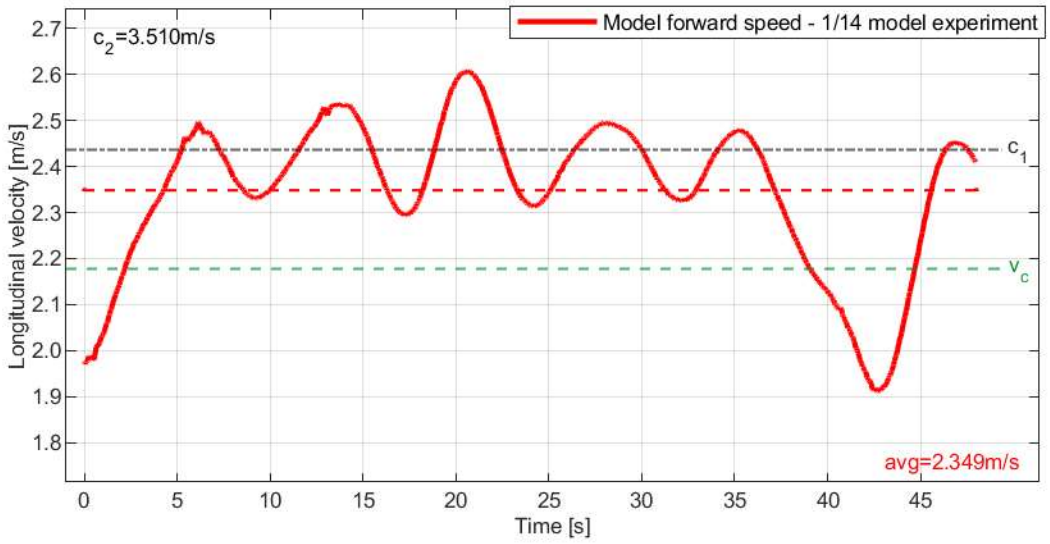

Figure 3.51 Case No. B119 Bi-chromatic wave; λ_1=3.802m; c_1=2.437m/s; A_1=0.032m; λ_2=7.888m; c_2=3.510m/s; A_2=0.013m; v_c=2.178m/s; T_{E1}=42.97s; T_{E2}=6.79s; Oscillatory surf-riding on primary wave

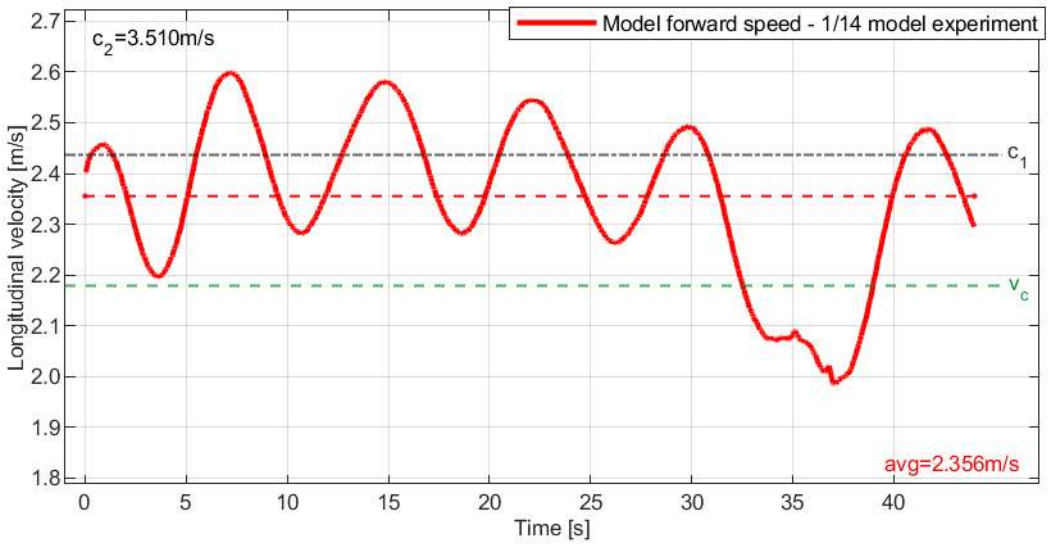

Figure 3.52 Case No. B117 Bi-chromatic wave; λ_1=3.802m; c_1=2.437m/s; A_1=0.030m; λ_2=7.888m; c_2=3.510m/s; A_2=0.015m; v_c=2.178m/s; T_{E1}=46.67s; T_{E2}=6.831s; Oscillatory surf-riding on primary wave

The three cases shown further on, presented in Figures 3.53, 3.54 and 3.55, demonstrate the sensitivity of the experiment to changes in the parameters of the runs. The cases B175, B176 and B177, were carried out using a bi-chromatic wave with the following parameters: $\lambda_1 \approx 2.84$ m, $A_1 \approx 0.008$ m, $\lambda_2 \approx 1.09$ m, $A_2 \approx 0.045$ m. In case B175 the commanded speed was v_c=1.839 m/s, in cases B176 and B177 the commanded speed was v_c=1.915 m/s.

The results of case B175 can be described as a hybrid of *high-runs on secondary wave* with *high-runs on primary wave* in between. Thru the run the ship model appears to oscillate with the characteristic of *high-run*, however, it seems to change the wave component to which it is attracted.

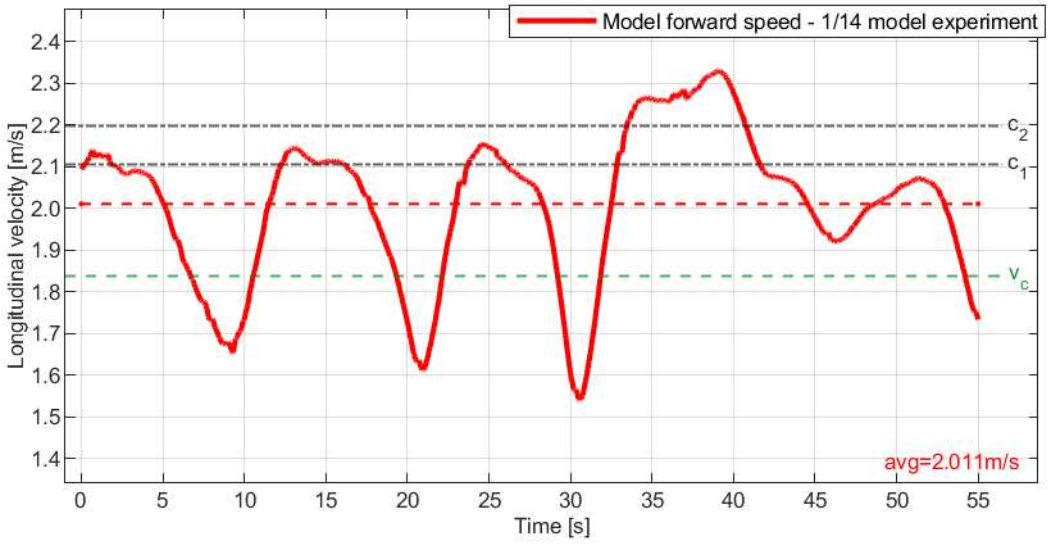

Figure 3.53 Case No. B175 Bi-chromatic wave; λ_1=2.837m; c_1=2.105m/s; A_1=0.009m; λ_2=3.090m; c_2=2.197m/s; A_2=0.045m; v_c=1.839m/s; T_{E1}=30.15s; T_{E2}=16.62s; High-runs on primary wave/ high-runs on secondary wave

Case B176 is difficult to categorize because there is no apparent attraction to any of the wave celerities. The ship model seems to be attracted to the secondary wave celerity up to 10th second of the run, however, around 25th second it accelerates up to 2.5 m/s. Then the ship model decelerates and changes the response type to *high-runs on secondary wave*.

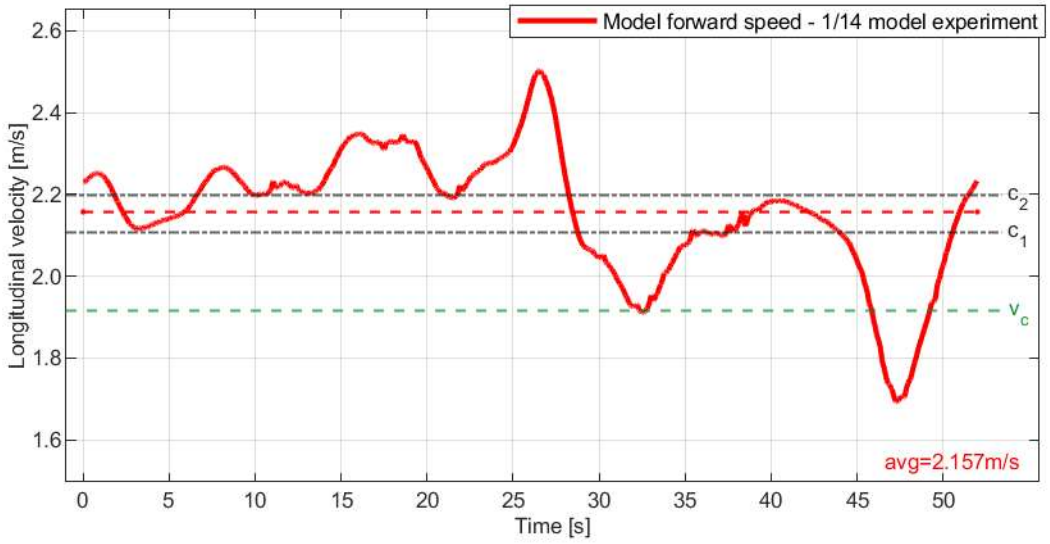

Figure 3.54 Case No. B176 Bi-chromatic wave; λ_1=2.837m; c_1=2.105m/s; A_1=0.008m; λ_2=3.090m; c_2=2.197m/s; A_2=0.042m; v_c=1.915m/s; T_{E1}=-55s; T_{E2}=76.86s; Uncertain case

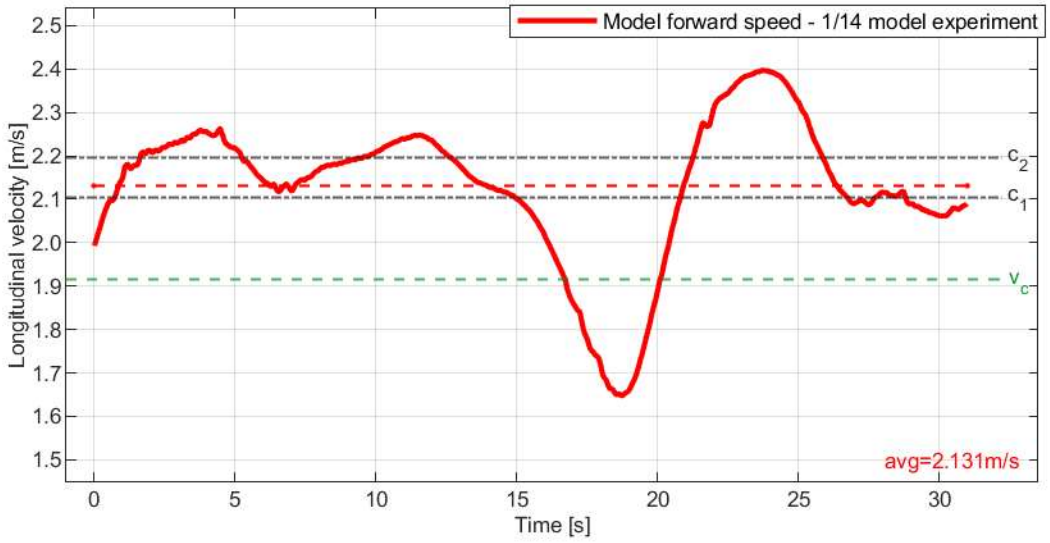

Figure 3.55 Case No. B177 Bi-chromatic wave; λ_1=2.837m; c_1=2.105m/s; A_1=0.005m; λ_2=3.090m; c_2=2.197m/s; A_2=0.046m; v_c=1.915m/s; T_{E1}=-109.9s; T_{E2}=46.84s; Uncertain case

The last runs of the 1/14 scale experiment were cases from B183 to B191, the results of which are shown in Figures 3.56 to 3.64, were carried out using the bi-chromatic wave with the following parameters: λ_1≈2.96 m, A_1≈0.008 m, λ_2≈3.30 m, A_2≈0.050 m. The varying parameter was the commanded speed, which was set up according to the scenarios presented in Table 2.8. This part of the study aimed to check what happens when the speed is reduced to a state close to *surf-riding on secondary wave*.

Case B183 shown in Figure 3.56, where the commanded speed was v_c=1.980 m/s, the phenomenon of *surf-riding on secondary wave* occurs between 10 and 30 second of the run. Rest of the run could be categorized as *high-runs on secondary wave*, however, the run-time is not sufficient to be certain. Case B184 shown in Figure 3.57 commenced for the same parameters results in *surf-riding on secondary wave* between 2nd and 15th second. In this case between 25th and 50th second *high-runs on secondary wave* are more evident.

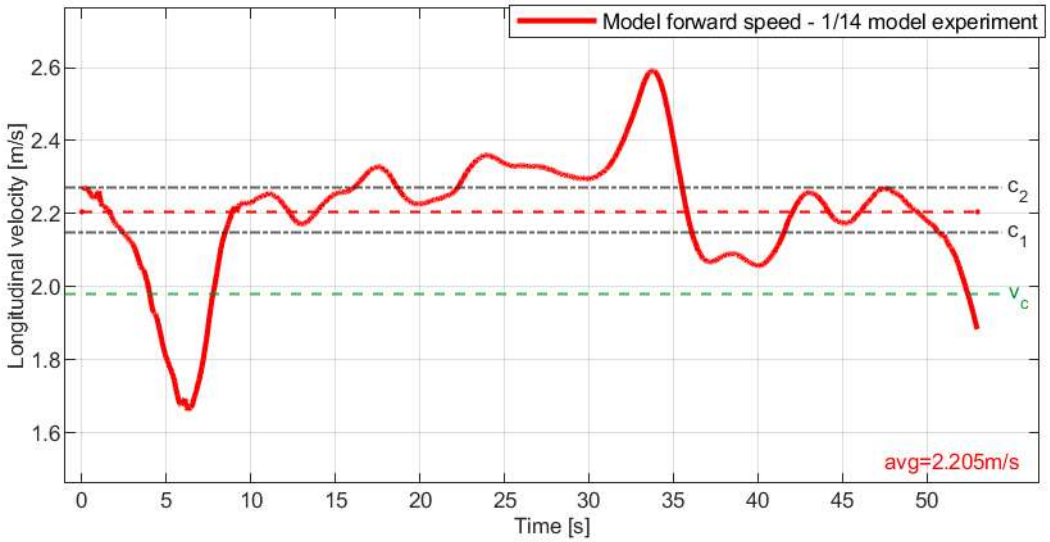

Figure 3.56 Case No. B183 Bi-chromatic wave; λ_1=2.956m; c_1=2.149m/s; A_1=0.009m; λ_2=3.300m; c_2=2.271m/s; A_2=0.049m; v_c=1.980m/s; T_{E1}=-52.48s; T_{E2}=50.4s; Surf-riding on secondary wave/ high-runs on secondary wave

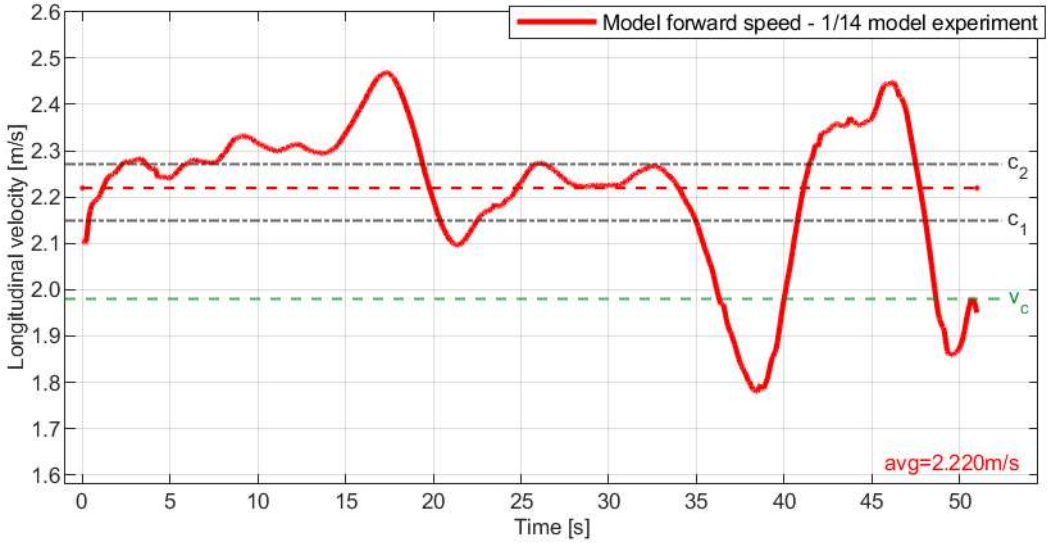

Figure 3.57 Case No. B184 Bi-chromatic wave; λ_1=2.956m; c_1=2.149m/s; A_1=0.009m; λ_2=3.300m; c_2=2.271m/s; A_2=0.051m; v_c=1.980m/s; T_{E1}=-41.71s; T_{E2}=64.79s; Surf-riding on secondary wave/ high-runs on secondary wave

In the case B185 shown in Figure 3.58, where the commanded speed was decreased to v_c=1.915 m/s, the phenomenon of *surf-riding on secondary wave* was not observed. From t=20s to t=40s *surf-riding on primary wave* seems to occur after a quick acceleration that started near t=18s. *Surging* started at t=40s and lasted until the end of the run.

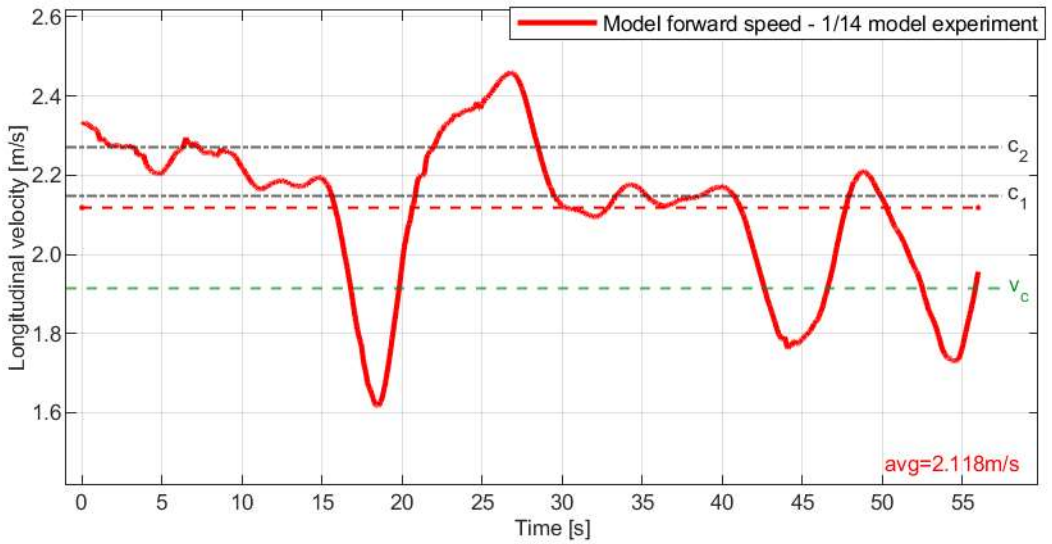

Figure 3.58 Case No. B185 Bi-chromatic wave; λ_1=2.956m; c_1=2.149m/s; A_1=0.006m; λ_2=3.300m; c_2=2.271m/s; A_2=0.050m; v_c=1.915m/s; T_{E1}=96.65s; T_{E2}=21.66s; Surf-riding on primary wave/ surging

In cases B186 and B187, shown in Figure 3.59 and Figure 3.60, conducted for the same parameters as case B185. In both cases *surf-riding* occurs, however, determining which of the wave components is attracting the model is challenging. In case B186 *surf-riding* is observed between t=17s and t=40s. In case B187 *surf-riding* is observed between t=20s and t=36s. The remaining time of the runs shows the *high-runs on secondary wave* phenomenon.

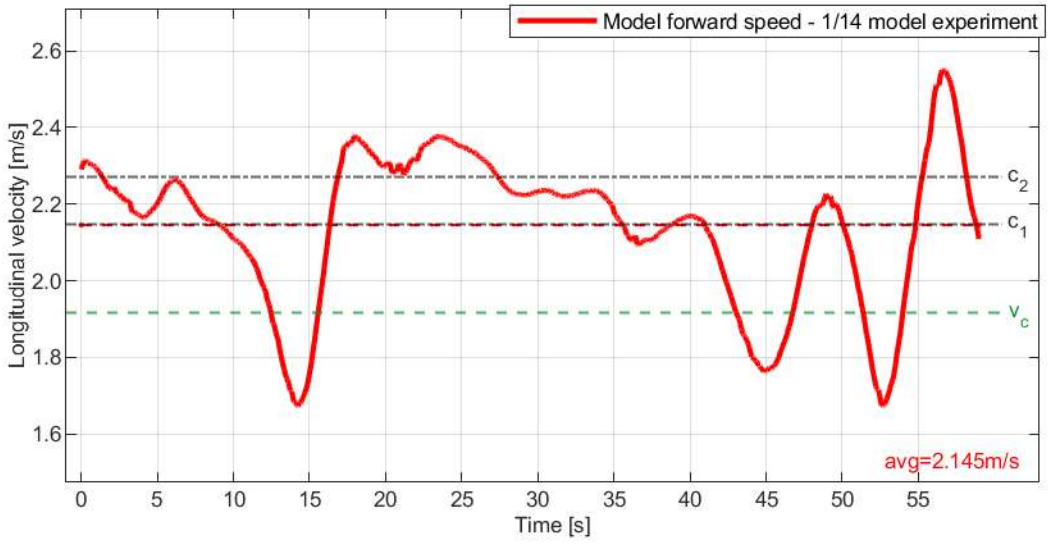

Figure 3.59 Case No. B186 Bi-chromatic wave; λ_1=2.956m; c_1=2.149m/s; A_1=0.009m; λ_2=3.300m; c_2=2.271m/s; A_2=0.049m; v_c=1.915m/s; T_{E1}=923.6s; T_{E2}=26.4s; Surf-riding/ high-runs on secondary wave

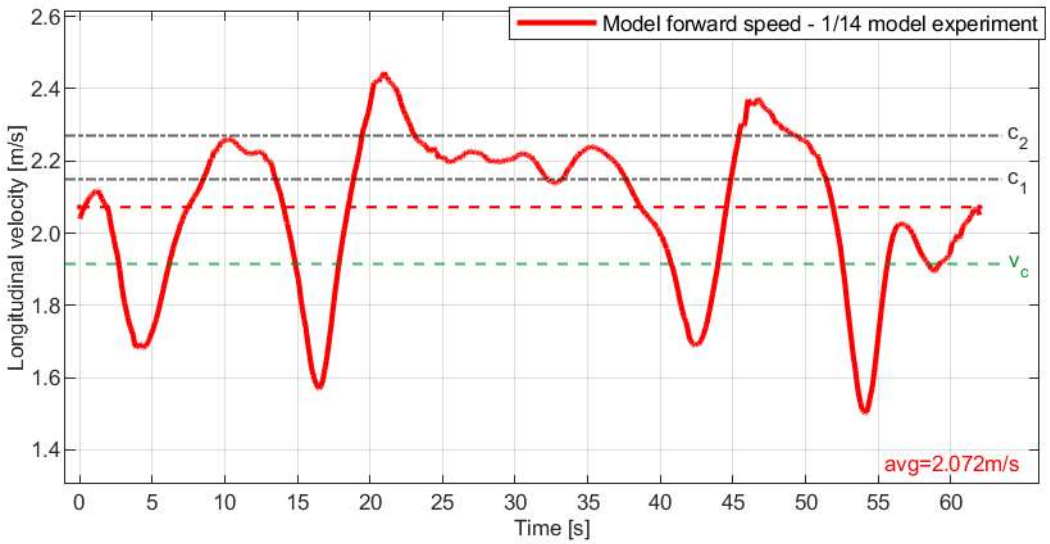

Figure 3.60 Case No. B187 Bi-chromatic wave; λ_1=2.956m; c_1=2.149m/s; A_1=0.007m; λ_2=3.300m; c_2=2.271m/s; A_2=0.050m; v_c=1.915m/s; T_{E1}=38.68s; T_{E2}=16.65s; Surf-riding/ high-runs on secondary wave

Cases B188 and B189, shown in Figure 3.61 and Figure 3.62, the commanded speed was further reduced down to v_c=1.839 m/s. In case B188 *high-runs* are observed except between t=20s and t=30s, when there was *surf-riding on secondary wave* occurring. In case B189, *high-runs on secondary wave* are observed up to t=40s, followed by *high-runs on primary wave*.

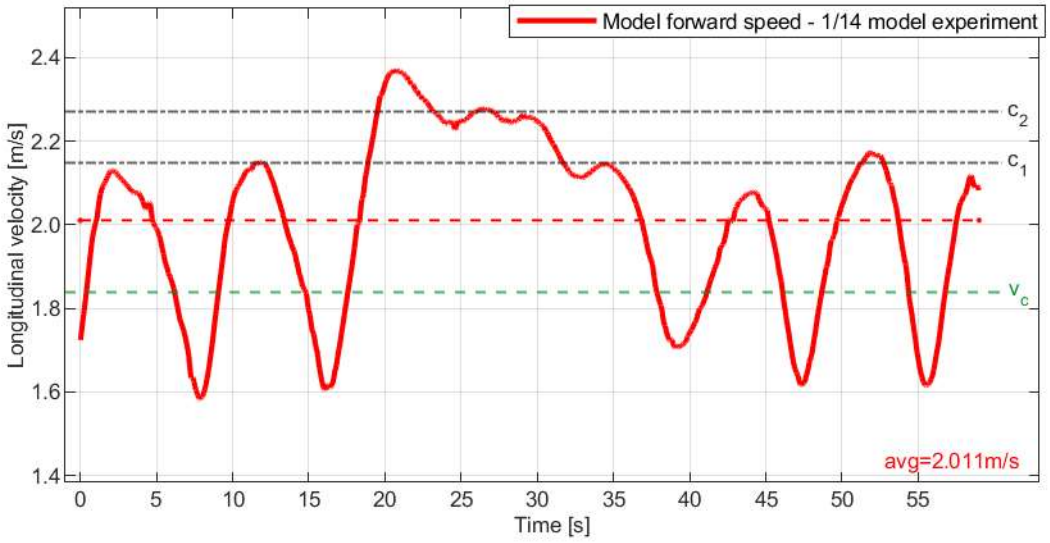

Figure 3.61 Case No. B188 Bi-chromatic wave; λ_1=2.956m; c_1=2.149m/s; A_1=0.006m; λ_2=3.300m; c_2=2.271m/s; A_2=0.050m; v_c=1.839m/s; T_{E1}=21.39s; T_{E2}=12.69s; High-runs on primary wave/ surf-riding on secondary wave

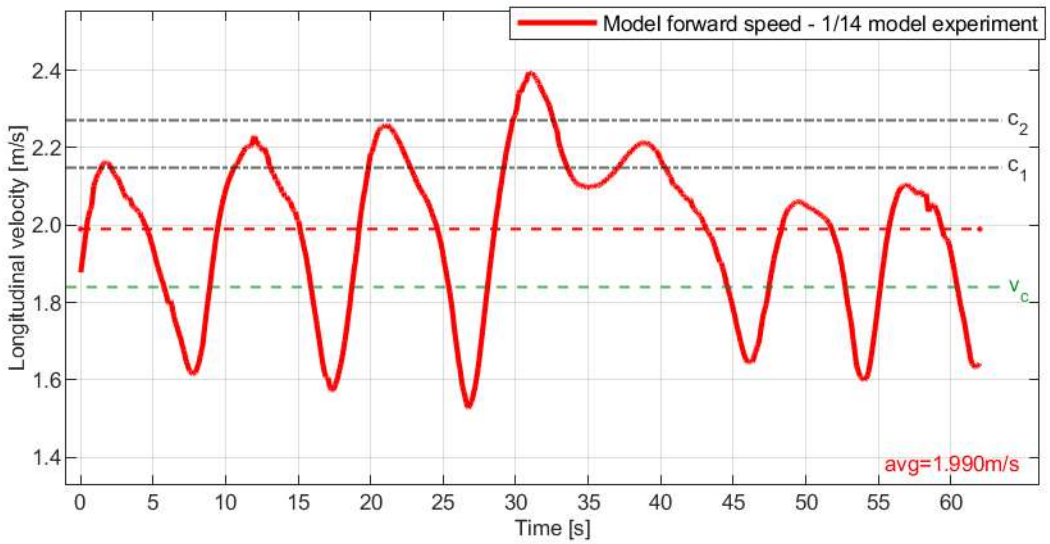

Figure 3.62 Case No. B189 Bi-chromatic wave; λ_1=2.956m; c_1=2.149m/s; A_1=0.009m; λ_2=3.300m; c_2=2.271m/s; A_2=0.051m; v_c=1.839m/s; T_{E1}=18.61s; T_{E2}=11.76s; High-runs on secondary wave/ high-runs on primary wave

In cases B190 and B191, shown in Figure 3.63 and Figure 3.64, the commanded speed was set to v_c=1.730 m/s. Both cases seem to be closer to *beating surging* than to *high-runs* because there is no significant asymmetry in *surging* observed. In each case one *high-run on secondary wave* is observed, in case B190 around t=20s, in case B191 around t=41s.

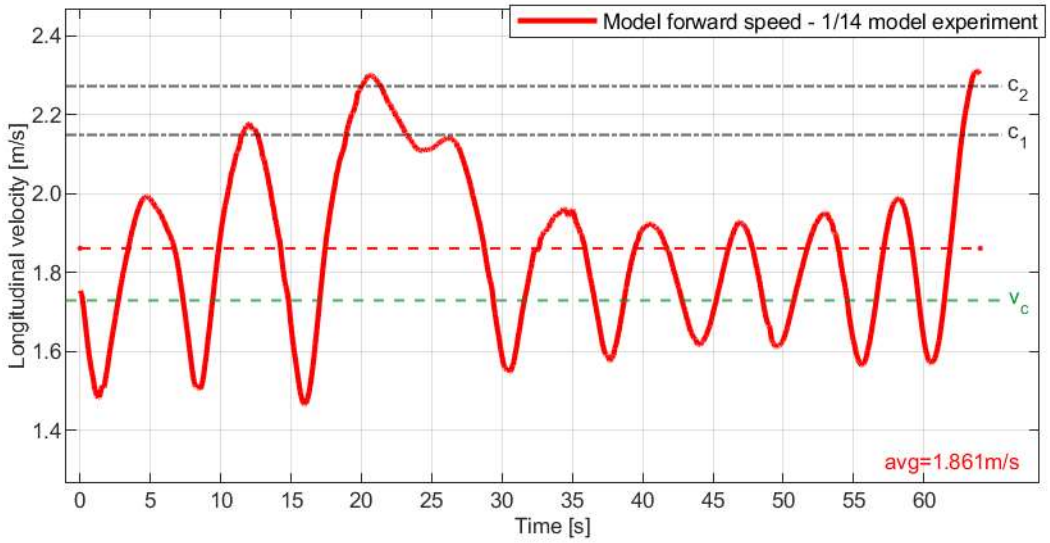

Figure 3.63 Case No. B190 Bi-chromatic wave; λ_1=2.956m; c_1=2.149m/s; A_1=0.007m; λ_2=3.300m; c_2=2.271m/s; A_2=0.051m; v_c=1.730m/s; T_{E1}=10.28s; T_{E2}=8.063s; Beating surging/ high-runs on secondary wave

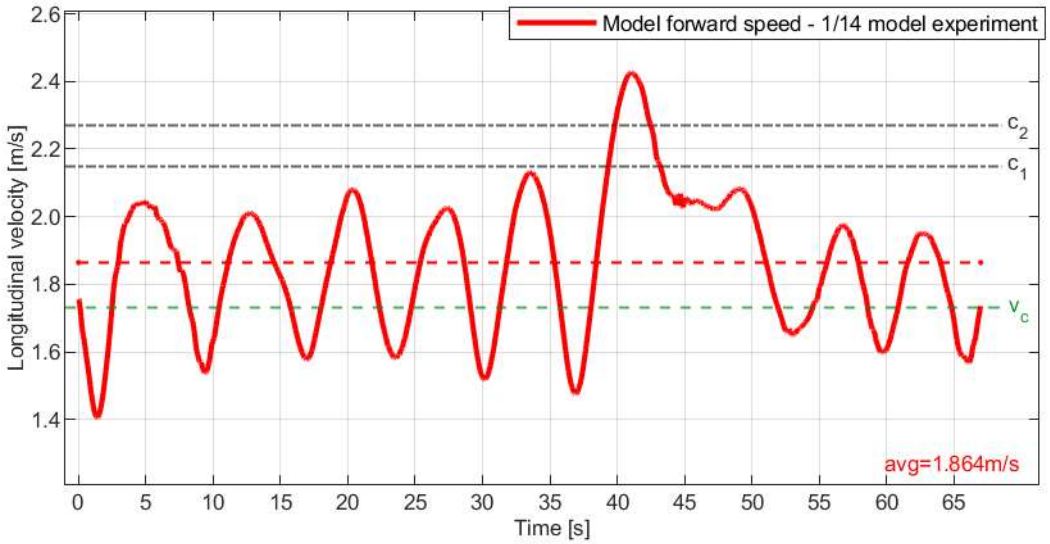

Figure 3.64 Case No. B191 Bi-chromatic wave; λ_1=2.956m; c_1=2.149m/s; A_1=0.008m; λ_2=3.300m; c_2=2.271m/s; A_2=0.050m; v_c=1.730m/s; T_{E1}=10.39s; T_{E2}=8.125s; Beating surging/ high-runs on secondary wave

The expanded results for all of the cases conducted in the bi-chromatic seas can be found in Appendix B.

3.4. Comparison of experiments: 1/64 vs. 1/14 scale

This part of the research compares the results obtained in the experiments conducted in a 1/14 scale and a 1/64 scale. The scenarios used to perform the following comparison are presented in Table 2.9. The results of experiment at a 1/14 scale are rescaled to a 1/64 scale. The data presented thru Figure 3.65 to Figure 3.78 consists of the model's longitudinal velocity in time, in case of the 1/64 model as a bold blue line, in case of the 1/14 model a bold red line, the commanded speed v_c (dashed green line), the two wave components celerities c_1 and c_2 (dashed black dotted lines) as well as the average speed of the ship model marked with a dashed line the same color as velocity plot. For clarity of the results representation, both experiments are presented in common plots, comparing the corresponding cases.

Surf-riding on primary wave in was observed at a scale of 1/14 in case C1 shown in Figure 3.65 and case C2 shown in Figure 3.66. While *beating surging* was observed at a scale of 1/64.

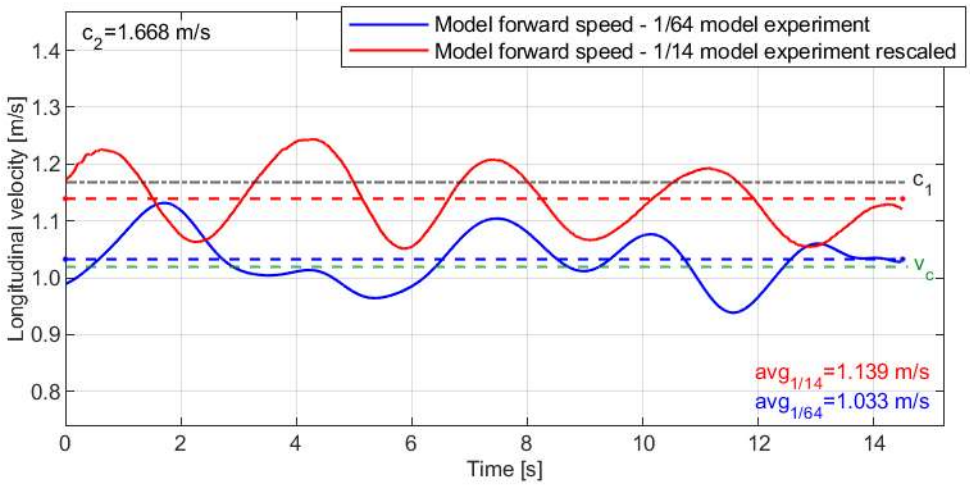

Figure 3.65 Case No. C1 Bi-chromatic wave; λ_1=0.875m=LBP*1.591; c_1=1.169m/s; A_1=0.006m; λ_2=1.781m; c_2=1.668m/s; A_2=0.004m; v_c=1.020m/s

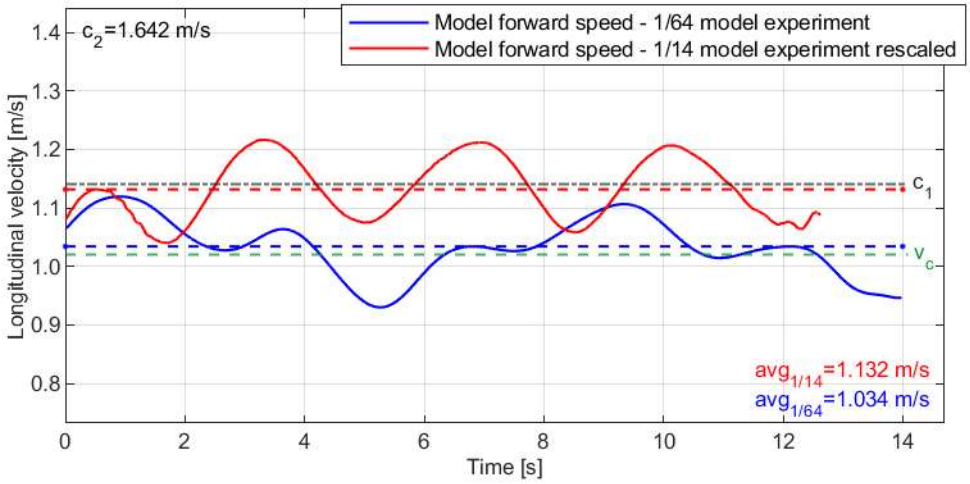

Figure 3.66 Case No. C2 Bi-chromatic wave; λ_1=0.832m=LBP*1.512; c_1=1.140m/s; A_1=0.006m; λ_2=1.726m; c_2=1.642m/s; A_2=0.003m; v_c=1.020m/s

In case C3 shown in Figure 3.67 at a scale of 1/14, a transition between celerities was observed at t=6s and release at around t=12s. At a scale of 1/64 high-runs are occurring at around 2nd, 6th, 10th and 15th second of the run.

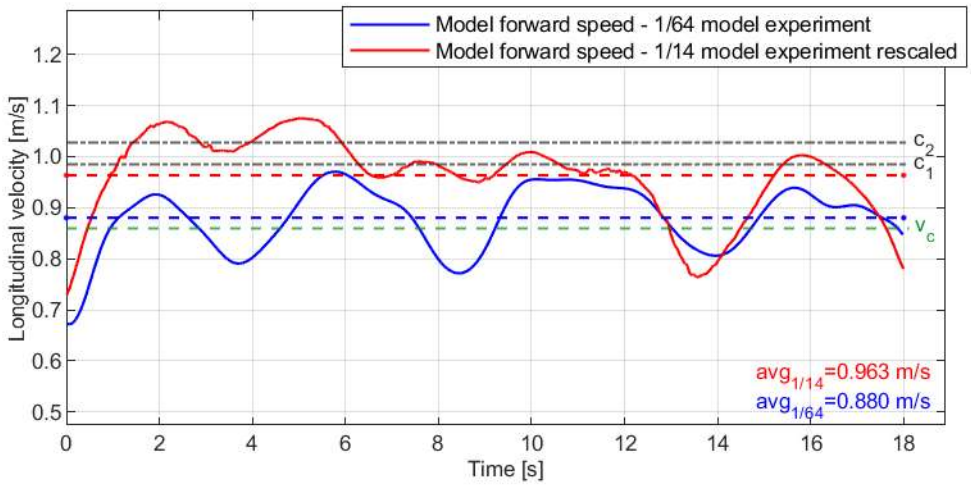

Figure 3.67 Case No. C3 Bi-chromatic wave; λ_1=0.621m=LBP*1.129; c_1=0.985m/s; A_1=0.001m; λ_2=0.676m; c_2=1.028m/s; A_2=0.010m; v_c=0.860m/s

Case C4 shown in Figure 3.68 for a scale of 1/14 a catch is observed at around t=5s and a transition between celerities occurs at around t=12s. At a scale of 1/64 *surging* is observed.

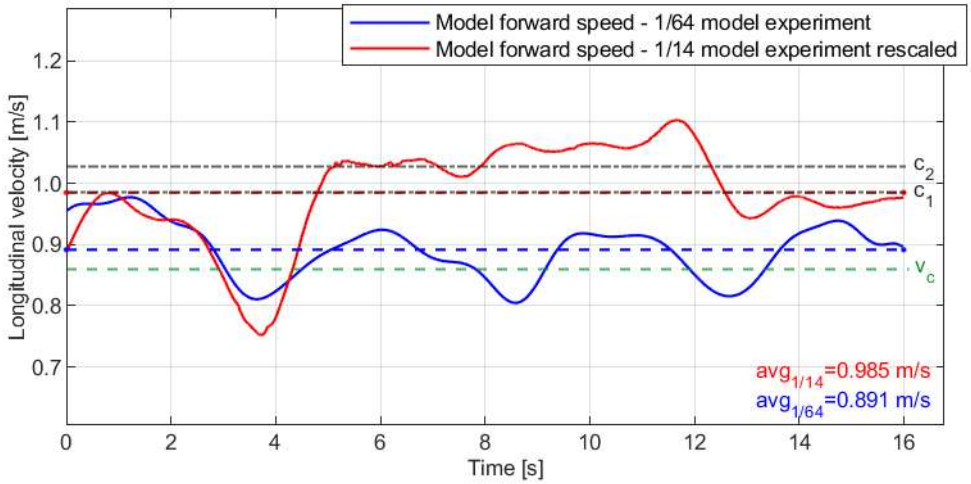

Figure 3.68 Case No. C4 Bi-chromatic wave; λ_1=0.621m=LBP*1.129; c_1=0.985m/s; A_1=0.002m; λ_2=0.676m; c_2=1.028m/s; A_2=0.010m; v_c=0.860m/s

In case C5 shown in Figure 3.69 at the 1/14 scale we observe *high-runs on secondary wave* while there is *surging* at a scale of 1/64. In case C6 shown in Figure 3.70 at both scales we can observe *high-runs on secondary wave*.

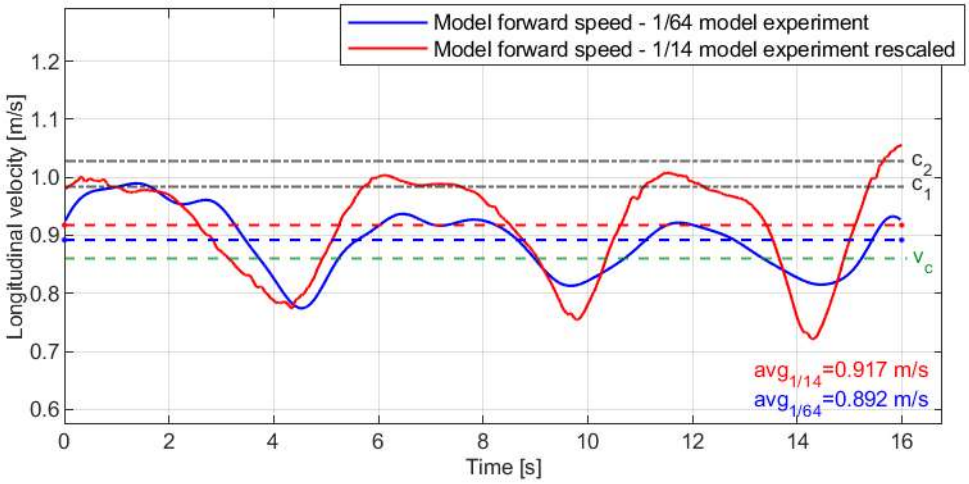

Figure 3.69 Case No. C5 Bi-chromatic wave; λ_1=0.621m=LBP*1.129; c_1=0.985m/s; A_1=0.002m; λ_2=0.676m; c_2=1.028m/s; A_2=0.010m; v_c=0.860m/s

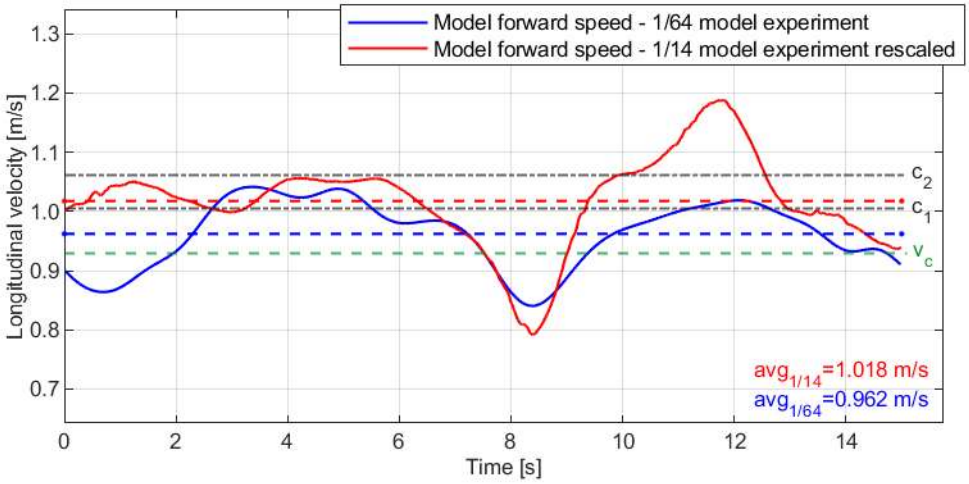

Figure 3.70 Case No. C6 Bi-chromatic wave; λ_1=0.647m=LBP*1.176; c_1=1.005m/s; A_1=0.002m; λ_2=0.722m; c_2=1.062m/s; A_2=0.010m; v_c=0.930m/s

Case C7, shown in Figure 3.71, at both scales is classified as *high-runs on secondary wave*, however at a scale of 1/14 timeframe indicates that *surf-riding on secondary wave* occurs. For the scale of 1/14 cases were categorized in a wider timeframe than shown on graphs. In case C8, shown in Figure 3.72, *surf-riding on secondary wave* occurs at the 1/14 scale while *high-runs on secondary wave* are seen at the 1/64 scale.

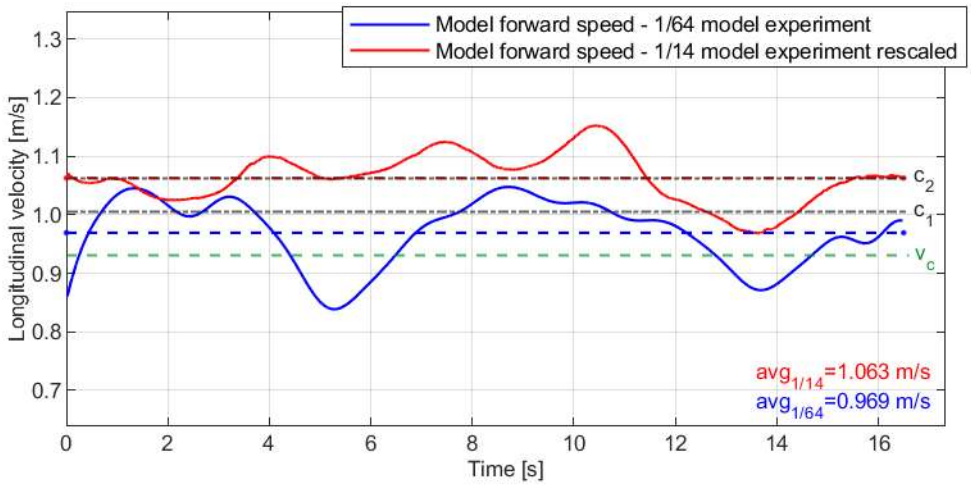

Figure 3.71 Case No. C7 Bi-chromatic wave; λ_1=0.647m=LBP*1.176; c_1=1.005m/s; A_1=0.001m; λ_2=0.722m; c_2=1.062m/s; A_2=0.011m; v_c=0.930m/s

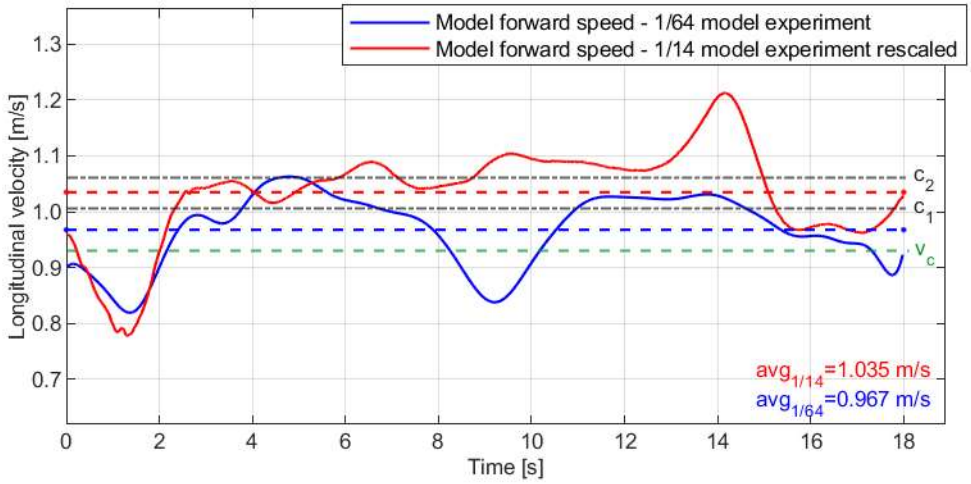

Figure 3.72 Case No. C8 Bi-chromatic wave; λ_1=0.647m=LBP*1.176; c_1=1.005m/s; A_1=0.002m; λ_2=0.722m; c_2=1.062m/s; A_2=0.011m; v_c=0.930m/s

In cases C9 and C10, shown in Figure 3.73 and Figure 3.74, at the scale of 1/64 *high-runs on primary wave* were observed, while at the scale of 1/14 catch and release with transition between celerities was observed.

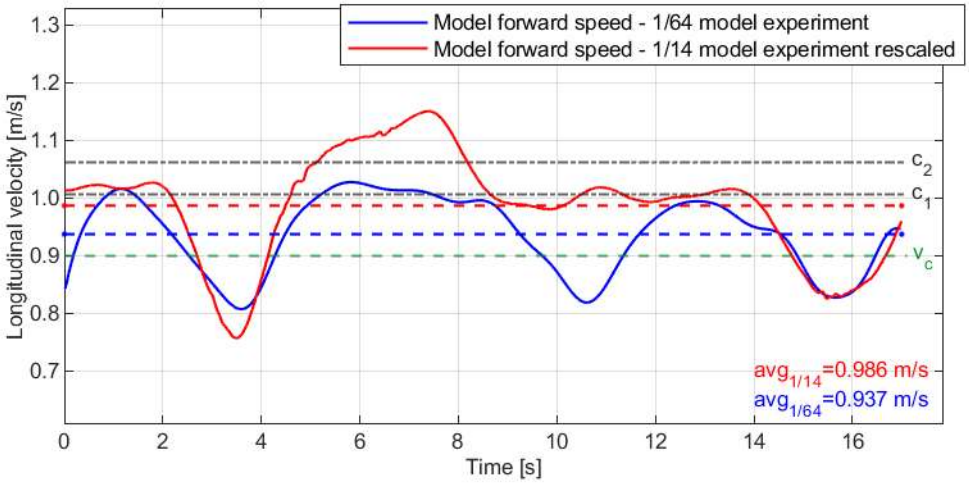

Figure 3.73 Case No. C9 Bi-chromatic wave; λ_1=0.647m=LBP*1.176; c_1=1.005m/s; A_1=0.001m; λ_2=0.722m; c_2=1.062m/s; A_2=0.011m; v_c=0.900m/s

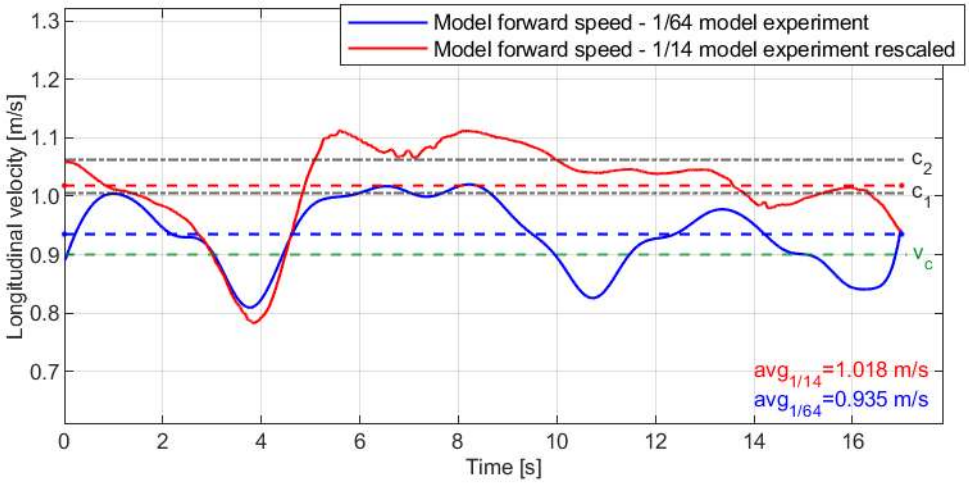

Figure 3.74 Case No. C10 Bi-chromatic wave; λ_1=0.647m=LBP*1.176; c_1=1.005m/s; A_1=0.002m; λ_2=0.722m; c_2=1.062m/s; A_2=0.011m; v_c=0.900m/s

In case C11, shown in Figure 3.75, there was *surging* at the scale of 1/64 and catch and release with transition between celerities at the 1/14 scale.

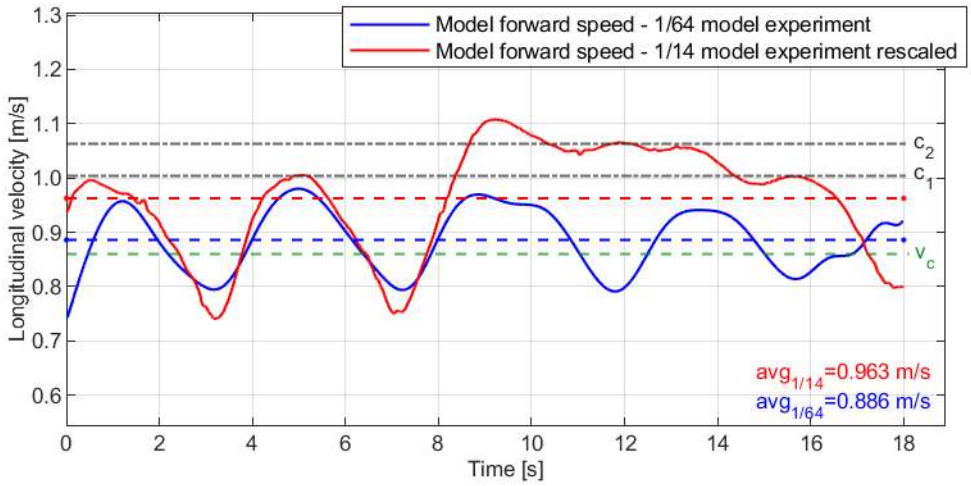

Figure 3.75 Case No. C11 Bi-chromatic wave; λ_1=0.647m=LBP*1.176; c_1=1.005m/s; A_1=0.001m; λ_2=0.722m; c_2=1.062m/s; A_2=0.011m; v_c=0.860m/s

In case C12, shown in Figure 3.76, there were *high-runs on secondary wave* at the 1/14 scale and *beating surging* at the scale of 1/64. In cases C13 and C14, shown in Figure 3.77 and Figure 3.78, all results show *beating surging* type response.

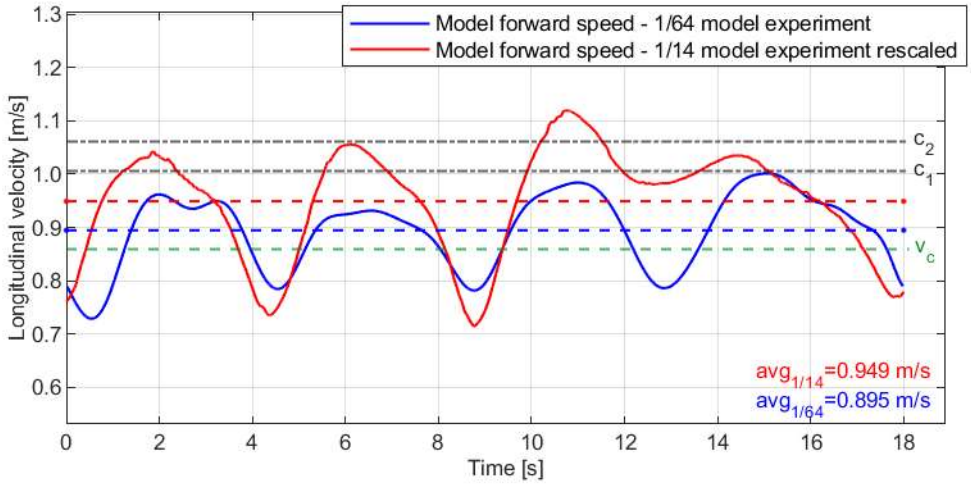

Figure 3.76 Case No. C12 Bi-chromatic wave; λ_1=0.647m=LBP*1.176; c_1=1.005m/s; A_1=0.002m; λ_2=0.722m; c_2=1.062m/s; A_2=0.011m; v_c=0.860m/s

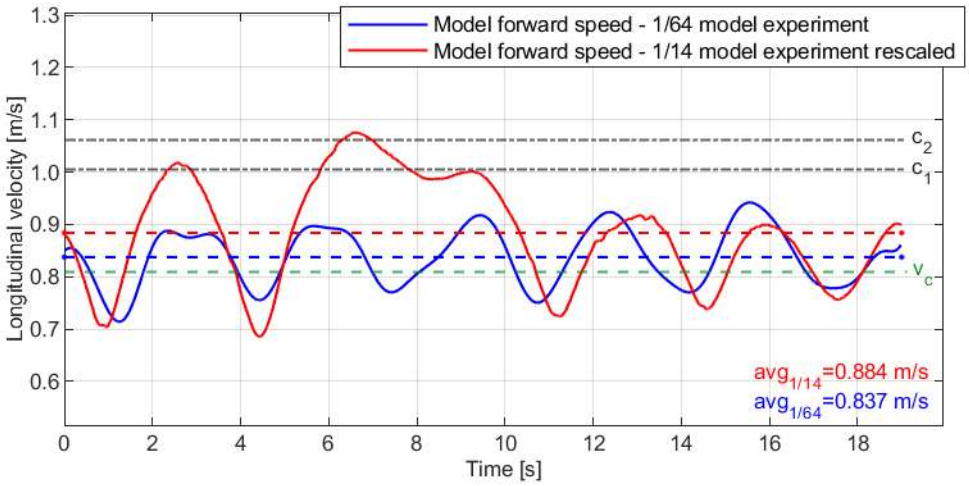

Figure 3.77 Case No. C13 Bi-chromatic wave; λ_1=0.647m=LBP*1.176; c_1=1.005m/s; A_1=0.002m; λ_2=0.722m; c_2=1.062m/s; A_2=0.011m; v_c=0.810m/s

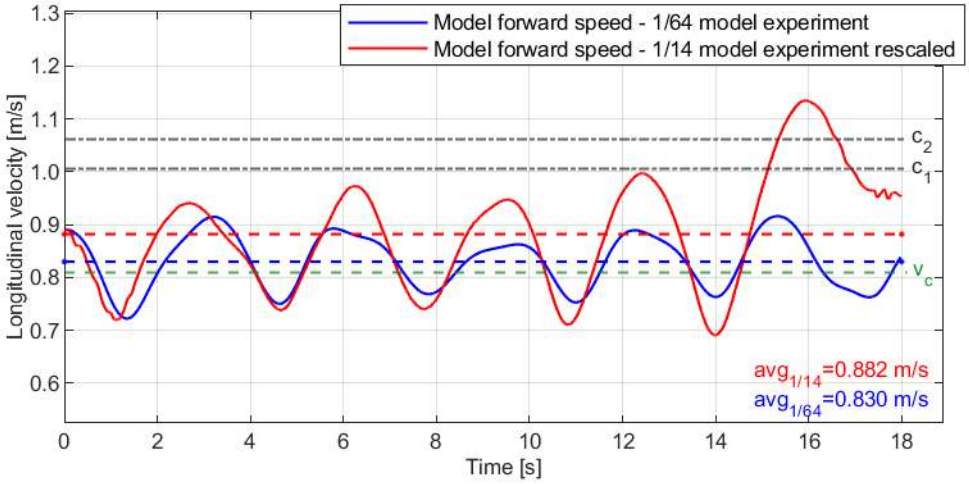

Figure 3.78 Case No. C14 Bi-chromatic wave; λ_1=0.647m=LBP*1.176; c_1=1.005m/s; A_1=0.002m; λ_2=0.722m; c_2=1.062m/s; A_2=0.011m; v_c=0.810m/s

Despite the seemingly substantial number of comparable cases ending in qualitatively different outcomes, overall, the results are not so divergent, as discussed in more detail in the discussion section.

4. DISCUSSION

4.1. Main findings

During the experiments at the scale of 1/14 and 1/64 in regular wave conditions known phenomena was observed including:

- Asymmetric surging behavior (e.g., case A11);
- Attraction to surf-riding equilibrium, observed as small-amplitude oscillations near the wave celerity (e.g., case A12, B78);
- "Catch-and-release" dynamics indicating potential coexistence of surging and surf-riding states (e.g., case A13, B80, B82);
- Homoclinic transitions: increasing commanded speed progressively shifts the system from surging to surf-riding, potentially through transient coexistence states (e.g., cases A10 -> A15).

These phenomena were consistently observed within the brief measurement timeframe, aligning with established theoretical predictions of surf-riding dynamics.

The expected results were observed on the regular wave, so it was decided that the experimental setup was sufficient for further bi-chromatic wave experiments and that the research methodology did not require any major changes. Experiments on regular waves were also used to determine the surf-riding commanded speed threshold. This value was later used, for example, in one of the series of runs for the 1/14 scale.

4.1.1.*Experiments involving bi-chromatic waves conducted at a scale of 1/64*

Experimental findings from the bi-chromatic wave runs illustrate velocity oscillations around the celerity of a dominant wave component as identified in Spyrou et al.(2016). These results demonstrate strong alignment with the observations in Warnke-Olewniczak & Krata (2024). The results reveal repeatedly captured six out of eight theoretically predicted phenomena, as follows:

- *Beating oscillations in surge (case A1);*
- *High-speed runs on primary wave (case A2);*
- *Surf-riding on primary wave (case A3);*
- *Low-speed runs on primary wave (case A4);*
- *Surging due to attraction to secondary wave (case A9);*
- *Surf-riding on secondary wave (case A7).*

Notably, the *high-runs on the secondary wave* and *low-runs on the secondary wave* remain unobserved, possibly due to limitations in the tank length and as well as the high sensitivity of these phenomena to operational parameters.

4.1.2. *Experiments in bi-chromatic waves conditions conducted at a scale of 1/14*

Similar to the experiments conducted at the 1/64 scale, a variety of ship response types were also observed at the 1/14 scale. These results further reinforce the validity of the findings presented by Spyrou et al. (2016). Table 4.1 summarizes the response types observed in the three sets of runs, which aimed to investigate changes in the response type as commanded speed increased. The results indicate that higher commanded speeds settings lead to a "higher energy" response in each experimental set. Under the same wave conditions, the ship could exhibit surf-riding, surging, or susceptibility to high-runs, depending on the propeller revolution rate, thus the thrust.

Oscillatory and hybrid responses were also observed. While the oscillatory behavior (e.g., case B132, B117) is easily identifiable, the hybrid responses (e.g., case B175, B189) are more challenging to characterize. It is likely that the proposed term "trebuchet" (e.g., case B45, B104), describes the hybrid response. The transition from the primary to the secondary wave during the initial surf-riding results in high acceleration indicating a strong attraction to the surf-riding quasi-equilibrium. Even though the term "trebuchet" is not yet sufficiently established among the community, it has been made up to analogize the observed phenomenon, namely the waves accelerating a vessel exhibit behavior similar to how a trebuchet uses a double-pendulum mechanism to propel a projectile.

Table 4.1 Classification of results of bi-chromatic wave cases conducted at a scale of 1/14 showing changes in response type observed with increasing commanded speed

Case No.	Figure	Response type
B29	3.22	*Beating surging*
B30	3.23	*High-runs on primary wave*
B31	3.24	*Surf-riding on primary wave*
B38	3.25	*Surf-riding on primary wave*
B40	3.27	*Beating surging*
B41	3.28	*Beating surging*
B42	3.29	*High-runs on primary wave*
B43	3.30	*High-runs on primary wave*
B44	3.31	*High-runs on primary wave*
B45	3.32	*Trebuchet*
B47	3.33	*Beating surging*
B48	3.34	*Asymetric surging*
B49	3.35	*Surf-riding on primary wave*

The summary in Table 4.2 shows that for each set of runs, the response type remains unchanged as the secondary wave amplitude increases. However, the amplitude of velocity oscillations caused by the secondary wave increases. It is worth noting that those three sets were carried out with relatively long secondary waves; it would require substantial ship velocity for the wave to influence the ship more than producing only the perturbation.

Table 4.2 Classification of results of bi-chromatic wave cases conducted at a scale of 1/14 showing change in response type while increasing amplitude of secondary wave

Case No.	Figure	Response type
B99	3.36	*Uncertain case*
B129	3.37	*Uncertain case*
B102	3.38	*Uncertain case*
B124	3.39	*Uncertain case*
B104	3.40	*Trebuchet*
B132	3.41	*Oscillatory surf-riding on primary wave*
B106	3.42	*Oscillatory surf-riding on primary wave*
B137	3.43	*Oscillatory surf-riding on primary wave*
B108	3.44	*Oscillatory surf-riding on primary wave*
B121	3.45	*Oscillatory surf-riding on primary wave*
B110	3.46	*Oscillatory surf-riding on primary wave*
B139	3.47	*Oscillatory surf-riding on primary wave*
B112	3.48	*Oscillatory surf-riding on primary wave*
B135	3.49	*Oscillatory surf-riding on primary wave*
B114	3.50	*Oscillatory surf-riding on primary wave*
B119	3.51	*Oscillatory surf-riding on primary wave*
B117	3.52	*Oscillatory surf-riding on primary wave*

Cases shown in Table 4.3 provide a great example of the sensitivity of phenomena related to surf-riding. Even miniscule changes in parameters could change the response type during a single experimental run due to wave degradation.

Table 4.3 Classification of results of bi-chromatic wave cases conducted at a scale of 1/14 showing sensitivity of the surf-riding related phenomena

Case No.	Figure	Response type
B175	3.53	*High-runs on primary wave/ high-runs on secondary wave*
B176	3.54	*Uncertain case*
B177	3.55	*Uncertain case*

The experimental runs summarized in Table 4.4 demonstrate that a decrease in commanded speed not only changes the response type but also affects the duration of oscillations across different phenomena. Under these wave conditions, multiple response types were observed by altering the commanded speed.

Table 4.4 Classification of results of bi-chromatic wave cases conducted at a scale of 1/14 showing decrease of high-run duration while lowering commanded speed

Case No.	Figure	Response type
B183	3.56	*Surf-riding on secondary wave/ high-runs on secondary wave*
B184	3.57	*Surf-riding on secondary wave/ high-runs on secondary wave*
B185	3.58	*Surf-riding on primary wave/ surging*
B186	3.59	*Surf-riding/ high-runs on secondary wave*
B187	3.60	*Surf-riding/ high-runs on secondary wave*
B188	3.61	*High-runs on primary wave/ surf-riding on secondary wave*
B189	3.62	*High-runs on secondary wave/ high-runs on primary wave*
B190	3.63	*Beating surging/ high-runs on secondary wave*
B191	3.64	*Beating surging/ high-runs on secondary wave*

4.2. Comparison of experiments: 1/64 vs. 1/14 scale ship models

Table 4.5 shows that only 4 out of 14 cases achieved high qualitative accuracy in classification. This discrepancy aligns with potential limitations in the 1/64 scale experiments, such as insufficient wave steepness or commanded speeds. That suggests that dimension and time rescaling alone cannot reliably reproduce scaled experiments, as certain responses are highly sensitive to minor condition changes.

Table 4.5 Classification of results by the type of surf-riding related phenomena

Case No.	Response type	
	1/64 scale model	1/14 scale model model
C1	Beating oscillations in surge	Surf-riding on primary wave
C2	Beating oscillations in surge	Surf-riding on primary wave
C3	High-runs on primary wave	Catch and release with transition between celerities
C4	Beating oscillations in surge	Catch and release with transition between celerities
C5	Beating oscillations in surge	High-runs on secondary wave
C6	High-runs on secondary wave	High-runs on secondary wave
C7	High-runs on secondary wave	High-runs on secondary wave
C8	High-runs on secondary wave	Surf-riding on secondary wave
C9	High-runs on primary wave	Catch and release with transition between celerities
C10	High-runs on primary wave	Catch and release with transition between celerities
C11	Beating oscillations in surge	Catch and release with transition between celerities
C12	Beating oscillations in surge	High-runs on secondary wave
C13	Beating oscillations in surge	Beating oscillations in surge
C14	Beating oscillations in surge	Beating oscillations in surge

Quantitative comparisons among cases C6, C7, and C14 (with similar response types) reveal varying velocity amplitude differences: +24% in case C6, +3% in case C7, and +58% in case C14 for the 1/14 scale experiments. However, these results should be interpreted cautiously due to the constrained run durations in the short towing tank.

4.3. Uncertainty assessment

In this experiment, sources of uncertainty were identified and divided into three categories: reproduction of the hull geometry and its mass distribution, wave generation with specified parameters, and uncertainties in position and velocity measurement.

Type A uncertainty estimation, which involves analyzing consistency of a series of repeated measurements, is not applicable to this study as there are no identical cases. Thus, the collected results do not allow for a sufficient statistical data analysis. As of this attempt at Type B uncertainty estimation was carried out that focus on judgments based on information other than repeated measurements. The source of data for such an analysis is the technical documentation of the manufacturing and measuring equipment, the determination of the reading error (important for the initial immersion reading), and possible parameter changes during the runs (e.g., change in weight and immersion due to water inflow). In Table 4.6 the uncertainty of all parameters and measurement devices was listed for both Gdańsk Tech and CTO towing tank experiment.

Table 4.6 Uncertainty assesment summary

Parameter	Unit	CTO 1/14 scale model			Gdańsk Tech 1/64 scale model		
		value	error	error %	value	error	error %
L_{BP}	m	2.51	0.001	0.04	0.55	0.001	0.18
Beam	m	0.543	0.001	0.18	0.119	0.001	0.84
Draft	m	0.189	0.003	1.59	0.041	0.002	4.88
Mass	kg	151.2	0.500	0.33	1.59	0.01	0.63
VCG	m	0.1169	0.001	0.86	0.0338	0.001	2.96
Carriage speed	m/s	2.5	0.005	0.20	1.3	0.002	0.15
Position measurment	m	-	0.005	-	-	0.002	-
Velocity calculation	m/s	2.5	0.007	0.28	1.3	0.003	0.22

For the 1/64 scale model, greater uncertainty was obtained than for the 1/14 model in terms of shape, mass parameters, and draft, which is to be expected due to the very large scaling factor. In the case of measuring the speed of the model, the uncertainties were similar, although the smaller measurement area in the Gdańsk Tech experiment resulted in a lower percentage uncertainty in position measurement. None of the measured parameters exceeded an error of 5 percent, so this can be considered a small enough error to consider the results reliable. However, in the case of a 1/64 scale experiment, it is important to remember the error of the method itself, resulting from different resistance scaling and the lack of the same Reynolds number. It was decided that the results obtained at a scale of 1/64 could be considered good

qualitatively, while the results obtained at a scale of 1/14 were considered good qualitatively and quantitatively.

4.4. Limitations of the experiment

4.4.1.*Limitations common for both experimental campaigns*

Despite performing the study with the highest possible level of care, a number of unavoidable limitations need to be mentioned. These result from a number of factors, including, above all, limited resources in terms of both funds and time.

The first limitation is that only one type of vessel was studied. The vessel was carefully selected, based on the literature on the subject and the results of earlier studies. It is also the benchmark vessel in the ITTC. This is precisely because of its known susceptibility to surf-riding. Nevertheless, this limits the applicability of the results obtained and the conclusions drawn. Therefore, the results cannot be generalized to all ships. However, this does not prevent the generalization of the final conclusions, which confirm that theoretical predictions are reflected in the physical world.

Another significant limitation was conducting tests in scale. On the one hand, it is obvious that tests on full-scale objects are least affected by the inability to maintain all the dimensionless quantities. However, due to the size of real ships, this limitation is typical for the vast majority of experimental studies conducted in the field of ship hydromechanics.

Furthermore, no autopilot was used; during all runs the operator manually controlled the ship course to maintain its position in the measurement area as well as to prevent broaching. However, influence of manual course corrections does not appear to have noticeable impact on the final results.

An additional limitation was the absence of phase shift measurement for the two wave components. While this does not prevent the analysis of results, it restricts the exact comparison in the same conditions, while the “same conditions” are to be understood here as the exact wave realization. The bi-chromatic wave components were adequately controlled; thus, the phase-shift remained the only parameter that could be considered random to a certain degree.

Due to the limitations in the manufacturing process, propellers and rudders were only roughly suited to the required scale. It should be noted that despite the accurate scaling of the mass in both models, the moments of inertia were not scaled due to the most crucial phenomena referring to the x-axis direction. The manufacturing limitations additionally resulted in slight alterations of hull geometry at sharp edges, but due to change being minimal the hulls can be considered properly manufactured.

The models may have had a minimal amount of water resulting from minor leaks. In the 1/64 scale model, the presence of water was checked between runs, while in the 1/64 scale model, a bilge pump installed in a sump was activated between runs to check for water and remove it if necessary.

The last but not least limitation was found to be the relatively small number of experimental runs. It is of note, that the variables governing the studied phenomenon are numerous, since four parameters of waves are required for the proper description of a bi-chromatic wave. Furthermore, the commanded speed remains essential. Therefore, once several states of each of the variable are considered, immediately many thousands of combinations are produced. Such a number of experimental runs is unfeasible, although it would be desired as to fully understand these phenomena.

4.4.2.*Limitations specific for the Gdańsk Tech towing tank experiment*

The primary constraint encountered at the Gdańsk Tech towing tank pertained to the dimensions of the tank, which is only 40 meters long. This limitation imposed an upper bound on the duration of the experimental runs, which could not exceed several seconds. Furthermore, the dimensions of the ship model itself were constrained, such that an increase in length would result in a reduction of the run time at real scale.

The rudder position and the shaft revolutions were not acquired live during the experiment at a 1/64 scale due to technological challenges of mass and space limitations of the platform being so small.

4.4.3.*Limitations specific for the CTO towing tank experiments*

The main constraint encountered at the CTO towing tank was wave generator unable to fully reliably and repeatedly generate waves. In order to overcome that challenge each wave had to be generated multiple times to get correct wave amplitudes as assumed in the list of considered scenarios. During the iterative determination of the required wave parameters, additional runs were performed in order to fully utilize the towing tank time. Repeating the scenarios on different days was also problematic, because the wave-maker parameters adjusted on one day did not generate the same wave the next day. Possibly the applied technology of the wave generator run by hydraulics, was pretty sensitive to oil temperature.

A limitation resulting from the towing tank requirements was securing the model on a mooring line. The towing tank crew did not allow the experiment to be carried out with a completely free-running model for concern that it would sink. For this purpose, only a thin 2mm diameter Dyneema line was used. Its small weight and diameter were intended to minimize the impact on the total resistance of the model. The mooring was adjusted by a student assistant only in case of hazardous proximity to the tank wall or in case of the model sinking. Therefore, the

motions of the model were not meaningfully affected, nor the model was slowing down during the runs.

5. CONCLUSION

The conducted research has been strictly focused on the ship surf-riding phenomenon, specifically with respect to the response observed in bi-chromatic following waves conditions. The main objective of this study was to either prove or disprove the standing theory of surf-riding by conducting towing tank experiments on surf-riding phenomena in bi-chromatic following seas. To archive this objective this dissertation addresses research questions:

- Are the surf-riding experiments feasible in bi-chromatic following wave conditions?
- Do phenomena observed in recent numerical studies actually occur in physical experiments? Can the theoretical predictions be confirmed by the experiment, if so, only qualitatively or also quantitatively?
- Can experiments in following seas conditions be conducted in a short 40 meters towing tank?
- Can surf-riding experiments be considered scalable?

All goals achieved through this work confirm the robustness of surf-riding theory, particularly the accuracy of the 1-DOF mathematical model by addressing all the stated research questions:

- free-running surf-riding experiments are feasible and yield significant insights;
- surf-riding phenomena predicted by numerical experiments occur in real-world conditions, matching them both qualitatively and quantitatively;
- following seas experiments in a 40-meter towing tank are feasible despite the low number of wave encounters;
- surf-riding experiments demonstrate scalability, though further research is required to identify the most critical ship-model parameters governing this scalability;
- six out of eight theoretically predicted phenomena were repeatedly captured in the experiments;
- oscillatory and hybrid response types were observed;
- miniscule parameter changes (e.g., wave degradation) can alter response types during a single run.

This validation underscores the alignment between numerical predictions and physical reality while establishing the experimental feasibility of surf-riding in practical towing tank settings. Ultimately it supports the standing theory of surf-riding through its real-world applicability. It is of note that this experimental work is the first one worldwide in terms of exploration the ship surf-riding in bi-chromatic waves, which speaks to their innovative nature. The obtained results provide the scientific novelty in the field.

The author of this dissertation wishes to acknowledge own contributions, which include:

- Design and development of ship models and experimental methodology;
- Development of equipment at the Gdańsk Tech towing tank to facilitate these experiments;
- Execution of all experiments, including crew management during testing and operation of models via radio remote control;
- Comprehensive data post-processing and presentation of results;
- Analysis and interpretation of results;
- Development of an experimental framework to streamline future studies using small free-running models.

This research is useful for fellow researchers working at towing tanks. However, numerical researchers specializing in ship dynamics should also be interested and fully aware of the implications of this work. The author hopes that more experiments will be conducted in facilities with limited capabilities, thereby expanding our knowledge of ship dynamics and increasing the number of people working in this field.

Future work will address the limitations identified in this study in order to enhance the confidence of the results. This will involve refining the experimental framework with a focus on low-cost, modular model design; developing a method for accurately measuring the position of the model relative to each wave component; and conducting further investigations into surf-riding dynamics in multi-chromatic following seas. Ultimately, the analysis will be extended to include fully irregular wave conditions.

BIBLIOGRAPHY

Belenky, V., Spyrou, K., Weems, K., 2019. Modeling of Surf-Riding in Irregular Waves, in: Contemporary Ideas on Ship Stability. pp. 347–358. https://doi.org/10.1007/978-3-030-00516-0_20

Belenky, V., Weems, K., Spyrou, K., 2016. On probability of surf-riding in irregular seas with a split-time formulation. Ocean Engineering 120, 264–273. https://doi.org/10.1016/j.oceaneng.2016.04.003

Bulian, G., Francescutto, A., 2013. Second generation intact stability criteria: On the validation of codes for direct stability assessment in the framework of an example application. Polish Maritime Research 20, 52–61. https://doi.org/10.2478/pomr-2013-0041

Chu, J., Gu, M., Lu, J., Zhang, P., 2024. A Prediction Method and Model Experiments on Surf-Riding and Broaching in Stern-Quartering Waves. J Mar Sci Eng 12, 1538. https://doi.org/10.3390/jmse12091538

Davidson, K., 1948. A note on the steering of ships in following seas., in: Proc. of 7th Int. Congress Applied Mech. London.

Du Cane, P., Goodrich, G., 1962. The following sea, broaching and surging. Trans. RINA.

Grim, O., 1951. Das Schiff von Achtern Auflaufender. Jahrbuch der Schiffbautechnischen Gesellschaf.

Gu Min, Chu Jilong, Han Yang, Lu Jiang, 2017. Study on Vulnerability Criteria for Surf-riding / Broaching with a Model Experiment , in: Proceedings of the 16th International Ship Stability Workshop.

Harold E. Saunders, 1965. Maneuvering and wavegoing, in: Hydrodynamics in Ship Design. The Society of Naval Architects and Marine Engineers, New York.

Hashimoto, H., Umeda, N., Matsuda, A., 2004. Importance of several nonlinear factors on broaching prediction. J Mar Sci Technol 9. https://doi.org/10.1007/s00773-003-0175-1

Horel, B., Guillerm, pierre-emmanuel, Rousset, J.-M., Alessandrini, B., 2014. Experimental database for surf-riding and broaching-to quantification based on captive model tests in waves.

IMO, 2023. Explanatory notes to the Interim Guidelines on second generation intact stability criteria. MSC.1-Circ.1652.

IMO, 2021. Physical background and mathematical models for stability failures of the second generation intact stability criteria. SDC 8/INF.2.

IMO, 2020. Interim Guidelines on the Second Generation Intact Stability Criteria. MSC.1/Circ.1627.

IMO, 2007. Revised guidance to the master for avoiding dangerous situations in adverse weather and sea conditions. MSC.1/Circ.1228.

IMO, 1995. Guidance to the master for avoiding dangerous situations in following and quarting seas. MSC/Circ.707.

ITTC, 2025. Facilities of member organizations of ITTC (https://ittc.info/facilities) [WWW Document].

Kan, M., 1990a. Surging of large amplitude and surf-riding of ships in following seas., in: Selected Papers in Naval Architecture and Ocean Engineering. Society of Naval Architects of Japan, Tokio.

Kan, M., 1990b. A Guideline to Avoid the Dangerous Surf-riding., in: Proc. 4th Int'l Conf. Stability of Ships and Ocean Vehicles. Naples.

Maki, A., Umeda, M., Renilson, M., Ueta, T., 2010. Analytical Formulae for Predicting the Surf-Riding Threshold for a Ship in Following Seas. J. Marine Science and Technology.

Makov, Y., 1969. Some results of theoretical analysis of surf-riding in following seas. Trans. Krylov Society, "Maneuverability and Seakeeping of Ships.".

Margari, V., Spyrou, K., 2025a. Eliciting the bifurcation structure of cumulative broaching, in: Proceedings of the 20th International Ship Stability Workshop. Chania.

Margari, V., Spyrou, K., 2025b. Robustness of Hydrodynamic Model Assumptions of Cumulative Broaching Predictions, in: Innovations in Sustainable Maritime Technology - IMAM 2025; Ship Motions, Hydrodynamics, Propulsion.

Matsubara, K., Umeda, N., Matsuda, A., 2023. Probabilistic estimation of the large heel due to broaching associated with surf-riding for a ship in short-crested irregular waves and its experimental validation. Ocean Engineering 269, 113540. https://doi.org/10.1016/j.oceaneng.2022.113540

Nakamura, M., Yoshimura, Y., Shiken, D., 2014. Model experiments in following and quartering seas using a small size ship model, in: The 14th International Ship Stability Workshop (ISSW).

Qualisys AB, 2013. Qualisys Track Manager User Manual. Gothenburg.

Sadat Hosseini, S.H., 2009. CFD prediction of ship capsize. University of Iowa, Iowa City, IA, United States. https://doi.org/10.17077/etd.c2qgkc5s

Sakai, M., Umeda, N., Maki, A., 2017. Analytical Solution of Critical Speed for Surf-Riding in the light of Melnikov Analysis., in: Proc. Conf. of the Japan Society of Naval Architects and Ocean Engineers.

Spyrou, K., 2017. Homoclinic Phenomena in Ship Motions. Journal of Ship Research 61, 107–130. https://doi.org/10.5957/JOSR.170012

Spyrou, K., 2010. Historical trails of ship broaching-to. The International Journal of Maritime Engineering 152, A163–A174.

Spyrou, K., 2006. Asymmetric Surging of Ships in Following Seas and its Repercussions for Safety. Nonlinear Dyn 43, 149–172. https://doi.org/10.1007/s11071-006-0758-6

Spyrou, K., 1997. Dynamic instability in quartering seas - Part III: Nonlinear effects on periodic motions. Journal of Ship Research 41, 210–223.

Spyrou, K., 1996a. Dynamic instability in quartering seas: The behavior of a ship during broaching. Journal of Ship Research 40, 46–59.

Spyrou, K., 1996b. Dynamic instability in quartering seas - Part II: Analysis of ship roll and capsize for broaching. Journal of Ship Research 40, 326–336.

Spyrou, K., Kontolefas, I., Themelis, N., 2016. Dynamics of the Surf-Riding Behaviour of A Ship in A Multi-Chromatic Sea Environment, in: 31st Symposium on Naval Hydrodynamics Monterey.

Spyrou, K., Themelis, N., Kontolefas, I., 2018. Nonlinear surge motions of a ship in bi-chromatic following waves. Commun Nonlinear Sci Numer Simul 56, 296–313. https://doi.org/10.1016/j.cnsns.2017.08.013

Spyrou, K.J., 1995. Surf-riding and oscillations of a ship in quartering waves. J Mar Sci Technol 1, 24–36. https://doi.org/10.1007/BF01240010

Spyrou, K.J., Belenky, V., Themelis, N., Weems, K., 2014. Detection of surf-riding behavior of ships in irregular seas. Nonlinear Dyn 78, 649–667. https://doi.org/10.1007/s11071-014-1466-2

Szozda, Z., Krata, P., 2022. Towards evaluation of the second generation intact stability criteria - Examination of a fishing vessel vulnerability to surf-riding, based on historical capsizing. Ocean Engineering 248, 110796. https://doi.org/10.1016/j.oceaneng.2022.110796

Themelis, N., Spyrou, K.J., Belenky, V., 2016. “High runs” of a ship in multi-chromatic seas. Ocean Engineering 120, 230–237. https://doi.org/10.1016/j.oceaneng.2016.04.024

Tigkas, I., Spyrou, K., 2023. Hybrid surging and surf-riding motions of a ship in steep Bi-chromatic following seas. Ocean Engineering 269, 113522. https://doi.org/10.1016/j.oceaneng.2022.113522

Tigkas, I., Spyrou, K., 2021. Continuation Analysis of Ship Motions in Bi-chromatic Following/Quartering Seas, in: 1st International Conference on the Stability and Safety of Ships and Ocean Vehicles (STABS 2021).

Umeda, N., 1999. Nonlinear dynamics of ship capsizing due to broaching in following and quartering seas. J Mar Sci Technol 4, 16–26. https://doi.org/10.1007/s007730050003

Umeda, N., 1990. Probabilistic study on surf-riding of a ship in irregular following seas, in: Proceedings of the 4th International Conference on Stability of Ships and Ocean Vehicles. University Federico II of Naples.

Umeda, N., Hamamoto, M., 2000. Capsize of ship models in following/quartering waves: physical experiments and nonlinear dynamics. Philosophical Transactions of the Royal Society of London. Series A: Mathematical, Physical and Engineering Sciences 358, 1883–1904. https://doi.org/10.1098/rsta.2000.0619

Umeda, Naoya, Hamamoto, M., Takaishi, Y., Chiba, Y., Matsuda, A., Sera, W., Suzuki, S., Spyrou, K., Watanabe, K., 1995. Model Experiments of Ship Capsize in Astern Seas. Journal of the Society of Naval Architects of Japan 1995, 207–217. https://doi.org/10.2534/jjasnaoe1968.1995.207

Umeda, N., Matsuda, A., Hamamoto, M., Suzuki, S., 1999. Stability assessment for intact ships in the light of model experiments. J Mar Sci Technol 4, 45–57. https://doi.org/10.1007/s007730050006

Umeda, N., Usada, S., Mizumoto, K., Matsuda, A., 2016. Broaching probability for a ship in irregular stern-quartering waves: theoretical prediction and experimental validation. J Mar Sci Technol 21, 23–37. https://doi.org/10.1007/s00773-015-0364-8

Umeda, N., Yamakoshi, Y., Suzuki S, 1995. Experimental Study for Wave Forces on a Ship Running in Quartering Seas with Very Low Encounter Frequency. Int. Sympo. on Ship Safety in a Sea Way, Kaliningrad, Russia.

Umeda, N., Yamamura, S., Matsuda, A., Maki, A., Hashimoto, H., 2008. Model Experiments on Extreme Motions of a Wave-Piercing Tumblehome Vessel in Following and Quartering

Waves. Journal of the Japan Society of Naval Architects and Ocean Engineers 8, 123–129. https://doi.org/10.2534/jjasnaoe.8.123

Wahab, R., Swaan, W., 1964. Coursekeeping and broaching of ships in following seas. J. Ship Res.

Warnke-Olewniczak, K., Krata, P., 2024. Numerical simulation of surging and surf-riding in bi-chromatic following waves in support of the model test., in: Proceedings of the 2nd International Conference on the Stability and Safety of Ships and Ocean Vehicles. Wuxi.

Wu, W., Spyrou, K., McCue, L., 2010. Improved prediction of the threshold of surf-riding of a ship in steep following seas. Ocean Engineering.

This page was intentionally left blank.

LIST OF FIGURES

LIST OF TABLES

This page was intentionally left blank.

Appendix A Experimental runs conducted at a scale of 1/14

Case No.	A_1 [cm]	λ_1 [m]	c_1 [m/s]	A_2 [cm]	λ_2 [m]	c_2 [m/s]	v_c [m/s]
B11	2.11	2.899	2.128	-	-	-	1.915
B12	2.47	2.899	2.128	-	-	-	1.996
B13	1.87	3.802	2.437	-	-	-	1.815
B14	1.88	3.802	2.437	-	-	-	1.915
B15	1.85	3.802	2.437	-	-	-	1.996
B16	1.93	3.802	2.437	-	-	-	2.074
B17	1.99	3.802	2.437	-	-	-	2.161
B19	1.74	3.161	2.222	0.84	3.459	2.325	1.580
B20	1.52	2.899	2.128	1.59	3.161	2.222	1.580
B21	1.08	2.777	2.083	1.69	3.161	2.222	1.678
B22	1.66	3.161	2.222	0.78	3.459	2.325	1.815
B23	1.62	2.899	2.128	1.62	3.161	2.222	1.996
B24	1.54	2.899	2.128	1.56	3.161	2.222	2.074
B25	1.57	2.899	2.128	1.60	3.161	2.222	2.126
B26	1.42	2.899	2.128	1.48	3.161	2.222	1.759
B27	2.79	2.899	2.128	1.90	7.102	3.331	1.455
B28	2.77	2.899	2.128	1.99	7.102	3.331	1.601
B29	2.97	2.899	2.128	1.88	7.102	3.331	1.638
B30	2.97	2.899	2.128	1.85	7.102	3.331	1.703
B31	2.96	2.899	2.128	1.98	7.102	3.331	1.879
B32	0.91	2.899	2.128	5.16	7.102	3.331	1.531
B34	0.83	2.899	2.128	5.18	7.102	3.331	1.915
B35	0.89	2.899	2.128	5.16	7.102	3.331	1.996
B36	0.91	2.899	2.128	5.17	7.102	3.331	2.196
B37	1.04	2.899	2.128	5.18	7.102	3.331	2.306
B38	3.11	2.777	2.083	2.17	7.102	3.331	1.996
B39	2.77	2.899	2.128	2.01	7.102	3.331	1.531
B40	2.01	2.899	2.128	1.39	3.300	2.270	1.557
B41	2.08	2.899	2.128	1.84	3.300	2.270	1.638
B42	2.07	2.899	2.128	1.82	3.300	2.270	1.759
B43	1.81	2.899	2.128	1.45	3.300	2.270	1.815
B44	2.08	2.899	2.128	1.75	3.300	2.270	1.860
B45	1.99	2.899	2.128	1.41	3.300	2.270	1.996
B46	2.36	2.777	2.083	1.49	3.300	2.270	2.306
B47	2.27	2.899	2.128	0.92	4.676	2.703	1.557
B48	2.91	2.837	2.105	0.77	4.676	2.703	1.703
B49	2.61	2.899	2.128	0.88	4.676	2.703	1.897
B50	2.67	3.398	2.304	3.44	3.630	2.381	1.703
B51	1.77	3.469	2.328	2.26	3.630	2.381	1.915
B52	2.36	3.398	2.304	3.16	3.630	2.381	1.996
B53	2.60	3.398	2.304	3.26	3.630	2.381	2.178

Case No.	A_1 [cm]	λ_1 [m]	c_1 [m/s]	A_2 [cm]	λ_2 [m]	c_2 [m/s]	v_c [m/s]
B54	4.33	3.459	2.325	1.68	8.143	3.566	1.394
B55	4.34	3.459	2.325	1.65	8.143	3.566	1.638
B56	3.95	3.459	2.325	1.64	8.143	3.566	1.839
B59	4.47	3.300	2.270	1.81	8.143	3.566	2.306
B60	1.36	3.459	2.325	4.64	8.143	3.566	1.340
B61	1.39	3.459	2.325	4.61	8.143	3.566	1.638
B62	1.29	3.459	2.325	4.55	8.143	3.566	1.915
B63	1.39	3.459	2.325	4.57	8.143	3.566	2.126
B64	1.26	3.459	2.325	4.52	8.143	3.566	2.306
B65	3.05	3.459	2.325	1.44	5.540	2.942	1.505
B66	2.98	3.459	2.325	1.46	5.540	2.942	1.839
B67	2.84	3.459	2.325	1.36	5.540	2.942	1.932
B68	3.02	3.459	2.325	1.45	5.540	2.942	1.897
B69	2.97	3.459	2.325	1.30	5.540	2.942	1.965
B70	2.96	3.459	2.325	1.35	5.540	2.942	2.178
B71	2.77	3.459	2.325	1.39	5.540	2.942	2.306
B72	3.14	3.459	2.325	1.24	3.999	2.499	1.703
B73	3.04	3.378	2.297	0.72	3.999	2.499	1.915
B74	3.13	3.378	2.297	0.62	3.999	2.499	1.965
B75	2.99	3.378	2.297	0.61	3.999	2.499	1.996
B76	2.93	3.378	2.297	0.73	3.999	2.499	2.074
B77	2.93	3.378	2.297	0.69	3.999	2.499	2.287
B78	2.92	3.802	2.437	-	-	-	2.074
B79	2.99	3.802	2.437	-	-	-	2.108
B80	2.98	3.802	2.437	-	-	-	2.126
B81	3.48	3.802	2.437	-	-	-	2.143
B82	2.99	3.802	2.437	-	-	-	2.161
B83	2.68	2.837	2.105	0.70	4.676	2.703	1.703
B84	2.13	3.378	2.297	2.60	3.630	2.381	1.915
B85	2.12	2.837	2.105	2.40	3.090	2.197	1.455
B86	1.06	2.837	2.105	3.53	7.102	3.331	1.788
B87	3.04	3.802	2.437	-	-	-	2.161
B88	3.11	3.802	2.437	-	-	-	2.178
B89	3.24	2.837	2.105	1.36	7.102	3.331	1.996
B90	2.95	2.899	2.128	1.77	7.102	3.331	2.074
B91	2.12	3.802	2.437	-	-	-	2.196
B92	2.07	3.802	2.437	-	-	-	2.215
B93	2.89	3.378	2.297	0.95	5.540	2.942	2.042
B94	2.79	3.378	2.297	1.01	5.540	2.942	2.091
B95	3.07	3.378	2.297	0.65	3.999	2.499	2.143
B96	3.21	3.378	2.297	0.64	3.999	2.499	2.215
B97	3.44	3.802	2.437	0.65	4.212	2.565	2.178

Case No.	A_1 [cm]	λ_1 [m]	c_1 [m/s]	A_2 [cm]	λ_2 [m]	c_2 [m/s]	v_c [m/s]
B98	2.73	3.802	2.437	0.86	4.212	2.565	2.178
B99	2.51	3.802	2.437	0.74	4.212	2.565	2.178
B100	3.37	3.802	2.437	1.28	4.212	2.565	2.178
B101	2.67	3.802	2.437	1.06	4.212	2.565	2.178
B102	2.61	3.802	2.437	1.08	4.212	2.565	2.178
B103	3.20	3.802	2.437	2.02	4.212	2.565	2.178
B104	3.16	3.802	2.437	1.62	4.212	2.565	2.178
B105	3.44	3.802	2.437	0.81	5.867	3.027	2.178
B106	3.05	3.802	2.437	0.81	5.867	3.027	2.178
B107	3.46	3.802	2.437	1.14	5.867	3.027	2.178
B108	3.06	3.802	2.437	1.06	5.867	3.027	2.178
B109	3.40	3.802	2.437	1.59	5.867	3.027	2.178
B110	3.19	3.802	2.437	1.63	5.867	3.027	2.178
B111	3.45	3.802	2.437	0.86	7.888	3.510	2.178
B112	3.15	3.802	2.437	0.74	7.888	3.510	2.178
B113	3.47	3.802	2.437	1.01	7.888	3.510	2.178
B114	3.15	3.802	2.437	1.09	7.888	3.510	2.178
B115	3.32	3.802	2.437	1.61	7.888	3.510	2.178
B116	3.28	3.802	2.437	1.57	7.888	3.510	2.178
B117	3.04	3.802	2.437	1.49	7.888	3.510	2.178
B118	3.38	3.802	2.437	1.24	7.888	3.510	2.178
B119	3.18	3.802	2.437	1.28	7.888	3.510	2.178
B120	3.06	3.802	2.437	1.36	5.867	3.027	2.178
B121	3.14	3.802	2.437	1.46	5.867	3.027	2.178
B122	3.43	3.802	2.437	1.18	4.212	2.565	2.178
B123	2.93	3.802	2.437	1.71	4.212	2.565	2.178
B124	3.40	3.802	2.437	0.96	4.212	2.565	2.178
B129	3.22	3.802	2.437	0.99	4.212	2.565	2.178
B130	3.43	3.802	2.437	0.72	5.867	3.027	2.178
B131	3.50	3.802	2.437	1.21	4.212	2.565	2.178
B132	3.20	3.802	2.437	0.62	5.867	3.027	2.178
B133	3.55	3.802	2.437	0.96	7.888	3.510	2.178
B134	3.11	3.802	2.437	1.07	7.888	3.510	2.178
B135	3.06	3.802	2.437	0.94	7.888	3.510	2.178
B136	3.39	3.802	2.437	1.01	5.867	3.027	2.178
B137	3.21	3.802	2.437	0.79	5.867	3.027	2.178
B138	3.48	3.802	2.437	0.68	7.888	3.510	2.178
B139	3.11	3.802	2.437	0.63	7.888	3.510	2.178
B149	2.83	3.378	2.297	2.59	3.630	2.381	2.196
B150	2.68	3.378	2.297	3.07	3.630	2.381	2.196
B151	2.70	3.378	2.297	3.04	3.630	2.381	2.196
B152	3.47	3.378	2.297	2.23	3.630	2.381	2.196

Case No.	A_1 [cm]	λ_1 [m]	c_1 [m/s]	A_2 [cm]	λ_2 [m]	c_2 [m/s]	v_c [m/s]
B153	2.56	3.469	2.328	2.60	3.630	2.381	2.196
B154	3.38	3.802	2.437	-	-	-	2.178
B155	1.67	2.837	2.105	4.74	3.300	2.270	1.580
B156	1.61	2.837	2.105	4.81	3.300	2.270	1.580
B157	1.90	2.837	2.105	4.60	3.300	2.270	1.580
B158	2.00	2.837	2.105	3.70	3.090	2.197	1.915
B159	1.30	2.837	2.105	4.04	3.090	2.197	1.915
B160	0.96	2.837	2.105	5.27	3.090	2.197	1.915
B161	1.14	2.837	2.105	5.27	3.090	2.197	1.915
B162	1.05	2.837	2.105	4.97	3.090	2.197	1.839
B163	1.11	2.837	2.105	5.04	3.090	2.197	1.839
B164	0.90	2.837	2.105	5.09	3.090	2.197	1.839
B168	2.72	2.899	2.128	1.79	7.102	3.331	1.996
B169	2.59	3.999	2.499	1.91	8.143	3.566	2.178
B170	2.95	3.802	2.437	1.46	7.888	3.510	2.178
B171	3.47	3.802	2.437	1.97	7.612	3.448	2.178
B172	3.01	3.802	2.437	1.44	7.888	3.510	2.178
B173	0.60	2.837	2.105	4.56	3.090	2.197	1.839
B174	0.88	2.837	2.105	4.41	3.090	2.197	1.839
B175	0.94	2.837	2.105	4.50	3.090	2.197	1.839
B176	0.81	2.837	2.105	4.23	3.090	2.197	1.915
B177	0.50	2.837	2.105	4.56	3.090	2.197	1.915
B178	0.73	2.837	2.105	4.77	3.300	2.270	1.915
B179	0.76	2.837	2.105	4.56	3.234	2.248	1.980
B180	0.50	2.956	2.149	4.30	3.234	2.248	1.980
B181	0.94	2.956	2.149	4.45	3.300	2.270	1.980
B182	0.61	2.956	2.149	4.98	3.300	2.270	1.980
B183	0.94	2.956	2.149	4.92	3.300	2.270	1.980
B184	0.92	2.956	2.149	5.07	3.300	2.270	1.980
B185	0.61	2.956	2.149	4.99	3.300	2.270	1.915
B186	0.90	2.956	2.149	4.88	3.300	2.270	1.915
B187	0.67	2.956	2.149	4.98	3.300	2.270	1.915
B188	0.58	2.956	2.149	5.04	3.300	2.270	1.839
B189	0.85	2.956	2.149	5.08	3.300	2.270	1.839
B190	0.69	2.956	2.149	5.10	3.300	2.270	1.730
B191	0.84	2.956	2.149	5.04	3.300	2.270	1.730